SHEAR STRENGTH AND PHYSICAL PROPERTIES OF VARIOUS DEEP SEA SEDIMENTS FROM THE CENTRAL INDIAN BASIN

THESIS SUBMITTED TO THE GOA UNIVERSITY

FOR THE DEGREE OF

DOCTOR OF PHILOSOPHY

IN

MARINE SCIENCE

BY

N. H. KHADGE

NATIONAL INSTITUTE OF OCEANOGRAPHY
DONA PAULA, GOA 403 004, INDIA

AUGUST 1998

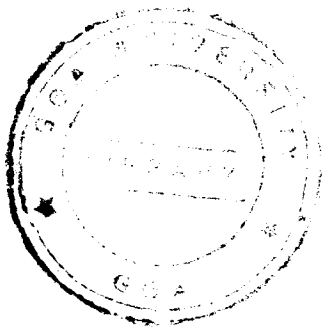

TO THE MEMORY OF

MY PARENTS AND BROTHER

CERTIFICATE

Mr. N. H. Khadge has been working under my guidance since 1995. The Ph. D. thesis entitled, ***'Shear strength and physical properties of various deep sea sediments from the Central Indian Basin'***, submitted by him contains the results of his original investigation of the subject. This is to certify that the thesis has not been the basis for the award of any other research degree or diploma of other University.

Place : Dona Paula

Date: 14.8.98

R. R. Nair
(Research Guide)
Former Deputy Director,
National Institute of Oceanography,
Dona Paula, Goa - 403 004.

The suggested corrections are incorporated in the Thesis

Expert

Guide

CONTENTS

STATEMENT

As required under the University ordinance O.19.8 (vi), I state that the present thesis entitled, ***'Shear strength and physical properties of various deep sea sediments from the Central Indian Basin'***, is my original contribution. To the best of my knowledge, the present study is the first comprehensive study of its kind from the area mentioned.

The literature concerning the thesis has been cited. Due acknowledgments have been made wherever facilities have been availed of.

(N. H. Khadge)

ACKNOWLEDGMENTS

I express my deep sense of gratitude to Shri. R. R. Nair, former Deputy Director of the National Institute of Oceanography, for his continuous guidance and encouragement during the entire work. His thought provoking suggestions from time to time were very much helpful to me. I am very much thankful to him for making himself available even after his retirement.

I am grateful to the Dr. E. Desa, Director, National Institute of Oceanography, for making the facilities available to carry out this work, and for permission to submit the thesis.

The Department of Ocean Development, New Delhi provided the financial assistance for the projects PMN and PMN - EIA under which present data and sample collection was possible.

I am thankful to the Head of Ocean Engineering Division for permission to use the geotechnical laboratory to carry out the study. This study is immensely benefited from discussions with Dr. S.T. Bhat and Mr. D. Illangovan.

I am highly indebted to my colleagues Drs. R. Mukhopadhyay, B.N. Nath, A. B. Valsangkar, S. M. Gupta, M. Sudhakar, V.N Kodagali, M. Shym Prasad, R. Sharma and S. Afzulpurkar for the help onboard various ships during sample and data collection.

The help rendered by Mr. R. L. Naik during laboratory analyses, by Mr. Girish Prabhu during x-ray diffraction, Mr. N.V. Ambre for microscopic examination of few samples was critical. Dr. S.M. Gupta is specially thanked for discussion on biostratigraphic data. Thanks are also due to Dr. V. P. C. Rao for discussion on clay minerals.

Assistance of Marine Surveyors and from Technicians of Geo-instrumentation and Mechanical Engineering groups of Geological Oceanography Division is gratefully acknowledged.

The cruise participants and crew members of the cruises *ORV Sagar Kanya 69, AA Sidorenko 4 and 17, and Yuzhmorgeologia INDEX 3A and 3B* are thanked for the assistance for sample and data collection. Thanks are due to Drs. J. N. Pattan, A. L. Paropkari for discussion, and to Dr. I. Ghosh, and Mr. S. Jai Sankar for helping me during use of software packages. The moral support from Drs. A.V. Mudholkar, V.K. Banakar, G. H. Ranade and the project colleagues during the work was extremely fruitful. Thanks are due to Mr. Shyam Akerkar for drafting nice figures.

Colleagues from the Geological Oceanography Division have helped me directly or indirectly at various stages of the work , to whom I would like to thank from my heart. I would like to thank the Head and office staff of Marine Science Department, Goa University for the cooperation. The help and facilities rendered by Mr. Wahidullah for colour xeroxing, and Mr. M. P. Tapswi, Mr. S. Jayakumar and D. Illangovan for final printing of the thesis are gratefully acknowledged

The inspiration and affection from my wife *Shailaja*, and daughters, *Harsha* and *Esha* helped me a lot in completing the work.

LIST OF TABLES

LIST OF FIGURES

CHAPTER 1

INTRODUCTION

Polymetallic nodules cover approximately 46 million square kilometer of area of the ocean floor with the estimated reserves of 1.7 to 3 trillion tonnes (Mero, 1965). The first nodule discovery was during HMS Challenger Expeditions (1873-1876) to the Pacific Ocean. They are considered as potential resource of the metals such as copper, nickel, cobalt, manganese and iron (Mero, 1965, Cronan, 1980). Similarly, manganese and cobalt rich crusts are also valuable metallic sources identified in the world oceans. It is expected that the exploitation of nodules in future will have profound effect on world economy, trade and metal consumption patterns. Since the land resources are diminishing fast, alternate deposits have to be identified in the oceanic areas. The Central Indian Basin in the Indian Ocean has been explored since 1981 for the non-living resources and has proved to be very rich in reserves of nodules and cobalt crusts. Because of their valuable metal contents and the large reserves, polymetallic nodules attracted interest of the Indian government and the program for nodule survey and exploration was launched by the Department of Ocean Development, New Delhi in the year 1981. Frazer and Wilson (1980) reported various basins in the Indian Ocean with nodule coverage. But the Central Indian Basin emerged as the most potential basin where extensive survey and exploration have been done. Because of entirely new technology with high investment in the exploration of the nodules, many companies in developed countries have pooled their expertise to form consortia. In so far as the India is concerned, the National Institute of Oceanography, Goa has been the lead organization in exploration in the Central Indian Basin. Nodules occupy about 10-15 million sq. km. area in the Indian Ocean (Siddiquie etal., 1978).

The Pacific ocean nodules have been extensively studied for the last five decades and the study reveals that the Clarian-Clipperton Zone ranging from 10°N to 20°N latitude and 115°W to 160°W longitudes is the most promising area as far as the abundance and metal content of nodules is concerned (Frazer and Wilson, 1980). The claims of all the Pioneer investors (Japan, France, Republic of China, South Korea and Inter Ocean Metal), except India, are in the Pacific Ocean. The Atlantic Ocean has relatively poor resources of nodules.

1.1 Central Indian Basin

The Central Indian Basin (CIB) extends from 0°S to 25°S latitudes and from 70°E to 90°E longitudes (Figure 1.1). The basin is bordered by Nintyeast Ridge on the eastern side, Central Indian Ridge and Chagos Laccadive Ridge on western side, South East Indian Ridge on the southern side. Four sedimentary facies are reported from the CIB (Udintsev, 1975; Rao and Nath, 1988). They are terrigenous facies dominant upto 5°S, siliceous sediments between 5°S and 15°S latitudes with isolated patches of calcareous sediments within, and pelagic sediments south of 15°S latitudes (Figure 1.2). The water depth of the nodule occurrence in this basin is 4800 to 6000 m. The major part of the basin is an abyssal plain and has the influence of terrigenous sediments from the Ganges-Brahmaputra, Krishna-Godavari rivers which distribute the sediments to 8°S (Kolla and Biscaye, 1973, Rao and Nath, 1988).

It is reported from single beam echosounding data that basin is punctuated by numerous seamounts and abyssal hills (Mukhopadhyay and Khadge, 1990). The CIB was then resurveyed with multibeam system - Hydrosweep during 1990-93 which showed new features with varying morphology (hills, fracture zones). It also revealed that the northern part of

the pioneer area (10°S- 12°30'S) is plain with gentle slopes while southern part (12°30'S-15°S) has rugged topography (Kodagali etal., 1995). The southern part shows seamounts of height range of 200 - 1000 m and more than 1000 m. Morphometric studies in the CIB showed that about 92 % of the area has slope angle less than 3 degrees and only 8 % has slope more than 3 degrees (Banakar and Kodagali, 1988). The average rate of sedimentation in the basin is 2-2.5 mm/ky (Banakar etal., 1991).

1.2 Nodules in general

Manganese nodules are probably the most widely known of the authigenic deposits found on the ocean floor, even though they are enigmatic. They have rounded shapes and range in size from micronodules of a few micron to up to 10 cm. They are most abundant where sedimentation rates are less than 5 mm/ky (5 m/Ma). These nodules show a patchy distribution in some areas or as a continuous mat for several square meters on the seafloor. Their concentration on the seabed can reach up to 25 kg/m^2. The systematic exploration for nodules in the world oceans started almost a century after their discovery. The concentric layers of Fe-Mn oxides and hydroxides are deposited around the nucleus to from the nodules of various sizes and shapes. The nucleus may be of biological origin e.g. shark tooth, but commonly a rock fragments. The growth rates of nodules are estimated to be few millimeters/Ma which are much less than sedimentation rates (Anonymous, 1989). Bonatti etal. (1972) attributed metal accumulations to multiple sources. The widely accepted theories for nodule formation are as follows.

a) Hydrogenous origin: overlying water column is the source of metals from which Fe-Mn hydroxides deposit around a nucleus along with trace metals (Goldberg and Arrhenius, 1958).

b) Diagenetic process: metals from overlying water column and from the sediments below accrete around the nucleous to form nodules (Murray and Irvine, 1894).

c) Hydrothermal origin: the metals are supplied from the solutions ejected from the submarine volcanic activities which on deposition form nodules of various sizes (Murray and Renard, 1891).

d) Halmyrolytic deposits are those in which the elements are at least in part, supplied by submarine weathering (halmyrolysis), generally of basaltic material. This type of nodules are in some limited areas of the Pacific Ocean.

Nodule composition shows three most commonly occurring manganese minerals i.e. todorokite, birnessite and δMnO_2. The accessory minerals include quartz, feldspar, zeolite, clay minerals etc. with quartz as the most common one (Burns and Burns, 1977). Several of the accessory minerals are alteration products of volcanic rocks. The growth rates of nodules have considerable variations (1-10 mm/Ma) depending upon environment of deposition and rate of supply of elements. In general, the growth rates are influenced by the nearness of deposit to the elemental supply. The internal structures show concentric banding of ferromanganese oxides and silica deposited around nucleous (Cronan, 1980).

1.3 Nodules from the Central Indian Basin

The first nodule recovery from the Indian Ocean was made onboard RV Gaveshani in 1981. Nodules are black in colour and vary in size from 2 to 10 cm in diameter. They have smooth or rough surface with variable shapes of round and spheroidal to ellipsoidal and flat. The rounded nodules have one nucleous but bigger ellipsoidal nodules show polynucleated growth. It is reported that nodules from the abyssal hills are more abundant but poor in metal content whereas the those from plain areas show reverse

phenomenon. Studies on various aspects of nodules from the Indian Ocean are reported by many. Frazer and Wilson (1980) reported occurrence of various morphological types of nodules from five basins. Siddiquie etal. (1978) reported todorokite and birnessite as main mineral phases. Cronan and Moorby (1981) based on x-ray diffraction analysis reported that todorokite in nodules from the deeper parts and δMnO_2 phase from elevated parts of Madgascar Basin. Cronan and Tooms (1967), Glasby (1972) reported abundance and grade of Indian and Pacific Ocean nodules.

Since 1987, data on mineralogical studies (Rao, 1987), morphological variations (Mukhopadhyay, 1987), abundance and grade distribution (Sudhakar, 1989), internal structures (Pattan, 1988), geochemical variation (Ahmed and Hussain, 1987; Jauhari, 1987), size analysis and metal grade variations (Valsangkar and Khadge, 1989; Valsangkar, 1995) of nodules from the Central Indian Basin; bathymetry and seamount morphology (Mukhopadhyay and Khadge, 1990) are published. An average abundance of nodules from the Pioneer Area is 4.39 kg/m^2 and the average metal grade is 2.31 % in which contribution of copper is 1.12 %, cobalt 0.14 % and nickel 1.05 %. The average percentage of manganese is 24 (Mudholkar etal, 1988). The rare earth element studies of sediments and nodules were reported by Nath etal. (1992) and Pattan and Banakar (1993). The studies (Rao, 1987; Sudhakar, 1989) showed that the nodules occurring in the siliceous sediments between 10° - 15°S in the CIB are rich in Mn, Cu and Ni and are more abundant; whereas nodules occurring in pelagic clays below $15^{O}S$ are rich in Fe and Co and are less abundant. Pattan etal. (1992) reported higher biogenic silica and radiolarian abundance in the siliceous sediments than pelagic sediments; and suggested that biogenic silica results in formation of Fe-rich montmorillonite; and nodules rich in Mn, Cu and Ni. Thus todorokite rich nodules are common in northern part (10°-15°S) of the CIB and δMnO_2-rich nodules are common in the southern part (beyond 15°S) of the CIB (Rao,

1987). The average composition of nodules from the Indian, Pacific and Atlantic Ocean is given in Table 1.1. Under water photography has confirmed the patchy distribution of nodules on the seafloor with variable abundance of 1-20 kg/m^2 and nodule size of 1-10 cm (Sharma, 1993). The in situ resources in the Indian Pioneer area are given in Table 1.2.

1.4 Background

The identification of nodule and metal reserves gave India the Pioneer Investor status under the United Nations Convention for Law of the Seas (UNCLOS) in August, 1987. Based on the close grid survey of nodule abundance and metal grade of the three elements viz. copper, nickel and cobalt, an area of 150,000 square kilometers known as Pioneer Area was allocated to India in the Central Indian Basin by International Seabed Authority in December, 1987 (Figure 1.3). This gave India exclusive rights to develop and exploit the nodule reserves therein. The next step was to delineate the bathymetric variations in the Pioneer area with the multibeam system and identify candidate mine site for nodule mining. The multibeam bathymetric survey gave three dimensional topographic features on the seafloor (like, hills, seamounts and ridges) with a resolution of 20 m. As an UNCLOS obligations, the relinquishment of 50 % of the Pioneer area in stages was also undertaken simultaneously. In the course of developing the nodule reserves, it was felt necessary to measure the geotechnical properties of sediments.

1.5 Worldwide developments

Exploration of the oceans has always engaged the attention of mankind. As conventional land based resources are diminishing, new

sources of energy and minerals critical to human existence are being sought from the oceans. Of these the most common are oil and gas which have been exploited from the shallow depth. Manganese nodules were reported first from deep water depths in 1873 and have been now reported from the Atlantic, Pacific and Indian Oceans (Poulos, 1988). The enormous investment and expensive ship time are required for the geotechnical studies essential for deep sea mining. Despite this reason, the development in this field started in late seventies/early eighties in the Pacific Ocean. The pioneer investors namely Japan, France, Republic of China, South Korea and Inter Ocean Metal (IOM is a joint organisation of governments of the Bulgaria, Cuba, Czech Republic, Poland, Russian Federation and Slovak Republic) identified their areas for nodule exploration in the Pacific Ocean. Nodules from the Atlantic Ocean did not get much attention due to their low abundance and poor metal content.

A knowledge of geotechnical properties is important to understand sedimentary processes i.e. erosion, deposition, slumping, consolidation whereas knowledge of sediment diagenesis and processes is essential to know sediment behaviour (shear strength, compressibility etc.). For example stress strain behaviour primarily controlled by the physico-chemical inter particle effects which in turn are largely related to the diagenesis of sediments, whereas many of the alterations that occur after the sediment deposition are in turn controlled by strength properties of the sediments. Detailed information on geotechnical properties is crucial in identifying correlation between various parameters that may provide supplementary information on tectonic processes and dating of stratigraphy (Silva, 1974). Marine geotechnique is a relatively new field that attempts to define mass physical and chemical properties of seafloor deposits and response of these material to applied static and dynamic forces (Keller, 1974).

The preliminary properties of sediments from the nodule mining areas in the Pacific Ocean were reported by many scientists (Simpson, 1976;

Richards etal., 1976; and references therein; Tsurusaki etal., 1994). The first in situ measurements of shear strength were made during *Le Nautile* submersible dives in the northeastern Pacific Ocean (Cochonat etal., 1992). At present the Pioneer Investors are involved in developing the resources in their respective areas in the Pacific and Indian Ocean. Most of these countries are planning to have combined efforts to the ultimate mining of nodules. As a prerequisite, the studies on environmental impact assessment of nodule mining have been carried out by these countries. Simultaneously designing and testing of a nodule collector have also been given importance.

1.6 Objectives

The vast reserves of nodules and metals therein could only be exploited in future provided suitable mining techniques are available to operate at the great depths (5000 m) in the Indian Ocean. For this, two aspects are thought to be most important. One is the design of mining system and the another is environmental impact assessment of deep sea mining on the surroundings. Since the geotechnial studies give sediment characteristics and their behavior under dynamic loading, it was necessary to determine these properties and their variation with depth by collecting long sediment cores from the Central Indian Basin. The properties include natural water content, specific gravity, porosity, wet bulk density, void ratio and undrained shear strength. These depend upon the grain size distribution and clay mineralogy of the sediments. Therefore, the data on these two aspects were also determined and related to measured properties. Such studies were suggested for the Indian Ocean sediments (Kolla and Hayes, 1974), but were not possible until the nodule exploration program was started. These studies give the depositional history of the sediment column and can be used as an additional tool for geological interpretation. The data is useful to mining

engineers for determining the bearing capacity and compressibility of sediments, and trafficability of mining module. The research work was undertaken with following objectives.

a) To measure shear strength and physical properties of the CIB sediments from nodule bearing area

b) to study variation in properties with depth below the seafloor.

c) to correlate them with grain size and clay mineralogy

d) To generate a data base of these properties which would be useful to mining engineers for design of nodule collector.

e) To assess impact of simulated disturbance on the properties

This research work is carried out for the first time on the CIB sediments and forms the part of the on going geotechnical program for the Central Indian Basin.

Table 1.1: Average composition of nodules from the world oceans and the Indian Pioneer area.

	Mn %	Fe %	Cu %	Ni %	Co %
Pacific Ocean[@]	19.78	11.96	0.392	0.634	0.335
Atlantic Ocean[@]	15.78	20.78	0.116	0.328	0.318
Indian Ocean[@]	15.10	14.74	0.294	0.464	0.230
Central Indian Basin*	24.4	7.1	1.04	1.10	0.11
Indian Pioneer Area**	24.0	-	1.12	1.05	0.14

[@] Cronan (1980)
* Jauhari and Pattan (1998)
** Mudholkar etal., (1988)

Table 1.2: In situ nodule and metal resources in the Pioneer area in the CIB

Resources	Quantity (Milli. Metric Tonnes)
Nodules (wet basis)	759
Nodules (dry basis)	607
Manganese	144
Cobalt	0.85
Nickel	7.0
Copper	6.5
Total Metal	14.35

PMN Status Report (1995)

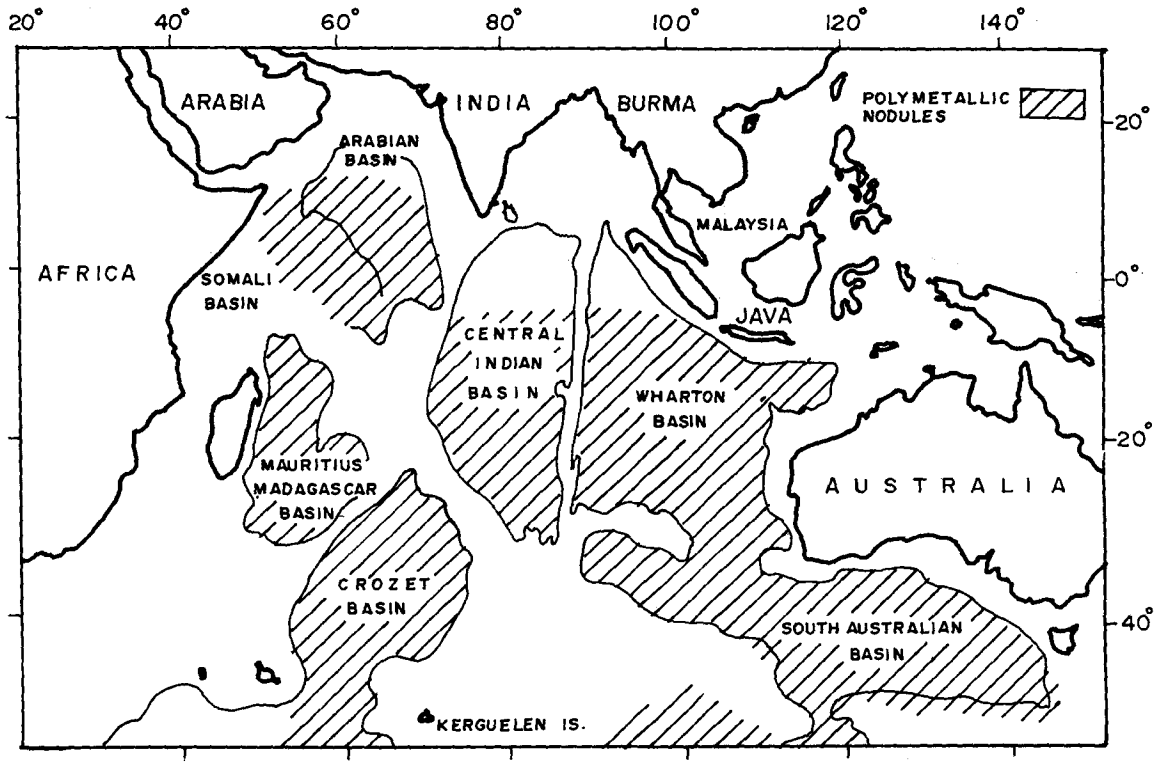

Fig. I.I DISTRIBUTION OF MANGANESE NODULES IN THE VARIOUS BASINS OF INDIAN OCEAN (Cronan and Moorby, 1981)

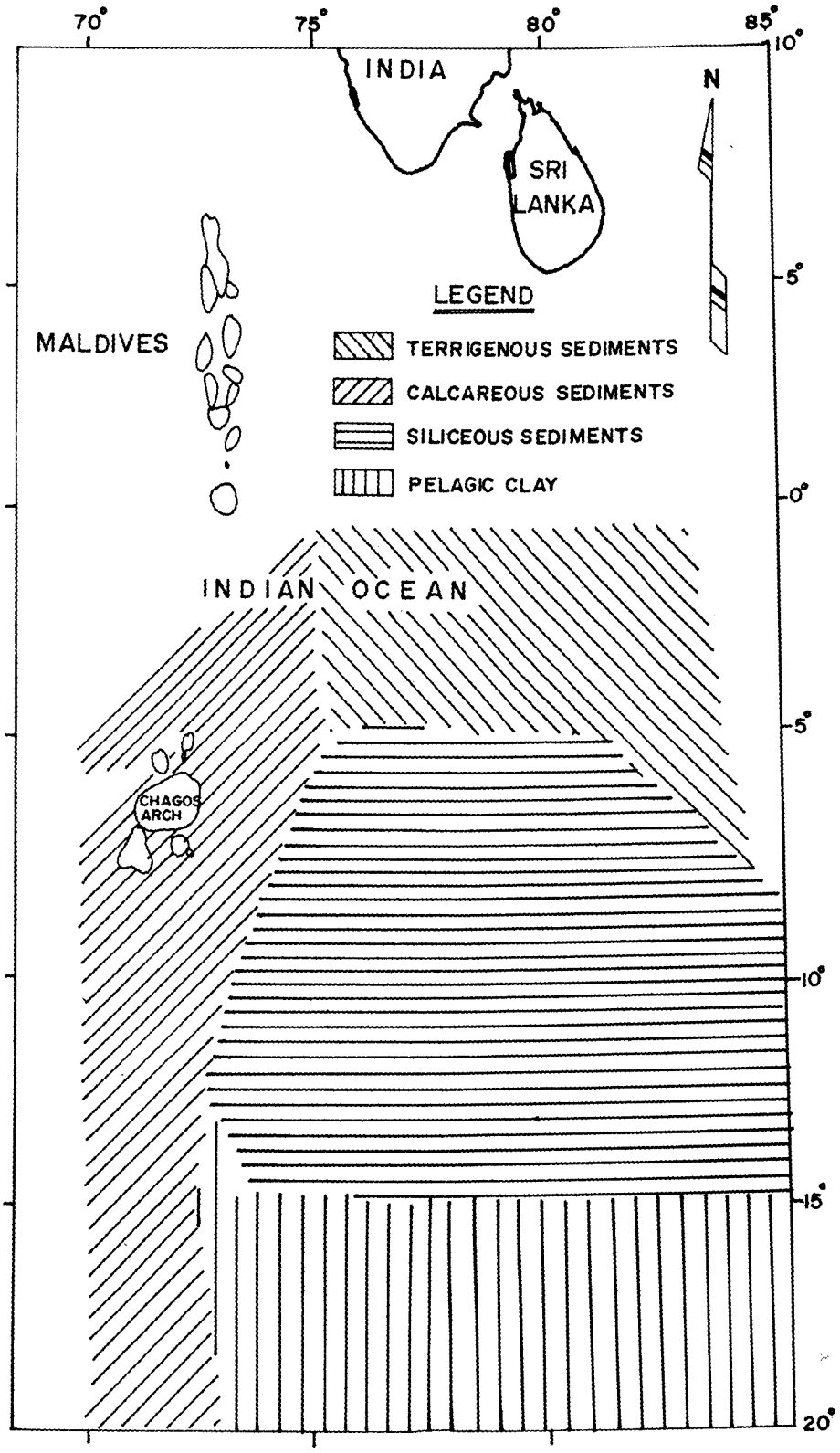

Fig. I.2 MAP SHOWING SEDIMENT TYPES IN THE CENTRAL INDIAN BASIN
(Rao & Nath, 1988)

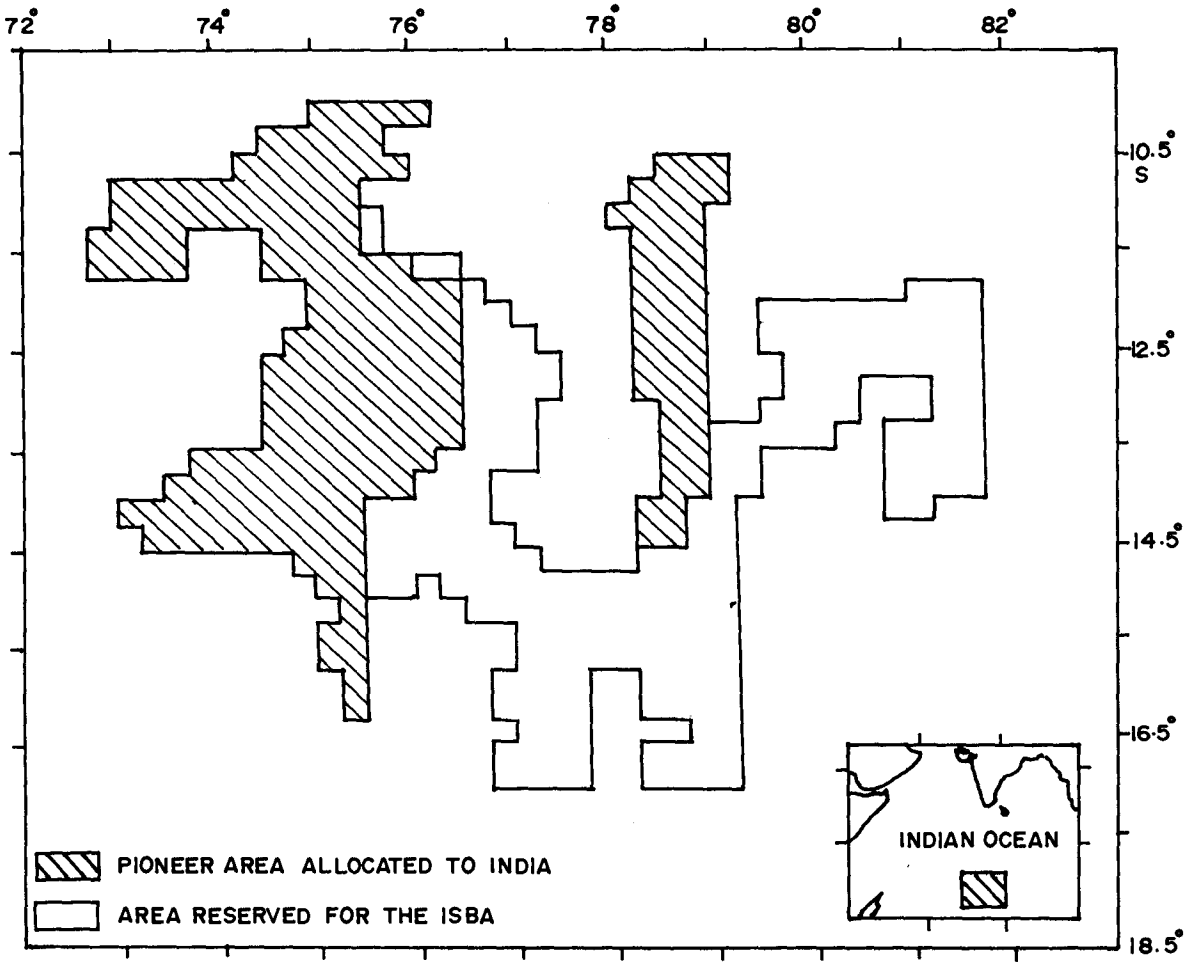

Fig. 1.3 THE INDIAN PIONEER AREA IN THE CIB. ISBA-INTERNATIONAL SEABED AUTHORITY.

CHAPTER 2

MATERIALS AND METHODS

To carry out the investigations, collection of undisturbed sediment cores was the basic necessity. The instruments used for sediment collection and methods followed for determination of various geotechnical parameters are described below.

2.1 Sediment cores

Two types of corers were used onboard ships to collect the sediment samples with the minimum possible disturbance.

a) Box corer (Okean Box Corer, Figure 2.2) of 50cm x 50cm x 50cm dimension was used onboard MV Yuzhmorgeologia with a wire rope and a winch. After the box core is onboard, two acrylic tubes of 6 cm diameter were inserted into sediments and removed. One was used to measure undrained shear strength immediately with the help of laboratory vane shear tester (AIMIL, New Delhi). The other tube was used to collect subsamples at different intervals to carry out tests in the shore laboratory. The subsamples were put in small polythene bags which were kept in a refrigerator at 4°C till various tests are carried out.

b) A 6 m gravity pipe corer (Figure 2.1) with 5 inch diameter and lead weights to facilitate sediment penetration was used to collect long cores. The PVC pipe of smaller ID was inserted in the tube before lowering the core sampler. The same pipe can be pulled out after core is onboard and can be cut for further processing. Subsampling is done at various intervals where notable variation in colour and lithology was observed. The subsamples were

put in the polythene bags and preserved at 4°C in the refrigerator. A gravity box core of 6 m length with 30cm x 30 cm was also used at one core location.

2.2 Parameters

2.2.1 Undrained Shear strength (SS)

It is a resistance of soil to deformation by continuos shear displacement of soil particles (ASTM, 1978). It is expressed in kilopascal (kPa). The test consists of inserting four-bladed vane in to the sediment, rotating the shaft connected to the blades, and measuring the torque required to shear the sediment (Winters, 1988).

Two equipments were utilized to measure the undrained shear strength.

a) Laboratory vane shear apparatus

b) Torvane shear apparatus

The undrained shear strength was measured with the Tovane shear apparatus (AIMIL, New Delhi) by rotating manually at a rotation rate of 90°/minute. This rate is recommended by Lee (1985), the USGS geotechnical laboratory and the ASTM (Winters, 1988) for fine grained sediments. The measurements were made on the plain surface by inserting vane blade perpendicular to the surface. This apparatus gives shear strength values directly.

Laboratory vane shear apparatus (AIMIL, New Delhi, Figure 2.3) was used in case of short cores at various depths depending upon the lithological change. This apparatus uses a spring of 4 cm kg torque capacity and gives the torque angle. A vane of 2.4 cm height and 1.2 cm diameter is used to measure angle of torque. The acrylic tube collected for this purpose is pushed from one side by plunger so that sample is filled in the stainless steel cup (7.5 x 3.8 cm). The vane of the apparatus is inserted in to the sample so

that the vane is about one vane height (2.4 cm) below the sediment surface. The centre of the vane should be at least 1.5 vane diameter away from the wall of the cup (Winters, 1988). Here the vane was rotated at the rate of 60°/minute (Noorany, 1985). The apparatus gives the angle of torque from which torque T can be calculated as,

T = angle of torque * spring factor/180 (cm kg)

In all the measurements spring factor of 4 cm kg was used.

Undrained shear strength (SS) can be calculated for vane blades of various dimensions using following formula (AIMIL manual; Winters, 1988)

$$SS = \frac{4T}{\pi (2D^2H + 0.667D^3)}$$

where SS = undrained shear strength (kg/cm^2)

D = diameter of the vane (cm)

H = height of the vane (cm)

T = torque (cm kg)

π = 3.142

The apparatus uses a vane of 1.2 cm diameter and 2.4 cm height. Therefore the final formula used for shear strength calculation is

SS = 0.343 * angle of torque (kPa)

(1 kPa = 9.8 gm/cm^2)

2.2.2 Natural water content (WC)

It is a natural moisture available in the pore spaces and grains of the sediments. To measure this, about 20 gm of sample was thoroughly mixed and kept in stainless steel cup for drying in the oven at 110°C for 24 hours and then weight loss was measured (ASTM, 1987, D-2216-80). For each

interval an average of two samples is considered. It is expressed in percent and given by the formula,

$$W = 100 * ((w1-w2)/w2) \qquad (\%\ \text{dry basis})$$

where w1 = wt. of sample before drying

w2 = wt. of sample after drying

Since the marine sediments have salt content, the water content is corrected for the salinity of deep-sea sediments at salinity of 35 ppt (0.035). Thus for correcting the water content following formula is used (Noorany, 1985). Error of 1 % is expected in the measurements.

$$WC = \frac{W}{[1-0.035(1+W)]} \qquad (\%)\ \text{dry basis}$$

2.2.3 Atterberg limits

Two index properties known as liquid and plastic limits were introduced by Atterberg (1911) to provide an empirical but quantitative measure of plasticity of sediments. They are also called as consistency limits. Their merits of classification purposes were emphasized by Terzaghi (1926) and modified by Casagrande (1932).

Liquid limit (LL) is a water content corresponding to the arbitrary limit between liquid and plastic states of sediments. For determining this, liquid limit apparatus (AIMIL, New Delhi) was used. The method is known as Casagrande drop cup method and is widely used. About 120 gm thoroughly mixed wet sample is filled in a brass cup as mentioned in ASTM (1987, D4318-84) and the groove is made at the centre of the cup. Then the cup is allowed to fall from 1 cm height by motorized mechanism till samples on both the sides of the groove join minimum 3 mm at the centre.

Plastic limit (PL) is the water content corresponding to the arbitrary limit between plastic and semisolid states of the sediment. Therefore, if water content is above liquid limit, the remolded sediments will behave like liquid; if it is below liquid limit but above plastic limit, then sample will exhibit plastic behavior.

The test is performed immediately after liquid limit test and provides lowest water content at which soil behaves plastically in remolded state. It is determined by first pressing a small portion of plastic soil together, rolling it into a 3 mm diameter thread which gradually removes the water, and repeating the process until the thread crumbles and can no longer be pressed and rerolled. The water content of this sample at this stage is called plastic limit. More details about the method are given in Winters (1988).

The Atterberg limits are very useful because they indicate the water content above which sediment behaves plastically. These limits are related to the amount of water that is attracted to the surface of the individual sediment particles. Non plastic behavior is typically exhibited by predominantly coarse grained material. Typically, the higher the clay mineral content of sediment, the greater will be the amount of absorbed water on the clay particles, hence, the higher the Atterberg limits (Winters, 1988).

Other sample parameters that can be estimated from these limits include plasticity index (PI) which is the difference between liquid limit and plastic limit i.e. (PI = LL-PL); and the liquidity index (LI) which relates to the in situ water content to the Atterberg limits and given as

LI = ((WC-PL)/PI).

The liquidity index is useful for estimating approximate stress history. The Plasticity Index is often plotted versus liquid limit on plasticity chart (Figure 2.4); the location of the data indicates what type of sediment is present and also the amount of compressibility that can be expected to follow engineering type loading (Peck etal, 1974).

2.2.4 Specific gravity (grain density, G)

It is a relative density or a ratio of density of sediments to density of water. Being a ratio, it does not have a unit and given by formula

G = wt. of solids / wt. of equal volume of water

For determining the specific gravity, sediments which are dried during water content determination are used after powdering them in agate mortar with pestle. Specific gravity bottles (25 ml capacity) were used to fill partially the powdered sample. The weights of empty bottle, bottle plus sample, bottle plus distilled water, and bottle plus sample plus water are taken from which G can be calculated from the following formula (ASTM, 1987, D854-83). As mentioned in Winters (1988), to remove the trapped air bubbles, bottles containing sample and distilled water were heated on hot plates for 2-3 minutes and allowed to cool to the ambient temperature before weighing.

$$G = \frac{(w2-w1)}{[(w4-w1)-(w3-w2)]}$$

where w1 = weight of empty bottle (gm)

w2 = weight of bottle + dry sample (gm)

w3 = weight of bottle + dry sample + distilled water (gm)

w4 = weight of bottle + distilled water (gm)

To reduce the error, average value of two measurements on each sample is considered.

2.2.5 Void ratio (e), Porosity (n), Wet bulk density (wbd)

These three parameters are estimated from the measured water content (WC) and specific gravity (G) of sediments (Bennett and Lambert, 1971) assuming full saturation of the sediments. Void ratio is a ratio of volume of void to volume of solids and is given as

$$e = WC * G$$

This ratio can be more than 1 which indicates volume of voids can be more than volume of solids in highly porous sediments.

Porosity (n) is a ratio of volume of voids to the total volume of solids, and is expressed in percent. However, it never exceeds 100 %. It can be calculated by formula

$$n = \frac{100 * e}{(1+e)} \quad (\%)$$

where, e = void ratio

Wet bulk density (wbd) is weight of solids per unit volume of water and calculated from the following formula

$$wbd = [(G+e)/(1+e)] * \sqrt{}_w \quad (g/cm^3)$$

where $\sqrt{}_w$ = density of the sea water = 1.028 g/cm^3

G = specific gravity,

e = void ratio

2.2.6 Grain Size Analysis

Marine sediments are composed of grains of various minerals, size and shape. Grains sizes of fine grained sediments are usually determined by pipette method. The procedure is based on Stoke's law which states that in suspension the velocity of a spherical particle is governed by the diameter of the particle and the properties of the suspension. Though the method is based on assumption, it is popular and widely used by the sedimentologists. Folk (1968) and McManus (1988) have described the method in detail. The

sample was oven dried for 24 hours at 60°C and about 10 gm of sample is dissolved in distilled water for 5-6 hours. After 6 hours, 20 ml of sodium hexametaphosphate solution was added to it for complete disintegration and defloculation of clays. The lumps were disintegrated with fingers slowly. This solution was passed through a sieve of 240 mesh (63 μm) which separates coarse fraction from the silt and clay. Wet sieving was carried out with distilled water without loosing any grains. The coarse fraction (> 63 μm) was kept for drying in preweighted beaker which is used to calculate the sand size fraction. This includes biogenic component like radiolarian and foraminifera tests. The sieved material was transferred in to 1000 ml cylinder and was analyzed for silt and clay contents using standard pipette method of settling (Folk, 1968).

Oriented slides for x-ray diffraction studies were prepared by pipetting 200 ml solution. The acetic acid and hydrogen paroxide (5 ml each) were added to remove organic carbon and calcium carbonate respectively. After two washings with distilled water, the slurry was spread uniformly on the glass slide and kept for natural drying. For each sample two oriented slides were prepared. These slides after drying were used on x-ray diffractometer for clay mineral identification.

2.2.7 Clay Mineralogy

Clay mineralogy from the x-ray diffraction patterns of the oriented slides was studied following Biscaye (1965). Sample slides were run through the Philips x-ray diffractometer (Model PW 1840) using CuKα radiations at 40 mv. The 2θ range was 3-30° at the rate of 3° 2θ per minute for fast scan and 0.6° 2θ per minute for slow scan from 3-15°. The clay minerals identified are common in the deep–sea sediments of the Indian Ocean. The montmorillonite, illite, kaolinite and chlorite are identified at d spacing of 14Å

(6.3° 2θ), 10Å (8.8° 2θ) and 7Å (12.4° 2θ) respectively. The kaolinite and chlorite could not be separated as zeolites are present in the sediments. The reflections of phillipsite and clinoptilolite interfere with combined reflections of kaolinite and chlorite at 7.0Å and 3.54Å respectively. Palygorskite encountered in few samples shows weak reflection at 10.4Å (8.4° 2θ). Other minerals include quartz and feldspar, the peaks of which are well developed at 26.8° and 28.1° 2θ respectively. For semiquntitative analysis of clays, the oriented slides were heated for 1 hour at 100°C in a dessicator containing ehthylene glycol, and then immediately run on x-ray diffractometer with slow scan with same instrumental settings. The areas below the glycolated peaks of three clays were taken as weightages for percent calculations using weighting factor of 1 for montmorillonite peak (17Å), 4 times for illite peak (10Å), two times for the kaolinite/chlorite peak (7Å) following Biscaye (1965) with assumption that these constitute 100 percent of the mineralogy of the sample in <2 μm fraction. Being a semiquantitative method, the mineral percentages are within an error of ± 5 %.

2.2.8 Activity of clays (A_c)

The activity of the sediment is the ratio of the plasticity index (PI) to percentage of the clay size fraction. Activity is a rough indication of the sediment's geological history, its clay mineralogy, and the degree of surface activity of the clay fraction with decreasing grain size (Kravitz, 1970). As the particle size decreases, the surface area of particle and the amount of water attracted to the soil surface increases. Based on activity values, Skempton (1953) proposed three varieties of clays. i.e. Inactive clays (activity, 0.0 - 0.75) normal clays (activity, 0.75 - 1.25), and active clays (activity >1.25). Figure 2.5 depicts the activity classification. Some workers have modified this classification subsequently in to five categories of clays.

2.2.9 Consolidation characteristics

Consolidation may be defined as a result of all processes causing the progressive transformation of the argillaceous sediment from a soft mud to clay and finally to mudstone or shale. These include inter-particle bonding, desiccation, cementation and above all, squeezing out of the pore water under increasing weight of overburden (Skempton, 1970). The consolidation and compaction are considered as synonymous terms. The consolidation study is generally conducted with oedometric tests. This requires exclusive sediments cores of specific diameter. Therefore in present study it could not be conducted. Nevertheless, consolidation state can be estimated from the formula (Skempton, 1970) using values of shear strength and plasticity index measurements. This method is rough but in absence of oedometer test data it can give some idea of consolidation characteristics of sediments. The formula is based on empirical relationships for predicting the shear strength /effective overburden stress ratio for normally consolidated marine sediments and given as follows:

Undrained shear strength/Effective overburden stress=0.11+0.0037*PI

where PI= plasticity index

This is plotted against the depth of shear strength measurement. The threshold value is 0.22 above which sediments are considered to be normally consolidated to overconsolidated, and below 0.22 they are assumed to be underconsolidated (Skempton, 1970).

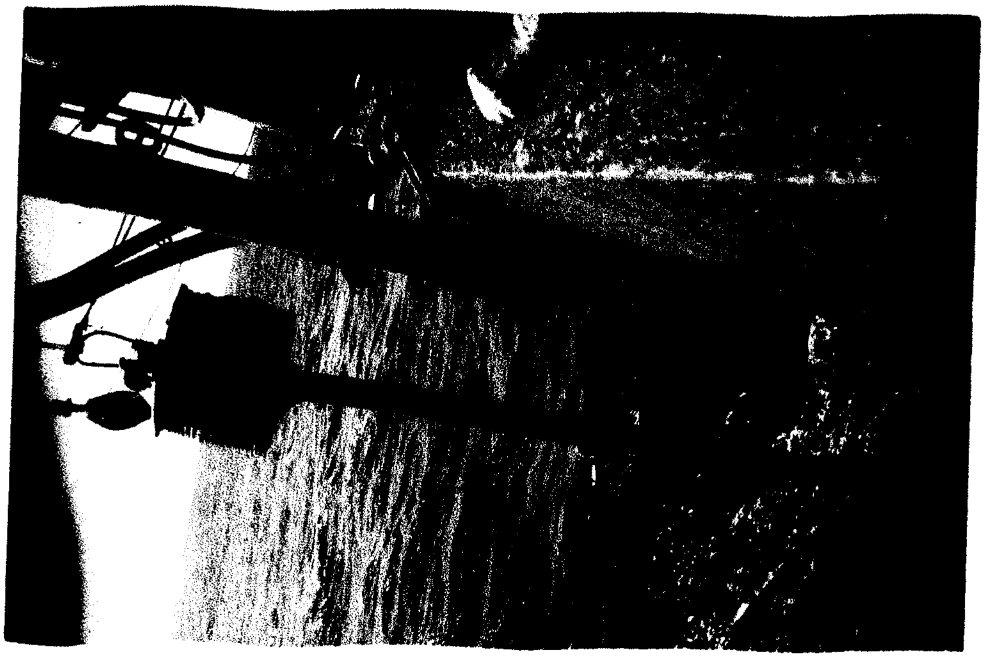

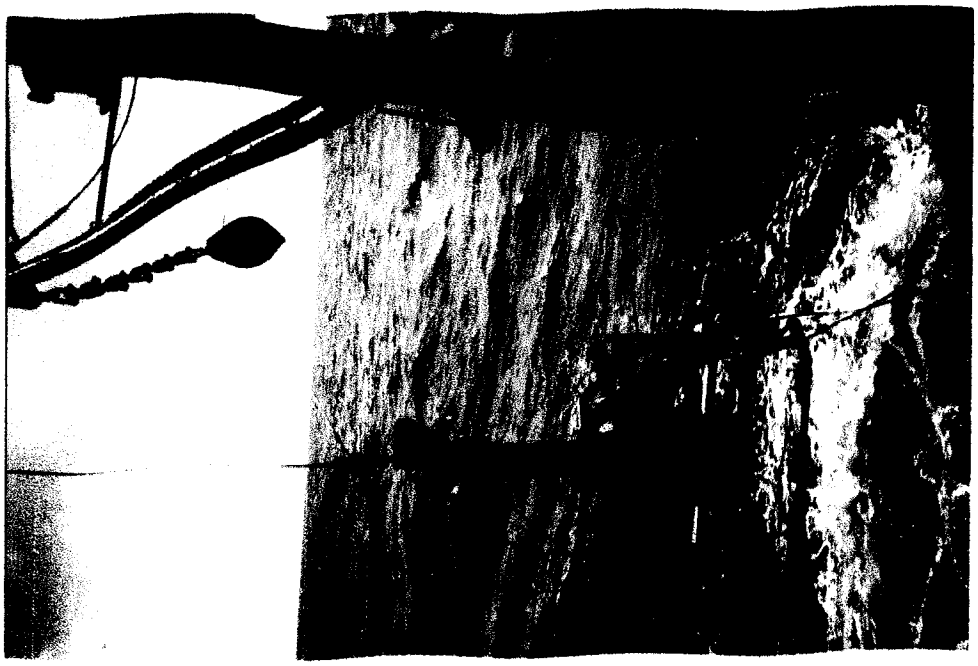

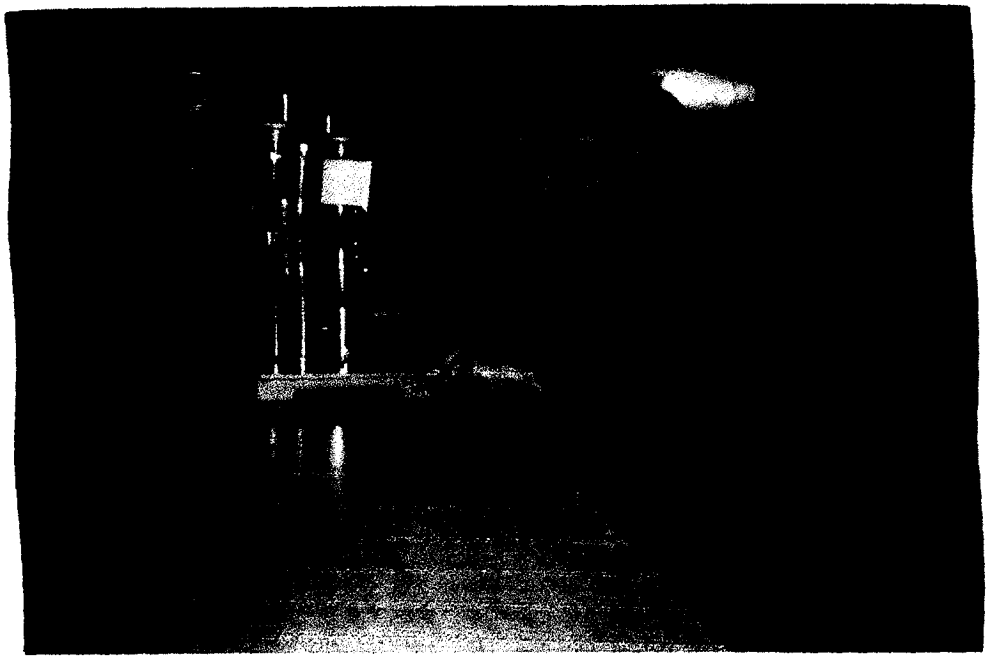

Figure 2.3: Laboratory vane shear tester used for the shear strength measurements of sediments

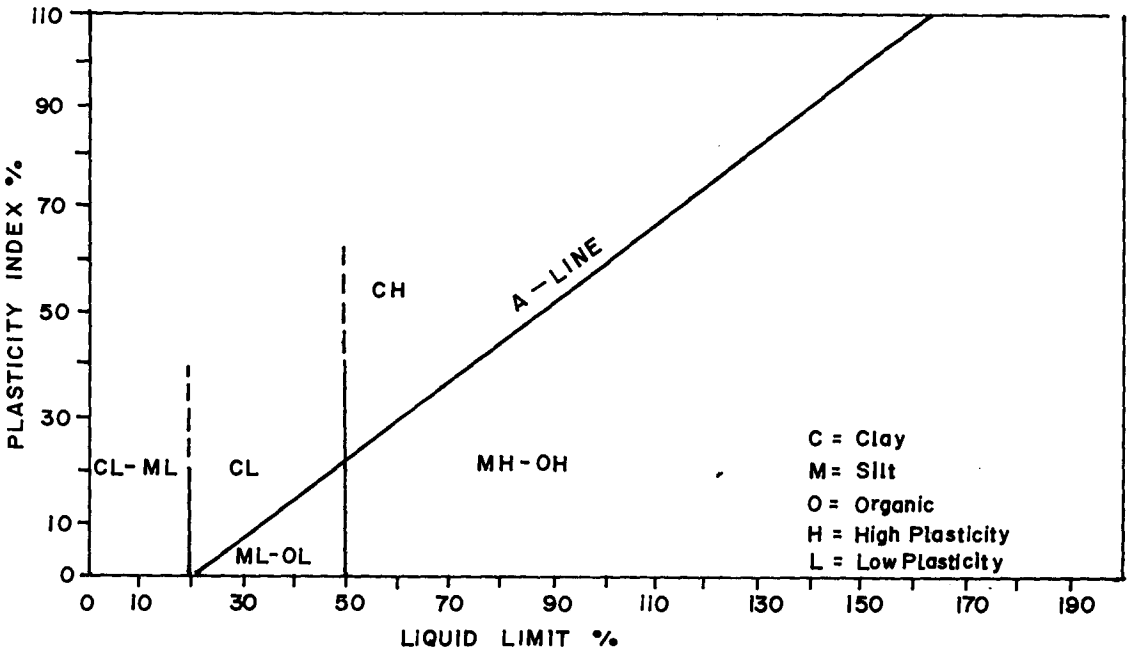

Fig. 2.4 PLASTICITY CHART (Lambe & Whitman, 1969)

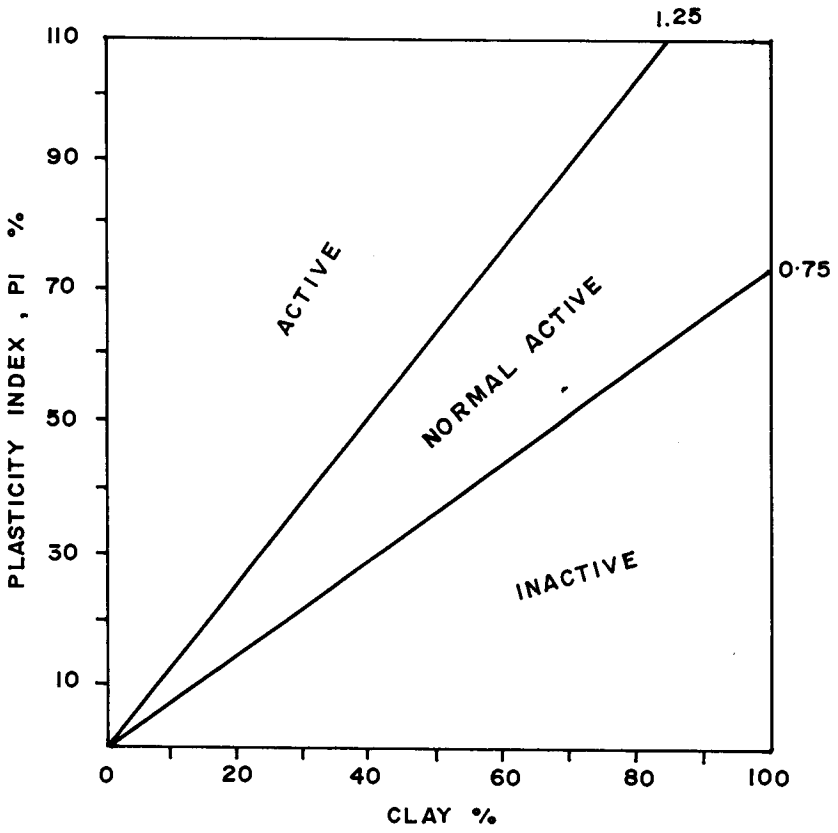

Fig. 2.5 ACTIVITY CHART (Skempton, 1953)

CHAPTER 3

CORE LOCATIONS AND DESCRIPTION

The Indian Ocean is known to have low depositional rates of 2-2.5 mm/ky (Banakar etal., 1991) despite influence of terrigenous material from the north. Such deposition could give almost homogenous sediments for long core depths. Eight cores were collected to determine geotechnical characteristics of deep-sea sediments. Seven cores represent siliceous composition and one shows calcareous composition. A core from pelagic sediment area was attempted but there was no recovery. The lithological and colour descriptions of sediment were noted down after each core is onboard using Munsell colour chart. While subsampling, structures representing bioturbated layers, thin intercalations were observed. Such bioturbated surface was noted down to decipher any change in properties especially shear strength and water content. In some cores buried nodules were encountered at deeper depths (75 cm, core A4/6; 510 cm core A4/5a). The core locations and other details are given in Figure 3.1 and Table 3.1.

3.1 Long cores

Core A4/1

This is 520 cm in length, siliceous ooze/clay in composition and collected from the uneven topographic area from a water depth of 5155 m. It showed homogenous sediment nature with very little colour variation. Dominant colour is dark brown (10YR). At 0-65 cm and 233-253 cm it is

grayish orange (10YR7/4). At 65-76 cm, 258-278 cm sediments are very pale orange (10YR8/2). At 76-88 cm, 315-329 cm, and 349-361 cm sediments are pale yellowish orange (10YR8/6). At 88-104 cm, 163-196 cm, 211-219cm, 329-349cm and 500-520 cm sediments are dark yellowish brown (10YR4/2). At 104-163 cm and 196-211 cm it shows moderate orange pink sediments (5YR8/4). At 219-233, 253-258 and 361-370 cm it is pale yellowish brown (10YR6/2).

Core GC-1

This siliceous core is recovered from the plain area of the CIB from a water depth of 5260 m. The top 55 cm shows moderate yellowish orange (10YR 5/4) with intercalations at 21-22 cm. The layer at 55-80 cm is moderate brown (3YR5/4) followed by mixed zone of moderate brown and grayish orange between 80-90 cm. The layer at 90-140 cm is grayish orange with light olive gray intercalations at 115 cm. Between 140-150 cm layer is dark yellowish orange (10YR 6/6); at 150-165 is dusky brown (5YR2/2) with intercalations of 5 cm. The layer at 165-175 represent mixed zone of dark yellowish orange and dusky brown color sediments. This is underlain by (175-210 cm) dark yellowish orange unit. The sediments at 210-225 show darker shade of dark yellowish brown color (10YR4/2). At 225-265 cm dark yellowish orange (10YR6/6) sediments are present. This is followed by 10YR 5/4 with intercalations at 263-268 cm of grayish to dark brown. At 305-330 dark yellowish orange (10YR6/6) followed by moderate yellowish brown (10YR5/4) up to 375 cm. Between 375-390 cm dark yellowish brown color observed. At 390-420 cm mottling of dark yellowish orange (10YR6/6) is seen. From 420 to 470 cm moderate yellowish brown (10YR5/4) sediments with bioturbated and mottled surface are observed. At 475 - 480 cm dusky yellowish brown sediments are present. Below this up to 510 cm sediments are dark yellowish orange color are seen. No nodule is encountered at any depth of the core.

Core A4/2

Core is siliceous in composition and collected from the uneven topographic area from the water depth of 5205 m. It was 565 cm in length and mostly bottom is homogenous in colour. Top 0-24 cm is moderate yellowish brown (10YR5/4) followed by grayish orange pink (5YR7/2) up to 33cm. At 33-63 cm colour 10YR5/4 is repeated. From 63-75 cm it shows 10YR7/4 (grayish orange). From 75-140 cm is homogenous with yellowish brown (10YR5/4). The layer at 140-170 cm is grayish orange. After this depth till 565 cm sediments are moderate yellowish brown with uniform nature. At 295 cm one nodule of 3 cm diameter was collected.

Core A4/5a

This is 552 cm in length, siliceous and collected from comparatively plain areas of the Central Indian Basin from a water depth of 5235 m. It has alternate units of moderate yellowish brown (10YR5/4) and grayish orange (10YR7/4) upto 447 cm. Below this (447-501 cm) sediments are yellowish orange (10YR5/4) with intercalations of 10YR7/4 (grayish orange). Between 501 cm and 549 cm the layer of light brown sediment is observed (5YR5/6). The intense bioturbation was observed at 450 cm. Moreover, small nodules were encountered at two depths (525 cm and 545 cm) of this core.

Core A4/6

This core is collected from uneven topographic area of the CIB (water depth 5180 m) away from earlier cores. It is siliceous in composition and its recovery was 580 cm. This core exhibits alternate units of 10YR5/4 and 10YR7/4 with intercalations into each other at three depths i.e. 50-110 cm, 122-155 cm and 285-297 cm. From 285 cm downwards up to 582 cm

sediments are somewhat sticky in nature indicative of consolidation. The core shows intense boiturbation at 40 cm, 115 cm, 200 cm and at 460 cm where lens like structures are seen. A nodule of 2 cm diameter was collected at 85-90 cm depth.

Core A4/12

This, comparatively shorter (350 cm) core is obtained from a water depth of 5070 m in the area of more topographic variations. Top unitsof 0-40 cm and at 185-205 cm are grayish orange (10YR7/4). Sediments at 40-75 cm and at 92-108 cm depths are moderate yellowish brown (10YR5/4). The layer at 75-92 cm is dark yellowish orange with intercalations of 10YR7/4. Thin unit at 108-118 cm is pale yellowish orange with intercalations of 10YR5/4. At 118-138 cm sediments are moderate brown (5YR4/4) and show colour difference from the other part of the core. The core is bioturbated at 85 cm and 210 cm depth.

Core A4/13

This is calcareous in composition and collected from the deep parts of Chagos Trench area. The water depth is 5800 m and core recovery was 352 cm. The sediments are fully homogenous with yellowish gray color (5Y8/1). The top 0-5 cm shows radiolarian ooze and sediments of grayish orange (10YR7/4) colour. The penetration of the gravity core in this case is less, most likely due to, cementation or overconsolidated nature of sediments as seen from the high strength values. The core does not show any bioturbation or nodule presence at any depth. It does not show slumping or mixing of the sediments.

Core SK69/2

The core is collected at 8° 59'S and 77°E using gravity box core (30cm x 30cm size) from a water depth of 5400 m and showed highest recovery (7.5 m). However, the top 2.3 m was disturbed and hence could not be used for any interpretation. The sediments of top unit (230-345cm) are alternate bands of light brown and dark brown clays. At 345-405 cm they are dark brown with light brown colour lens like structures indicative of bioturbation. At 405-420 cm fine laminations of light and dark brown colour are observed. Below this at 420-450 cm, dark gray/brownish colour layer has very sticky sediments with sharp contact with underlying light brown colour sediments. This layer does not show any bioturbation. Similar layers are encountered at 470-490 cm and 560-580 cm. Below 580 cm again alternate light and dark brown coloured sediments with intense bioturbation and mottled appearance are observed. Among all the cores this core is unique in the sense that it clearly shows Plio-Pleistocene sediment boundary based on biostratigraphic data analysis (Gupta SM, 1996) which is represented by the change in the sediment type and the environment of deposition. In addition, the layers of similar characteristics within the core indicate cyclic process of deposition in the geological past.

3.2 Short cores

These cores were collected using box core for the environmental impact assessment studies during pre- and post-disturbance cruises. These cores represent surface sediments from a very small area around the strip of disturbance. Since the cores are from a small area, their lithology does not vary with depth. In general, all the cores have dark brown (5YR3/4) homogeneously distributed sediments in top 10 cm overlying light yellowish

brown clays (10YR5/4) with gray, green and dark brown mottling, intercalation and features of bioturbation.

In core 1 (30 cm length), top 5 cm was dark brown and remaining 25 cm is light and dark brown with gray intercalations.

In core 2 (32 cm length), the top (0-17 cm) showed dark brown (5YR3/4) followed by gray colour intercalations (10YR6/2, 17-22 cm) and light brown (10YR5/4) with gray intercalations. Two nodules are collected in this core.

Core 3 (32 cm) showed dark brown colour upto 13 cm and moderate yellowish brown (10YR3/4) between 13-32 cm. Mottled and bioturbated lighter sediments with intercalations of grayish color are in the lower portion.

Core 4 (27 cm) shows 0-15 dark brown, 15-21 moderate yellowish brown, and 21-27 cm moderate yellowish brown sediments with green-grayish intercalations.

Core 5 (33 cm) shows 0-23 cm as dark brown and below it upto 33 cm as moderate yellowish brown sediments with grayish intercalations.

Core 6 (30 cm) has four zones. 0-11 dark brown, 11-15 light brown with lens like structures, 15-25 mixed layer of dark and light brown, and 25-30 cm light brown with mottling of gray color.

Core 7 (32 cm) 0-13 cm is dark brown, 13-19 cm is dark and light brown, 19-32 cm is light brown with many intercalations, lens, mottling of gray colour sediments.

Core 8 (31 cm) 0-14 is uniform dark brown and 14-31 cm is light brown with intercalation of green colour and mottling.

Core 11 (28 cm) has 0-13 cm of dark brown homogenous color and 13-28 cm with light brown and intercalations of dark brown and grayish colour. Buried nodules are collected from this core.

Core 12 (32 cm) shows 0-12 cm dark brown and homogenous sediments, 12-17 light brown with intercalations of dark brown sediments. At 17-33 cm light brown sediments with intercalations of gray colour are present.

Core 13 (35 cm) has 0-28 cm uniform and longest layer of homogenous dark brown; unit at 28-35 cm is light broom with gray intercalations.

Core 14 (27 cm) exhibits 0-12 dark brown sediments; and 12-27 cm as light brown layer with gray intercalations.

Core 15 (31 cm) has 0-13 cm as dark brown sediments; and 13-18 cm lenses of dark and light brown sediments, 18-31 cm is light brown unit with grayish intercalations.

Core 16 (30 cm) shows 0-10 cm as uniform dark brown layer, 10-14 cm light brown sediments, and 14-30 cm as light brown unit with grayish intercalation.

Table 3.1: Details of the sediment cores investigated in the present study

Core	Latitude S	Longitude E	Water depth (m)	Recovery (cm)	Sediment type
A4/1	11° 15.661	75° 00.706	5155	520	siliceous
A4/2	12° 00.105	75° 29.967	5205	555	siliceous
A4/5a	12° 30.500	76° 30.900	5235	552	siliceous
A4/6	12° 37	78° 29	5180	580	siliceous
A4/12	12° 30	74° 30	5070	350	siliceous
A4/13	11° 07.5	72° 30	5800	352	calcareous
SK69/2	8° 59	77° 00	5400	750	siliceous
GC-1	10° 00.218	75° 19.851	5260	510	siliceous

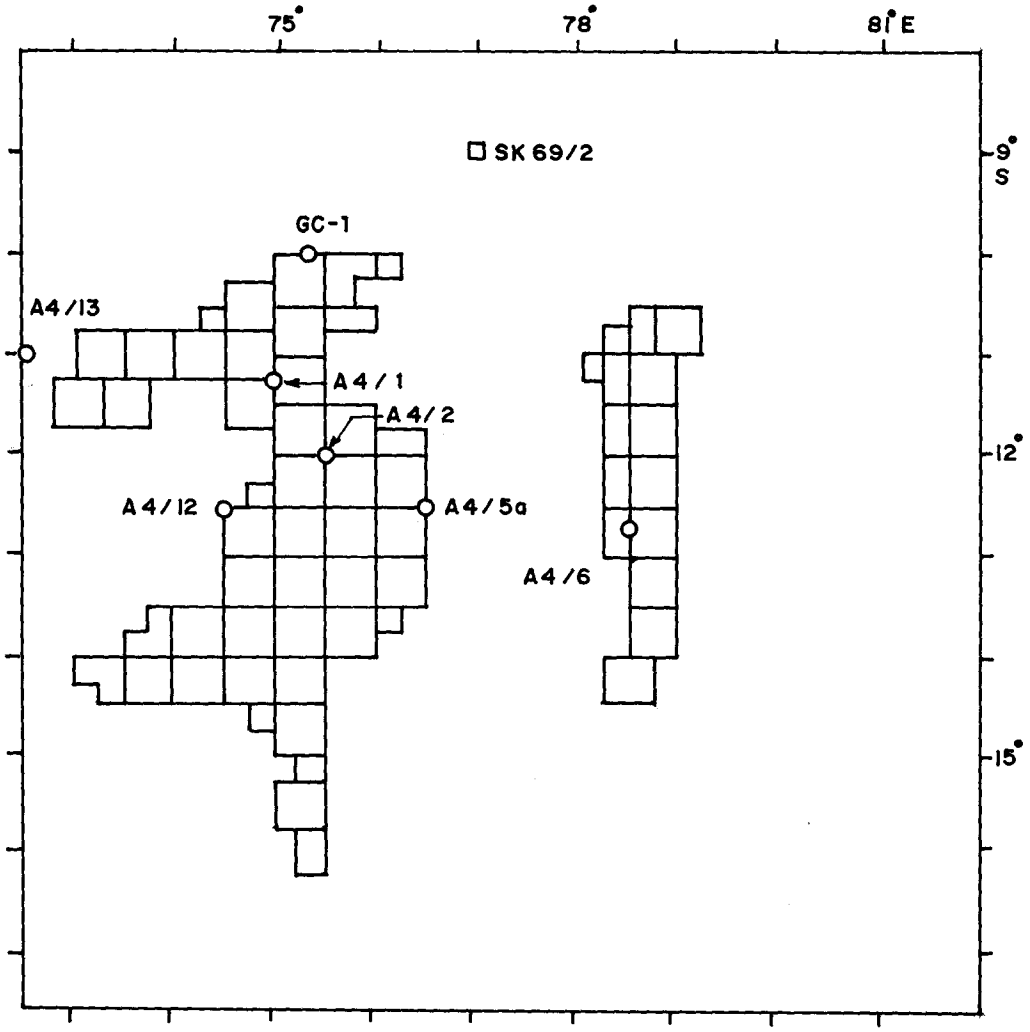

Fig. 3.1 CORE LOCATIONS IN THE CENTRAL INDIAN BASIN.

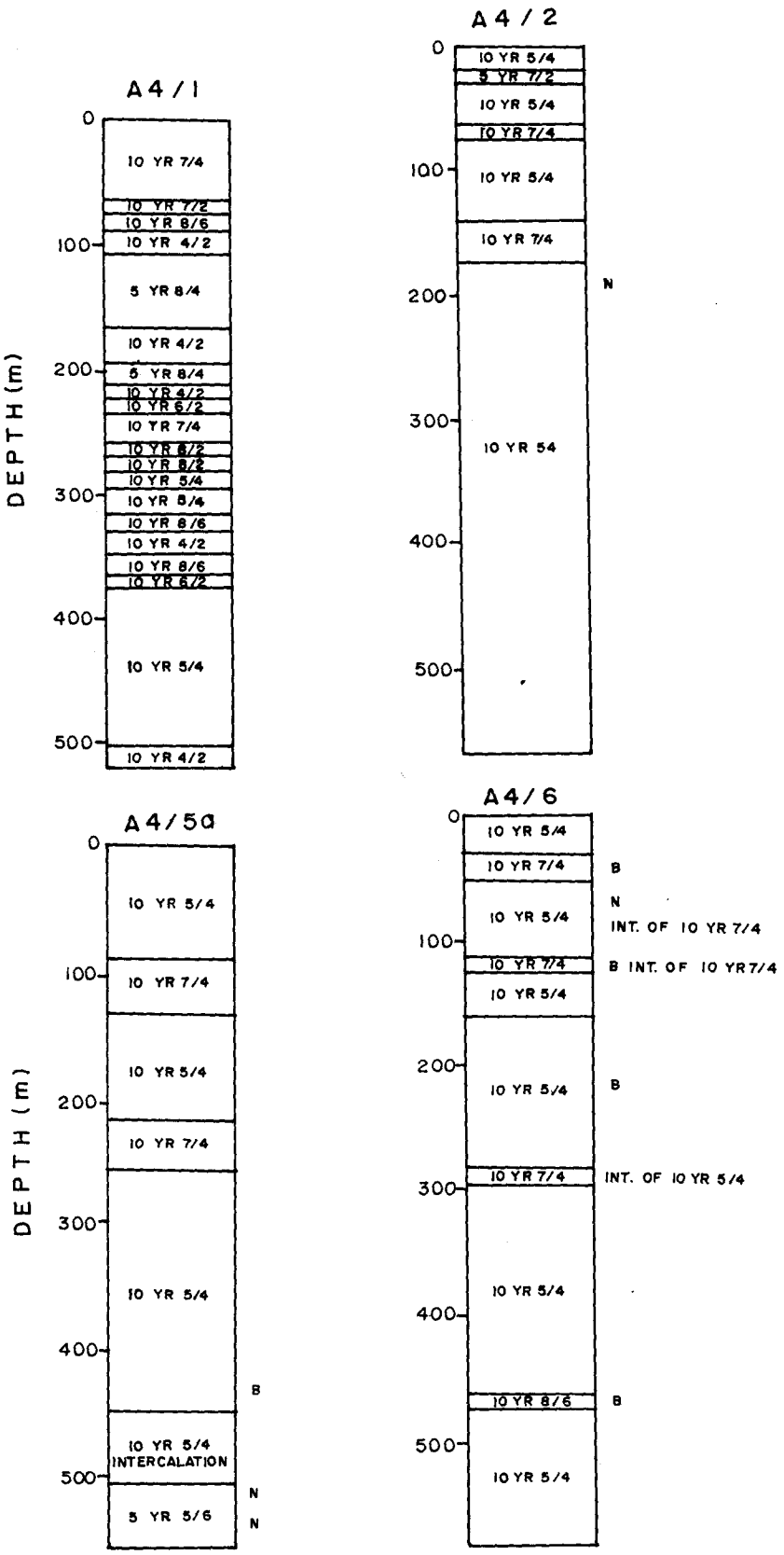

Fig.3.2 LITHOLOGS OF THE SEDIMENT CORES FROM THE CIB

N= NODULE , B = BIOTURBATION , INT = INTERCALATION

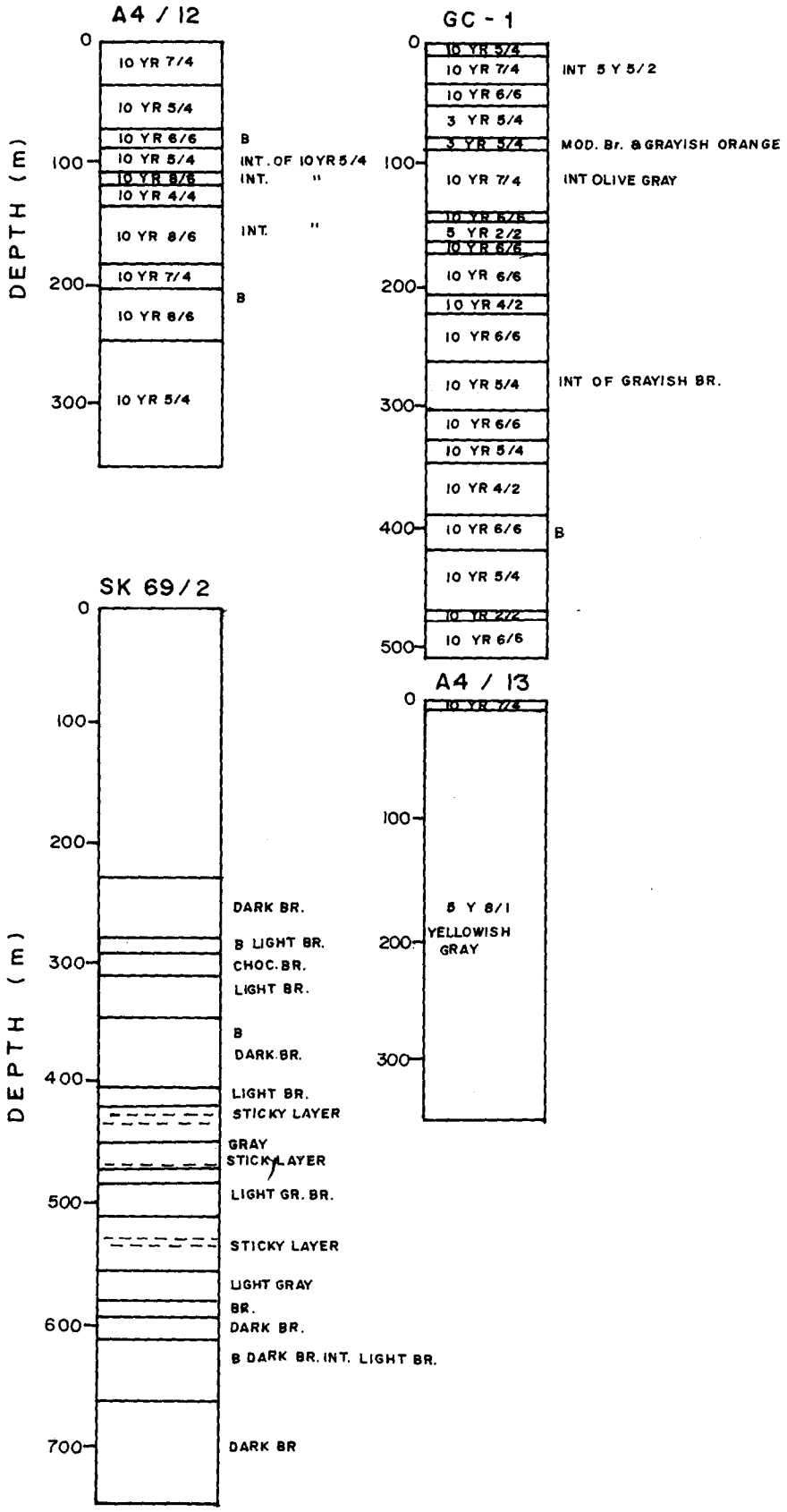

Fig.3.3 LITHOLOGS OF THE SEDIMENT CORES FROM THE CENTRAL INDIAN BASIN

N= NODULE, B = BIOTURBATION, INT = INTERCALATION

CHAPTER 4

RESULTS

The studied core samples comprise of siliceous and calcareous sediment from different locations in the Central Indian Basin. About 171 subsamples from siliceous and calcareous sediment cores were analyzed for measurement of natural water content, specific gravity, consistency limits, undrained shear strength, grain size analysis and clay mineral composition. From this parameters void ratio, wet bulk density and porosity were calculated using formulae (Bennett and Lambert, 1971). Figure 3.1 gives the core locations of long cores from the Central Indian Basin. Table 3.1 gives the core locations, water depth, core recovery and sediment type encountered. The lithological descriptions of sediment cores are given in Figures 3.2 and 3.3.

The data on minimum, maximum, average and standard deviation of all estimated and measured properties are tabulated for each core in the Tables 4.1 to 4.8. Cores A4/1, A4/2, A4/5a (Table 4.1, 4.2 and 4.3) indicate the dominance of silt over clay contents. Table 4.4 which represents data of core A4/6, indicates low activity of clay (1.29); and high clay content (62 %) than silt (28 %) and coarse fraction (8 %) percent. The cores A4/12, A4/13, SK69/2 and GC-1 (Table 4.5, 4.6, 4.7 and 4.8) also show higher silt abundance than clay and sand size fraction. Montmorillonite and illite abundance in cores A4/1, A4/12 and GC-1 are same. In other cores illite dominates other clay minerals. Only in core SK69/2 montmorillonite is more than the illite despite higher silt content than clays. In all cores sand size fraction is present in small amount (less than 15 %).

The downcore variations in measured and estimated properties of all the studied cores are depicted in Figures 5.1 to 5.16. Figures 5.17 and 18

depict the x-ray diffraction peaks of clay minerals namely montmorillonite, illite and kaolinite after glycol treatment encountered in siliceous core SK69/2. All the siliceous cores range from silty clay to clayey silts in composition with less sand size fraction and variable degree of bioturbation. On the contrary calcareous core is almost uniform and composed mostly of ooze. The range and average values of all parameters of siliceous and calcareous sediments are summarized in Table 5.1. Table 5.2 and 5.3 give correlation coefficients on various parameters of siliceous (Cores A4/1, A4/2, A4/5a, A4/6, A4/12, GC-1, SK69/2) and calcareous (A4/13) sediments respectively. Table 5.4 gives geotechnical properties of various sediment types from Pacific Ocean published by various researchers.

Activity chart (Figure 5.19 to 5.26) is prepared by plotting plasticity index against the clay percent. The lines in the graph show three fields marked for inactive (IN), normal active (NA) and active (A) type of clays based upon activity values. Most of the siliceous and calcareous sediments fall in the zones of normal active to active field.

The plasticity chart known as the Casagrandes plasticity chart is prepared by plotting plasticity index versus liquid limit for each core (Figure 5.19 to 5.26). The A-line separates the fields of various type of clays and silts in the four categories namely organic clays of low to medium plasticity, organic clays of high plasticity, Inorganic clays/silts of low to medium plasticity and inorganic clays/silts of high plasticity. This graph implies whether sediments belong to one or variable regime of sedimentation. The activity and plasticity charts show less scatter in the points for siliceous cores. The relationships among properties measured on siliceous sediments such as water content, shear strength, clay mineralogy and grain size are shown through scatter diagrams (Figures 5.27 to 5.29) showing interdependencies of the parameters.

Figure 6.1 and Table 6.1 give locations of the short cores collected from the small area at 10°S and 76°E before and after the simulated disturbance. Accuracy of the core locations before and after disturbance was ±25 m. Figure 6.2 depicts the photograph of the disturber that was used for disturbing the top sediment layer in the CIB. Figure 6.3 shows the thickness of the four sediment layers (a, b, c, d) encountered during subbottom surveys in the disturbance area. The effect of disturbance on natural water content and undrained shear strength measured on sediment cores is shown in Figures 6.4 to 6.7 by stationwise plotting the values of water content and shear strength of sediments before and after the simulated disturbance. Figure 6.8 shows the scatter diagrams of water content and shear strength before and after the simulated disturbance.

Table 4.1: Summary of geotechnical properties measured on core A4/1

	Minimum	Maximum	Average	Std. Dev.
WC %	362	489	427	35
LL %	112	159	132	10.08
PL %	58	81	70	5.35
PI %	49	87	63.5	8.76
LI	3.3	7.47	5.79	1.02
G	1.99	2.17	2.04	0.05
e	7.40	10	8.73	0.79
n %	88.05	91.4	89.7	0.86
wbd g/cm^3	1.12	1.16	1.14	0.01
sand %	4.00	26	14.07	4.63
silt %	43.00	62	54.00	4.79
clay %	17.00	49	28.83	8.12
M %	23	43	34.13	4.76
I %	27	46	35.77	5.12
K+C %	24	38	29.77	3.03
A_c	1.18	3.78	2.32	0.70
SS kPa	0.82	6.73	3.57	1.64

Note : WC = water content, LL = liquid limit, PL = plastic limit, PI = plasticity index, LI = liquidity index, G = specific gravity, e = void ratio, n = porosity, wbd = wet bulk density, sand = sand size fraction, M = montmorillonite, I = illite, K = kaolinite, C = chlorite, SS = shear strength, A_C = activity

Table 4.2: Summary of geotechnical properties measured on core A4/2

	Minimum	Maximum	Average	Std. Dev.
WC %	394	520	444	37.84
LL %	144	212	174	22.07
PL %	85	131	106	9.92
PI %	36	104	68.4	17.86
LI	2.98	10.6	5.32	1.63
G	2.19	2.42	2.28	0.06
e	9.1	11.7	10.1	0.82
n %	90.1	92.13	90.95	0.66
wbd g/cm^3	1.13	1.16	1.15	0.01
sand %	1.30	12	8.92	2.33
silt %	47.00	63.3	54.46	408
clay %	29.40	42	36.32	3.5
M %	8.2	30	19.05	5.31
I %	36	64	46.2	6.23
K+C %	25	43	34.96	5.30
A_c	1.17	3.02	~~0.36~~ 1.90	0.~~70~~52
SS kPa	0.82	8.98	4.53	1.16

Table 4.3: Summary of geotechnical properties measured on core A4/5a

	Minimum	Maximum	Average	Std. Dev.
WC %	374	460	414	25.49
LL %	159	238	187	22.62
PL %	92	127	108	7.84
PI %	53	121	78.2	19.34
LI	2.4	6.3	4.18	1.17
G	2.18	2.29	2.24	0.03
e	8.31	10.3	9.26	0.54
n %	89.30	91.1	90.22	0.51
wbd g/cm^3	1.14	1.16	1.15	0.01
sand %	5.4	11.0	8.47	1.38
silt %	50	64	57.52	3.62
clay %	28	40	34.04	2.95
M %	14	34	24.13	5.16
I %	34	64	43.35	6.18
K+C %	23	43.75	32.52	4.94
A_c	1.44	3.9	2.33	0.68
SS kPa	1.63	5.71	3.94	1.37

Table 4.4: Summary of geotechnical properties measured on core A4/6

	Minimum	Maximum	Average	Std. Dev.
WC %	337	451	397	32
LL %	141	248	175	31
PL %	69	124	95	12.38
PI %	53	129	81	22
LI	1.91	5.38	3.94	0.97
G	2.14	2.53	2.33	0.08
e	8.08	10.2	9.23	0.66
n %	89	91.1	90.18	0.65
wbd g/cm^3	1.1	1.2	1.18	0.04
sand %	2.0	14.0	8.82	3.13
silt %	16	35	28.77	5.32
clay %	51	82	62.14	8.04
M %	11.8	45.2	24.49	8.69
I %	25.7	53.7	41.66	6.21
K+C %	25	45	33.82	4.72
A_c	0.93	1.85	1.29	0.23
SS kPa	1.22	6.53	3.84	1.32

Table 4.5: Summary of geotechnical properties measured on core A4/12

	Minimum	Maximum	Average	Std. Dev.
WC %	429	574	490	46
LL %	144	225	194	21
PL %	96	132	115	9.29
PI %	48	112	79.2	18.23
LI	3	9	5.29	1.75
G	2.14	2.31	2.23	0.04
e	9.5	13.3	10.93	1.06
n %	90.5	93	91.55	0.73
wbd g/cm^3	1.12	1.15	1.14	0.01
sand %	5.7	10.9	7.96	1.56
silt %	48	59	53.79	3.75
clay %	34	44	38.21	3.26
M %	26	40	35	4.07
I %	23	42	33.6	5.15
K+C %	26	37	31.5	2.99
A_c	1.14	3.2	2.1	0.56
SS kPa	0.00	3.88	1.30	1.07

Table 4.6: Summary of geotechnical properties measured on core A4/13

	Minimum	Maximum	Average	Std. Dev.
WC %	192	214	201	6.89
LL %	114	160	144	11.46
PL %	50	79	67.6	8.28
PI %	64	92	76.5	8.45
LI	1.38	2.56	1.76	0.29
G	2.31	2.36	2.33	0.01
e	4.45	5.01	4.69	0.17
n %	81.7	83.4	82.4	0.52
wbd g/cm^3	1.26	1.28	1.27	0.01
sand %	3.10	23.9	7.32	4.82
silt %	45	65	60	4.61
clay %	27.1	35.2	32.26	2.23
M %	42	48	45.36	2.26
I %	28	35	32.07	2.22
K+C %	19	27	22.51	2.05
A_c	2.06	2.71	2.4	0.18
SS kPa	3.26	13.9	8.9	3.06
CaCO3 %	58.8	64.8	61.71	1.54

Table 4.7: Summary of geotechnical properties measured on core SK69/2

	Minimum	Maximum	Average	Std. Dev.
WC %	92	363	312	67
LL %	94	260	207	41
PL %	47	131	109	23
PI %	47	143	99	24
LI	0.96	3.01	2.08	0.56
G	1.9	2.6	2.23	0.17
e	2.39	8.26	6.84	1.35
n %	70.5	89.2	86.5	4.31
wbd g/cm^3	1.15	1.51	1.2	0.08
sand %	0.9	16	8.77	4.22
silt %	56.1	84.4	67.42	7.92
clay %	13.5	41.4	23.78	6.6
M %	20.8	65.5	41.42	11.23
I %	14.3	48	33.97	9.29
K+C %	15.4	36	24.61	1.54
A_c	1.14	7.41	4.49	0.09
SS kPa	2.4	12.8	9.01	3.37

Table 4.8: Summary of geotechnical properties measured on core GC-1

	Minimum	Maximum	Average	Std. Dev.
WC %	361	489	416	29.27
LL %	135	206	171	19.65
PL %	74	113	93	10.27
PI %	53	98	77	15.17
LI	2.9	5.8	4.32	0.81
G	2.1	2.5	2.3	0.08
e	8.09	11.7	9.58	0.75
n %	89	92	90.48	0.75
wbd g/cm^3	1.1	1.2	1.16	0.05
sand %	6.4	12.9	8.7	1.45
silt %	54	68	61.84	3.25
clay %	22	39	29.56	3.24
M %	27	45	37	4.5
I %	26.3	46.3	37	5.15
K+C %	21	32	26	2.8
A_c	1.46	3.9	2.63	0.58
SS kPa	~~1.9~~ 0.2	~~24~~ 4.9	~~10.94~~ 2.2	~~7.03~~ 1.46

CHAPTER 5

DISCUSSION

The sedimentation rate in the Central Indian Basin is in the range of 2-2.5 mm/ky (Banakar etal., 1991). This implies that the deposition of fine grained sediments in the area is very slow. The Pioneer area is mostly (95 %) composed of siliceous sediments (Sudhakar, 1989). As an obligation of UNCLOS, 50 % of the Pioneer Area has to be relinquished in stages. Due to this, the scope of the present investigations was reduced to an area of 75000 sq. km. Already, part of the relinquishment work is over in which area below $15^{o}S$ is discarded. Due to this, the core collection of pelagic sediments could not be attempted more number of times. Therefore, all the cores except one are siliceous in composition. The calcareous core lies out of the Pioneer area.

The cores are collected with minimum disturbance. Nevertheless, the disturbance caused due to decrease in pressure and increase in temperature after the sediments are onboard is out of control. The effect of such disturbances might give the values which may be high or low. Therefore, it is expected that these values will be different from the in situ measured values. The in situ measurements are not very common for all the parameters discussed here due to high water depth and non- availability of technology, though attempts have been made for in situ shear strength measurements through submersible in the Pacific Ocean (Cochonat etal., 1992).

5.1 Natural water content (WC)

The water content (dry basis) can indicate possible grain size of a sample because clay particles tend to adsorb water on their surfaces. For

instance, a high water content typically indicates sediments with high clay content. Some clay minerals such as montmorillonite, have a greater tendency than others to attract water particles (Lambe and Whitman, 1969). A low water content, on the other hand, may mean that coarser grain size is present or that clay is heavily loaded, which caused some of the adsorbed water to be squeezed out. Water content can be used to predict certain engineering behaviour or may be evidence that particular geologic processes have occurred (Winters, 1988).

Figures 5.1 to 5.16 depict down core variation in water content, liquid and plastic limits and other parameters. Core A4/1, 4/2, GC-1 show decrease in water content with depth where correlation coefficients are significant (Table 5.2). However, other cores do not show such significant relationship though general decrease with depth is seen. Instead water content varies directly with void ratio (Table 5.2).

Water content and grain size are commonly inversely proportional, coarser the sediments, the lower the water content. An exception to this rule is found in foraminifera rich sediments. Although large number of forams will constitute sandy texture, the framework of these tests with its large central cavity is such that relatively large amount of water is trapped within, thus resulting higher water content associated with coarse grained material (Keller, 1974). In the present cores the radiolarian ooze is common constituent which increases the water holding capacity of sediments. It is reported that these sediments have abundant radiolarian fossil tests (Pattan etal., 1992; Gupta SM, personal communication) which are hollow in structure and change the physical properties considerably (Poulos, 1988). The surface sediments are fluffy in nature due to sediment-water interface. This is the reason for very high water contents in surface sediments. Water content for siliceous sediments varies between 92 - 574 %, in wide range, (average 416 %). In core SK69/2 drastic reduction in water content at 470 cm depth is observed. Calcareous sediments exhibit lower water content that varies from 192 to 214

%, in a narrow range, due to uniform nature and compaction of sediments. Richards etal. (1976) reported water content for Pacific sediments in the range of 135 to 476 % for siliceous pelagic clays.

Water content for the Pacific siliceous sediments (Table 5.4) is in the range of 315 - 400 % (Tisot and Gerard, 1981, Table 5.4) and for pelagic sediments (Tsurusaki etal., 1994) is 180-300 % for surface (up to 40 cm) sediments. Comparatively sediments from Central India Basin show higher values of water content due to abundant fossil tests and loose packing of grains as evidenced from high porosities. Water content of calcareous sediments from the Pacific is reported 70 - 80 % (Tisot and Gerard, 1981). Water content of similar sediments from the CIB is 192 - 214 % (average 201 %) which varies in narrow range.

5.2 Atterberg limits (LL, PL)

The Atterberg limits are based on the concept that a fine grained soil exist in any of the four states depending on its water content. Thus, a soil is solid when dry, and upon addition of water it proceeds through the semisolid, plastic and finally liquid state (Lambe and Whitman, 1969).

Index properties known as liquid limit (LL) and plastic limit (PL) have two advantages. The first, that they reflect both the amount and type of minerals present in the clay and are therefore functions of cation exchange and total surface area of particles. Secondly, they are expressed as water contents, and thus can be compared directly with the ratio called liquidity index ((WC-PL)/PI). For wide variety of normally consolidated clays the liquidity index lies in rather narrow range of values, at any given effective pressure, although the corresponding water contents of clays may vary between wide range. This enables to reduce scatter of results due to small variation in clay types (Skempton, 1970). The Atterberg limits of montmorillonite are highest and vary in wide range (LL 140-710 %; PL 54-98

%,) which is followed by illite (LL 79 -120 %; PL 45 - 60 %) and kaolinite (LL 38 - 59 %; PL 27 - 37 %) (Lambe and Whitman, 1969).

These limits have proved to be useful for soil classification for engineering purpose. The plasticity index (LL-PL) indicates the magnitude of water content range over which the soil remains plastic whereas liquidity index indicates the nearness of a natural soil to the liquid limit. The Atterberg limits depend mainly on a) the type and amount of clay fraction, b) exchangeable cations and c) pore water chemistry (Mitchell, 1976). Under given chemical conditions, factors (b) and (c) are assumed to be constant, and parameter (a) can be approximated by specific surface area (Rabitti etal., 1983).

The liquid limit of siliceous sediments is in a wide range of 94-260 % (average 173 %) and the plastic limit varies in a range of 47 - 132 % (average 97 %). This is indicative of variation in clay content, mineralogy and exchangeable cations. The calcareous core shows narrow range of Atterberg limits (LL 114-160 %; PL 50-79 %) indicating uniform nature of sediments. Tisot and Gerard (1981) reported average liquid limit of 239 % (Table 5.4) and average plasticity index of 61 % for the siliceous ooze collected from the Pacific Ocean. Average plasticity index (PI) of siliceous sediments is 76 % with wide range (36 -143 %), that for calcareous sediments is also 76 % but with little variation (64 - 92 %) and calcareous whereas average liquidity index (LI) for siliceous cores is 4.5 and for calcareous core 1.76.

5.3 Specific gravity (G)

Specific gravity or grain density of sediments indicates mineralogical contrasts as each mineral has different specific gravity (Keller and Lambert, 1980). Lambe and Whitman (1969) gave specific gravities of various minerals which include montmorillonite (2.75-2.78), illite (2.84), kaolinite (2.61-2.64), chlorite (2.6-2.9), quartz (2.65), feldspars (2.54-2.76). Fragments of radiolaria

and diatoms have specific gravities of 2.3 (Hamilton, 1970). This shows that the illite has highest specific gravity among four clay minerals. The specific gravity in case of siliceous sediments from the CIB varies widely from 1.90 to 2.60 with an average of 2.23. The low specific gravity indicates silica fragments are common in the sediments. The specific gravity of calcareous sediments is 2.31-2.36 (average 2.33) indicating less variation in clay minerals. The positive correlation of specific gravity with clay (0.427) and negative with sand size fraction and silt (r = -0.602, -0.191 respectively, Table 5.2) show that it is governed by the clay minerals. The fact is that siliceous sediments have highest amounts of illite and radiolarian test which account for lower values of specific gravities. Richards etal. (1976) reported specific gravity of 2.3 for Pacific Ocean pelagic clays associated with polymetallic nodules.

5.4 Wet bulk density (wbd), Void ratio (e) and Porosity (n)

The well defined correlation between wet bulk density, porosity and water content is given by Keller (1974) for given specific gravity. Inverse relationship of wet bulk density to porosity and void ratio exists. It is commonly accepted that wet bulk density increases as depth below the sea floor increases. This is obviously not linear function but depends on grain size changes, shape, sorting and mode of packing (Bryant etal., 1981), overburden and depositional history. For example sand dominated sediments have less porosity as they have less surface area, and thus less absorbed substances. More surface area of flat or platy grains than the spherical grains of equal volume increases porosity i.e. angularity of sediment particles can increase the porosity, and roundness in grains can reduce it (Fraser, 1935). Both wet bulk density and porosity are closely related with sediment grain size. Although the relationships are not linear throughout their respective limits, there is a defined inverse correlation between mean grain size and

porosity (Hamilton, 1972). The decrease in porosity in homogenous sediments with depth is an indication of the amount of consolidation due to overburden pressure (Richards and Hamilton, 1967).

Grain size, carbonate content and clay mineralogy might cause change in porosity to 10 - 20 % in short depth. Unlike grain size, the influence of calcium carbonate on porosity is more pronounced with depth. As depth increases, less reduction in porosity is observed for calcareous sediments than non-calcareous sediments. Clay minerals have less control on porosity than either grain size or carbonate content (Bryant etal., 1981).

All the three parameters are calculated using measured values of water content and specific gravity. The cores A4/2, GC-1, A4/5a, A4/6, A4/12 indicate notable variation in these properties with depth. The wet bulk density of siliceous cores varies from 1.12 to 1.51 g/cm^3. Void ratio and porosity for these sediments vary widely 2.39 to 13.3 and 70 to 93 % respectively. This indicates the siliceous sediments are more porous and less dense than calcareous sediments. The high porosity and void ratios help in increasing the natural water content of the sediments. Calcareous sediments have low porosity (81.7 - 83.4 %) and void ratio (4.45 - 5.01) values. This implies that probably due to uniform sedimentation above the CCD (carbonate compensation depth); and cementation of pore spaces, compaction in calcareous sediments has occurred. Thus, in calcareous core (A4/13) due to uniform nature of sediments their physical properties vary in a narrow range. The wet bulk density of this core has a range of 1.26-1.28 g/cm^3.

In core SK69/2, sediments do not show much variation in these parameters till 470 cm which might be indicative of uniform and slow sedimentation in the area. But a drastic change in porosity, void ratio and wet bulk density at 470 cm (Figure 5.13) is observed due to climatic change in deposition during Plio-Pleistocene. The wet bulk density increases to 1.51 g/cm3, whereas porosity and void ratio decrease at this depth. This shows a control of geological processes on physical properties of sediments.

5.5 Grain size distribution

Seven cores are siliceous clay/ooze in composition and fall in the Pioneer Area. They show variable presence of silt and clay with little amount of sand size fraction. The coarse fraction varies from 1-26 % (average 9.7 %), silt content from 16-84 % (average 53.7 %) and clay from 13.5-82 % (average 35.9 %). But overall, the silt is dominant in sediments which is followed by clay and coarse fraction, thus, they are clayey silt in composition. The dominance of silt could be due to the influence of detrital sediments supply from the north which may be from Ganges-Brahmaputra river discharge to the abyssal depths of the Indian Ocean (Kolla and Hayes, 1974; Rao and Nath, 1988, Debrabant etal., 1993). The illite rich sediments are transported due to waning turbidity currents generated north of the Central Indian Basin. In most of the cores (A4/1, A4/5a, A4/12 and GC-1) it can be seen that sedimentation is uniform as the change in the grain size is not much. Downward variation in all the three grain sizes remain almost unchanged

In core SK 69/2, silt is more than clay content with very less sand size fraction. However, clay content increases drastically from 13 % to 41 % at 470 cm depth (Figure 5.14) and silt and sand size fraction reduce to their minimum. Similarly, in the core A4/6 at all depths clay percent is dominant (average 62 %) over silt (average 29 %), and sand size fraction (average 9 %), and thus shows silty clay composition. At the bottom of the core (450 cm downwards, Figure 5.10), the sand size fraction and silt percentages reduce significantly and attain their lowest values whereas clay content increases to its highest value (82 %) showing siliceous clay composition. Both these cores

indicate change in sedimentation during the geological past which is reflected in other properties too.

Calcareous core shows coarse fraction between 3-24 %, silt 45-65 % and clay 27-35 %. Higher coarse fraction could be due to nannofossils and radiolarian tests. In calcareous sediments also silt is dominant over other two grain sizes. Kolla and Biscaye (1973) and Goldberg and Griffin (1970) have reported similar grain size distribution for the India Ocean sediments.

5.6 Clay mineralogy

Four clay minerals are encountered in all the siliceous cores. They are illite, montmorillonite, kaolinite and chlorite with variable abundance, in general. The kaolinite and chlorite could not be separated as zeolites are present in the sediments. The reflections of phillipsite and clinoptilolite interfere with combined reflections of kaolinite and chlorite at 7 Å and 3.54 Å respectively (Rao and Nath, 1988). In most samples the illite and kaolinite peaks were narrow, well developed and sharp whereas montmorillonite peaks were less sharp and broader. Figures 5.17 and 5.18 depict x-ray diffraction peaks of glycol treated clay minerals of siliceous sediments analyzed from the core SK69/2. It is known that the montmorillonite group has minerals with variety of composition (Carroll, 1970). In siliceous sediments, the illite content varies between 14.3 - 64 % (average 39 %). The montmorillonite varies between 8 - 66 % (average 30 %) and kaolinite+chlorite between 15 - 45 % (average 31 %). The earlier investigations have shown that the montmorillonite appeared to be diversified and from several sources and processes (Bouquillon etal., 1989; Rao and Nath, 1988; Nath etal., 1989). For instance Rao and Nath (1988) identified two varieties of minerals - a montmorillonite reworked from volcanic areas and a Fe-rich montmorillonite from in situ formation in the metal rich environments. The distribution pattern of this mineral suggested large variations in its abundance within the CIB and

also within sediment facies. Bouquillon etal. (1989) showed montmorillonites of various types which are formed from exposed land masses and host sediments. Nath etal. (1989, 1992) and Pattan and Banakar (1993) reported geochemical evidence for terrigenous flux in the deep sea sediments in the Central Indian Basin. Illite, chlorite and kaolinite were mostly attributed to detrital supply, whereas montmorillonite was supposed to be mainly derived from submarine volcanic activity. Palygorskite which is present in some samples is considered to result essentially from aeolian supply (Kolla etal., 1976a).

In the present study the sediments have high illite content followed by montmorillonite. In fact illite is inversely related to montmorillonite abundance in siliceous sediments (Rao and Nath, 1988). In core A4/6, below 450 cm depth montmorillonite increases significantly (Figure 5.10) but water content does not reflect this change (Figure 5.9), although specific gravity and wet bulk density show an increase. This could be due to consolidation of clays at greater depth of the core. The other possibility is that the montmorillonite at this depth could be originating from different source. The latter is more possible as the x-ray diffractograms at this depth show well developed and sharp peaks of montmorillonite in contrast to the montmorillonite peaks at the top. In core SK69/2, montmorillonite percent shows drastic increase at 470 cm and despite this water content shows decrease. The peaks of montmorillonite become sharp at this depth (Figure 5.17) indicating authigenic source. Being an expandable clay mineral, it is expected that with increase in montmorillonite, water content should show an increase. The reverse relationship of water content and montmorillonite at this depth of the core is due to depositional change during Plio-Pleistocene sedimentation and overconsolidation of sediments. Debrabant etal. (1993) reported increase in abundance in montmorillonite during late Pliocene - early Pleistocene sediments (SHIVA cores 942 - 947 from the CIB) and attributed it to the erosion of Indian coastal zones favored by worldwide drop in sea level.

Similarly an increase in illite during the late Quaternary (Holocene) is attributed to the tectonic activity in the Himalaya range. Fe-rich montmorillonite might have formed during early diagenesis by interaction between iron and biogenic silica which are common in siliceous sediments (Lyle etal., 1977). Rao (1987) found that polymetallic nodules associated with siliceaous sediments contain less amounts of Fe and those associated with pelagic clay contain higher amount of iron (Fe). This further confirms that more iron (Fe) content is utilized in the formation of Fe-rich montmorillonite in siliceous sediments thus leaving free manganese to form todorokite-rich nodules. On the contrary nodules from pelagic clays are rich in Fe; and δMnO_2 phase is dominant. The x-ray diffraction patterns also show that montmorillonite peaks are broader which might indicate the early diagenetic process.

The calcareous sediments indicate no variation in clay mineralogy and their content with depth (Figure 5.16) due to uniform sedimentation above the CCD. Montmorillonite varies from 42 - 48 %, illite 27 - 35 % and kaolinite/chlorite 19.6 - 27 %. Absence of Fe-rich montmorillonite in calcareous sediments may indicate that either no or less diagenetic process takes place in these sediments (Rao and Nath, 1988). The montmorillonite peaks in calcareous sediments are broad and short, therefore might be indicative of less diagenetic process of montmorillonite formation.

5.7 Shear strength (SS)

Undrained shear strength of sediments associated with nodule deposits is a critical parameter as far as the design of the nodule collecting head is concerned. Therefore, this forms the essential data base for the development of the mining system. The strength is measured in kilopascal (kPa). Usually, shear strength increases linearly with depth; and is function of

sediment type and age (Keller, 1974). It has been observed that shear strength increases more rapidly with depth for hemipelagic, terrigenous and calcareous ooze than for siliceous or nannofossil ooze (Bryant etal., 1981). It's measurements at various depths in each core could be indicative of change in the sediment characteristics such as bioturbated layer, overconsolidated unit.

The cores show strength variation with depth, in some cases despite uniform lithology (A4/1, Figure 5.2). The shear strength varies in case of siliceous cores from 0.41 kPa to ~~24~~ 13 kPa with an average of ~~5.5~~ 2.7 kPa. The strength variations in the cores were observed at different depths. It shows general increase with depth of burial of sediments, specific gravity, and decrease with increase in clay and water content (Core A4/2, Figures 5.5 and 5.6). The homogenous sediments generally show this trend. The shear strength measured here might reflect the effect of unknown coring disturbance and the release of hydrostatic pressure and temperature. Therefore, higher strength values are expected in case of in situ measurements. In case of long cores, the disturbance is caused due to the friction on the sides of the corer during penetration. Some times sediments get compressed if they are highly compressible in nature. In the present case this possibility can not be totally ruled out. Therefore, the measurements made on small cores seems to be preferable and more accurate.

Numerous previous studies (Richards, 1961; Simpson, 1976; Richards and Parks, 1977; Richards etal., 1976; Tisot and Gerard, 1981; Bryant etal., 1981; Noorany, 1985; Tsurusaki etal., 1994) have determined the shear strength of deep sea pelagic clays of the Pacific Ocean by laboratory methods. Similar measurements on the CIB sediments are carried out by the author (Khadge, 1992, 1995, 1997). It is assumed to be the most significant parameter to study fine grained sediments. In situ measurements of shear strength made in the nodule mining area in the North Central Pacific Ocean (Cochonat etal., 1992) showed strength of <1 to 8 kPa in the surfacial pelagic

sediment layer of 10 cm. This study also showed that there is a fluffy layer at the sediment-water interface which is acoustically transparent and causes change in the strength. The thin acoustically transparent layer gives strength of 5.5 - 8 kPa, thicker layer of similar characteristics and abundant nodules gives strength of 2 - 5.5 kPa. It was revealed that though laboratory studies give mean value of strength, it could not discriminate several clusters of various ranges of shear strength values which is possible through in situ measurements. The other observation was that the manganese nodules are more abundant (>10 kg/m^2) and more rich in Cu+Ni (2.5 %) when overlying acoustic transparent unit is thicker. Similar observations were made on the CIB nodules overlying siliceous sediments (Mukhopadhyay and Nath, 1988). The extremely slow rates of deposition in the deep sea apparently allows the sediment strength to increase to such an extent that there is little reduction in porosity due to weight of overlying sediment column (Richards, and Hamilton, 1967). This might be the condition in the CIB area where porosity and water content of the sediments are high, and despite this shear strength is also high. Noorany (1985) reported strength values between 5 -13 kPa for the 60 cm pelagic sediments from the Pacific areas. Tsurusaki etal. (1994) have shown lower values of shear strength of 1 - 3 kPa upto 30 cm depth in pelagic clays of Penrhyn Basin in South Pacific.

Undrained shear strength in core SK69/2 increases with depth from 2 kPa at surface to 10 kPa at 430 cm (Figure 5.14). Below this, at 470 cm, it significantly increases to 12.2 kPa at a sticky layer and then reduces to 10 kPa at 510 cm depth. This strength spike is due to different sediment type having sharp contact with underlain and overlain lithological units. This also shows the Plio-Pleistocene sedimentation change that is reflected in all other properties.

Shear strength of the calcareous core, unlike siliceous sediments, shows gradual increase with depth (Figure 5.16) despite homogenous sediments. At surface itself the strength is 5 kPa which increases with depth

and attains value of 14 kPa at 200 cm and then exhibits reduction. The sudden decrease in shear strength below 225 cm of the core is enigmatic but could be due to loose/disturbed sediments. At this part of the core specific gravity and wet density shows decrease whereas porosity and void ratio show an increase (Figure 5.15). Bryant etal (1981) have observed that shear strength in calcareous ooze increases rapidly with depth than in siliceous ooze. The calcium carbonate might be controlling these properties, but can not be concluded as only one core is collected and number of sample is very less (n = 14). This can be confirmed with more calcareous cores from the area in future. The core has higher strength than siliceous sediments indicating more compaction at all depths. Tisot and Gerard (1981) have reported shear strength up to 30 kPa for calcareous ooze from the Pacific Ocean.

5.8 State of Consolidation

An object placed on the seafloor normally will sink immediately as a result of shear failure if the bearing capacity of the sediment is insufficient to carry the load. The object will initially remain on the surface if the sediment has sufficient strength to bear the load. In either case there will probably be relatively slow and gradual settlement of the object as sediment consolidates. Deep water sediments are generally stronger than might be expected because of very slow rate of deposition, grain-to-grain deposition, great age and presence of large amount of clay minerals and biogenic component (Richards and Hamilton, 1967).

Consolidation is a reduction of the volume of a sediment under an imposed load. Volume reduction in saturated sediments can take place only when there is a loss of pore or interstitial water. The load can be from a man made structure or overburden pressure exerted by the sediment itself. Consolidation test is necessary to know rate and amount of settlement that is

expected under any given pressure. Consolidation test requires a cylindrical sample from the core collected from seafloor. In the absence of this test, consolidation state can be given using formula (Skempton, 1970) which is a rough estimation.

$$USS/EOS = 0.11+0.0037 * \text{Plasticity index}$$

The ratio of undrained shear strength to effective overburden stress (USS/EOS) less than 0.22 indicate underconsolidated state of sediments and above 0.22 indicate normal to overconsolidation of sediments (Skempton, 1970). Using this value, it is seen that all the cores show mostly overconsolidated state (Figures 5.2, 5.4, 5.6, 5.8, 5.10, 5.12 and 5.14) of sediments. Siliceous sediments have this ratio varying mostly between 0.28 to 0.64. This could be due the hydrostatic pressure and the overlying sediment column of 2 - 3 Ma age. Siliceous cores show wide range of the ratio than calcareous core (Figure 5.16). Noorany (1985) measured such ratios for pelagic sediments from the Pacific Ocean which varied between 0.28 and 0.60 indicative of normal to overconsolidated characteristics of sediments.

Overconsolidated sediments are result of great age, cementation of mineral grains and development of rigid bonds as a result of absorbed water around clay particles attributed to the incipient lithification from solution and redeposition of various minerals. In addition, the removal of overburden by erosion or tectonic forces can create condition of overconsolidation. Consolidation tests conducted on various sediment types have indicated (Bryant etal., 1981) that calcareous sediments consolidate similar to argillaceous except that the calcareous sediment maintain higher porosity at greater applied pressure. The calcareous core (A4/13) has very narrow range of porosity (81-83 %, Figure 5.15 and Table 4.6) for the full core length which could be indicative of the phenomenon of cementation and compaction.

5.9 Activity of clays (A_c)

As the particle size decreases, the surface area of the particle and amount of water attracted to the surface increases. The ratio of plasticity index to clay percent is known as the activity and represents the surface activity of clay fraction, such as increased ion exchange capacity and absorption of water with decreasing grain size (Skempton, 1953). Activity of sodium montmorillonite is highest (7.2) followed by illite (0.9) and kaolinite (0.38) (Lambe and Whiteman, 1969). Skempton (1953) proposed activity classification for clays as inactive clays (A_c less than 0.75), normal active (A_c= 0.75-1.25) and active clays (A_c more than 1.25). The cores show scatter of points in the activity chart which can give indication to clay minerals present in the sediment. The siliceous cores A4/1, A4/2, A4/6, A4/12 and SK69/2 exhibit the activity ranges from normal active to very active (Figures 5.19, 5.21, 5.23, 5.24 and 5.25). This implies that plasticity of these sediments is controlled by montmorillonite and illite. Cores A4/5a, GC-1 show all points falling in the active field only (Figure 5.20 and 5.22) indicating only montmorillonite is governing the plasticity of these sediments.

An exception is observed in core A4/6 sediments which fall mostly in normal active field (Figure 5.23) represented by illite. This is due to the fact that illite is dominant (average 41 %) over other clay minerals. The x-ray diffraction peaks of the sediments from the lower part (below 450 cm) showed very well developed peaks of all the clay minerals. The montmorillonite peaks of sediments from this part of the core are more sharp indicting well crystalline nature of mineral than those from overlying sediments. It might indicate the episodic supply of authigenic, well crystalline illite, kaolinite/chlorite and montmorillonite, the last being mostly from weathered rocks. No sample point lies in the field of inactive clays represented by kaolinite rich clays. Thus, in case of siliceous cores this helps to decipher the effect of variable clay minerals on the plasticity index. The activity range of

siliceous sediments is 0.93 to 7.41 which covers clays rich in montmorillonite and illite.

Richards (1962) attempted to use these data as an indicator of mineralogy of clay fraction. But in case of calcareous sediment (Core A4/13) this may not hold good as it has high calcium carbonate content (58 - 64 %) and the mineralogy does not change with depth though montmorillonite is dominant (42-48 %) over other clays. This core also exhibits uniform sedimentation (Figure 5.16). Therefore, all sample points of this core lie in the active field only (Figure 5.26).

5.10 Plasticity characteristics

Most of the sediments are silty clay or clayey silt in composition which means that there is only small difference in the grain size distribution. Plasticity chart is prepared by plotting liquid limit against plasticity index. Liquid and plastic limits, and plasticity index are in general directly related to the clay content of the sample. According to Terzaghi (1955), the Atterberg limits of minerals would plot on the chart as a line parallel to the A-line and could be located above or below the line depending upon mineralogical composition of the grains. Points representing different samples from a geologically well defined sedimentary deposit would be on a line parallel to the *A-line* because the mineralogical composition of the clay size fraction would be similar. If the points representing two members in the plasticity chart were located on very different lines it would be almost certain that the sediments had been derived from two different sources. These relationships are valid for sediments investigated. Figures 5.19 to 5.26 show plasticity charts for all the core sediments that are analyzed for Atterberg limits. It is clear that cores A4/1, A4/2, A4/5a, A4/6, A4/12, A4/13, GC-1 and SK69/2 are plotted below and parallel to A-line indicating the field of organic clays of medium to high plasticity. They also show similar source of deposition.

However, the scatter of points of core A4/1 (Figure 5.19) and A4/13 (Figure 5.26) is very narrow whereas all other cores have wide scatter parallel to A-line implying homogenous sedimentation with same source of supply. It can also be noted that an isolated point from the core SK69/2 (Figure 5.25) which lies in the same field represents sample indicating change during Plio-Pleistocene (Gupta, 1996). Nevertheless, this point also has medium to high plasticity (PI = 47 %). Similarly in core A4/6 (Figure 5.23) two distinct clusters are seen below A-line which imply same source but at different geological time. Such clusters to some extent are also seen in Figure 5.22 (Core A4/5a) showing similar phenomenon.

5.11 Interrelationships

The relationships among the parameters was essential to know dependencies of properties among themselves. The correlation coefficients (r) were calculated using the computer program. For this purpose all siliceous core data was collated. The data on calcareous core was only from one core from which firm interpretation was not possible. Table 5.2 and 5.3 show correlation matrix for the siliceous and calcareous sediments respectively. Some significant relationships for siliceous sediments are shown in Figures 5.27 to 5.29.

Siliceous sediments

Correlation matrix for siliceous core data (Table 5.2) shows positive correlation of depth with wet bulk density(r = 0.341), montmorillonite (r = 0.362) and shear strength (r = 0.428). Water content generally, correlates significantly with porosity (r = 0.850) and wet density (r = -0.804). Its inverse relationship with depth could be anticipated due to increasing overburden

pressure with depth (Keller, 1974). Shear strength and water content are also inversely related (r = -0.425, Figure 5.28). Water content and sediment grain size are commonly inversely proportional. The coarser the sediments, the lower the water content with an exception to this is the sediments rich in foraminifera. Although the large number of forams constitute a sandy texture, the framework of their tests with large central cavity is such that large amounts of water are trapped within, thus, resulting in high water content. The siliceous cores show abundant radiolarian tests present in the sediments (Gupta SM, Pers. comm.) which increase the water content to considerable extent. Water content is also controlled by expandable clay mineral i.e. montmorillonite. It has high water holding capacity among the common clay minerals. The surface area of clay particles per unit mass is referred as specific surface. Clays with smallest particles have largest specific surface. The specific surface area of kaolinite, illite and montmorillonite are 15, 90 and 800 m^2/gm respectively (Purushothama Raj, 1995). However, in present cores water content shows inverse relationship with montmorillonite (r = -0.347, Figure 5.27). This probably is due to the dewatering of the sediments because of overconsolidation. This also confirms the consolidation state calculated from Skempton's (1970) empirical formula which showed overconsolidated characteristics of these deep sea sediments.

Wet bulk density is inversely related to void ratio (e) and porosity (n). It is commonly accepted that wet bulk density increases with depth. This is not a linear function but dependent on such factors and changes in grain size, cementation, overburden etc. (Keller, 1974). Both wet bulk density and porosity are closely related with sediment grain size. Although the relationships are not linear throughout their respective limits, there is a definite inverse correlation between mean grain size and porosity (Hamilton, 1972) and direct correlation with wet bulk density. However, no such relationship was observed for the present investigation. This could be due to less variation in grain size with homogenous sedimentation and consolidated nature of

sediments. In the present cores void ratio shows strong positive relationship with porosity (r = 0.879), water content (r = 0.928, Figure 5.27) and negative with wet bulk density (r = -0.693). Porosity also shows inverse relationship with wet bulk density (r = -0.908).

Specific gravity of sediments depends upon the minerals present in it as each mineral has certain specific gravity (Keller and Lambert, 1980). Specific gravity is directly proportional to clay content (r = 0.427) and wet bulk density (r = 0.398) and inversely to sand size fraction (r = -0.602).

Montmorillonite content varies inversely with the illite percentage (r = -0.839, Figure 5.29) and with k+c content (r = -0.635). Such observation is reported for CIB sediments by Rao and Nath (1988). Silt abundance varies inversely with clay content (r = -0.927, Figure 5.29) and thus indicates either would be dominant in the siliceous sediments.

Shear strength increases with depth of burial due in part to overburden pressure (Keller, 1974). Studies of Richards (1962) showed that shear strength is inversely proportional to porosity. The shear strength of siliceous sediment (Table 5.2) shows positive relationship with depth of burial (r = 0.428, Figure 5.28), wet density (r = 0.324), silt content (r = 0.368, Figure 5.28) and montmorillonite content (r = 0.334) and inverse relationship with water content (r = -0.425, Figure 5.28) and kaolinite+chlorite content (r = -0.362). In fact with increase in montmorillonite percent in sediments, increase in water content and as a consequence, decrease in shear strength is expected. But overall siliceous sediments are overconsolidated, and as an effect of dewatering, shear strength shows increase despite increase in montmorillonite and silt. It can also be said that shear strength is more dependent on depth below the seafloor and water content due to high correlation coefficients than on any other parameters.

From above discussion the strength relationship for the siliceous sediments of the CIB could be given by the equation as

SS = ~~0.0113~~ 0.0076 * (depth) + ~~2.4082~~ 2.0312

SS = -0.0329 * (WC) +19.153

Here depth is in cm and shear strength is in kPa and water content is in percent.

Similar to this, other equations for the siliceous sediments could be derived based on the correlations which are as follows

Void ratio = 0.0213 * (WC) +0.3773

Clay = -0.9873 * (Silt) +88.957

Illite = -0.6525 *(Montmorillonite) + 58.839

All the parameters except void ratio are expressed in percentage. Using these equations we can calculate one parameter if other is known. Nevertheless, more data should be considered in future to modify the equations.

Calcareous sediments

The population of calcareous sediments is very small (n = 14). Nevertheless, some relationships are observed but should not be taken as a general trend. Water content of these sediments varies positively with void ratio (r = 0.989) due to the fact that void ratio represents the pore space available for saturation. Liquid limit is inversely proportional to sand size fraction (r = -0.755) which shows influence of grain size over liquid limit. Further, coarse fraction correlates inversely with silt (r = -0.932) which implies that either of them only would dominate the sample. The silt content in the core varies from 45 % to 65 % whereas sand size fraction varies from 3 % to 23 %. The interesting thing about this core is that it was collected from a water depth of 5800 m which is deeper compared to the carbonate compensation depths (CCD) reported (Belyaeva and Burmistrova, 1985) in the Indian Ocean. But Kolla etal. (1976b) have reported CCD more than 5100 m in the equatorial area of the Indian Ocean between 10°N and 10°S. There

seems to be a deepening trend of the CCD in the Chagos Trench area. The uniform nature of the core also rules out possibility of slumping of sediment in the trench area as there is no mixing of sediments. The calcium carbonate content for the sediments ($CaCO_3$ %) determined by weight loss after hydrochloric acid treatment does not vary much (58.8 - 64.8 %) though it shows change at 175 cm in the core (Figure 5.16). In fact, unlike siliceous cores, most of the properties of this core remain unchanged with depth except shear strength which varies widely from 3 to 14 kPa. The variation in shear strength may be due to compaction of sediment. The USS/EOS ratio remains almost constant through the depth. Study on more calcareous cores is needed to know the relationships.

5.12 Bioturbation

Benthic invertebrates are known to rework and modify sediments mechanically through activities such as burrowing, tube building and deposit feeding. The results are a variety of identifiable structures which are abundant both at sediment-water interface and preserved at deeper layers (Rowe, 1974). Bioturbation by benthic animals alters the physical and acoustical properties of marine sediments by their direct effect on sediment physical properties and by their influence on erosional and depositional events (Richardson, etal 1983). The changes in geotechnical properties due to bioturbation of sediments are related to fabric changes (Chernow etal., 1986). However, a direct comparison between bioturbated and non-bioturbated sediments of similar composition is difficult to make because sediment physical properties are also affected by the conditions that prevent bioturbation, i.e. mainly rapid deposition and oxygen-free bottom waters (Wetzel, 1990).

In present study only siliceous cores are bioturbated at various depths. The oval and lens like structures are observed with mottled appearance on

sediment surface. The porosity is usually increased due to bioturbation, although it may occasionally be reduced (Rhoads and Boyer, 1982). The consequent effect of this is increase in water content and decrease in shear strength.

In cores GC-1, A4/5a, A4/6, A4/12 and SK69/2 the bioturbated layers are seen which are marked by 'B' in Figures 5.3 to 5.16 depicting the downcore variation of properties. The change in porosity at such layers is not only increase but also the little reduction. For example, in core GC-1 a bioturbated layer at 425 cm (Figure 5.3) reduces porosity, specific gravity and wet bulk density but water content remains same (398 %) whereas shear strength shows decrease (Figure 5.4). In core A4/5a, bioturbated layer at 500 cm shows (Figure 5.7) little increase in porosity and decrease in shear strength. In core A4/6, layers at 35 cm and 110 cm show an increase in porosity and layers at 200 cm and 450 cm show decrease in porosity (Figure 5.9). Shear strength on the contrary shows decrease at all these layers (Figure 5.10). Such phenomenon could be due to the fact that sediments are overconsolidated and thus despite bioturbation, porosity shows a reduction in few layers. Core A4/12 is bioturbated at 75 cm and 205 cm. In case of former layer porosity and water content increase very little from the overlying sediments but in the latter layer which is at deeper level, there is no change in both parameters. However, the shear strength shows an increase at both these layers (Figure 5.12). The core SK69/2 shows interesting layers of bioturbation and non-bioturbation. The bioturbated layers are seen at 281 cm, 347 cm, 405 cm and 610 cm. In first three layers there is no change in porosity but at fourth layer porosity shows an increase (Figure 5.13). The water content also does not change much at these layers. Shear strength increases a little at every layer except at second layer (347 cm). The non-bioturbated layers at 470 cm and 590 cm are sticky in nature and without any fossil tests. These layers show drastic decrease in water content and porosity and increase in shear strength (Figures 5.13 and 5.14).

The effect of bioturbation is mixed for these sediments and no firm correlationships and conclusions could be drawn. In general, it can be said that bioturbated layers show general increase in water content and porosity, and decrease in shear strength. Probably the consolidation state of sediments plays more important role in controlling the effect of bioturbation on the properties.

Table 5.1 : Range and average values of geotechnical properties of the CIB sediments

	Min.	*Max.*	*Ave.*	*Std.dev.*
Siliceous sediments				
Water content (%)	92	574	416	57
Liquid limit (%)	94	260	173	33
Plastic limit (%)	47	132	97	18
Plasticity Index (%)	36	143	76	20
Liquidity Index	0.96	10.6	4.5	1.6
Specific gravity	1.9	2.6	2.23	0.13
Wet bulk density (g/cm^3)	1.12	1.51	1.16	0.03
Porosity (%)	70.5	93	90	2.0
Void ratio	2.39	13.3	9.24	1.32
Sand (%)	1	26	10	3.7
Silt(%)	16	84	53	12
Clay(%)	14	82	36	13
Montmorillonite(%)	8	66	30	10
Illite(%)	14	64	39	8
Kaolinite+Chlorite(%)	15	45	31	5
Shear strength (kPa)	0.41	~~24~~13	~~5.5~~4.09	~~4.4~~2.7
Calcareous sediments				
Water content (%)	192	214	201	6.9
Liquid limit (%)	114	160	144	11.5
Plastic limit (%)	50	79	67	8.3
Plasticity Index (%)	64	92	76	8.5
Liquidity Index	1.38	2.56	1.76	0.29
Specific gravity	2.31	2.36	2.33	0.01
Wet bulk density (g/cm^3)	1.26	1.28	1.27	0.01
Porosity (%)	81.7	83.4	82.4	0.52
Void ratio	4.45	5.01	4.69	0.17
Sand (%)	3.1	23.9	7.3	4.8
Silt(%)	45	65	60	4.6
Clay(%)	27	35	32	2.2
Montmorillonite(%)	42	48	46	2.3
Illite(%)	28	35	32	2.2
Kaolinite+Chlorite(%)	19.6	27	22.5	2.05
CaCO3 (%)	58.8	64.8	61.7	1.5
Shear strength (kPa)	3.26	13.9	8.9	3.06

Table 5.2: Correlation coefficients on properties of siliceous sediments from the CIB.

	Dep	WC	LL	PL	G	e	n	wbd	sand	silt	clay	M	I	K+C	SS
Dep	1.0														
WC	**-.531**	1.0													
LL	.282	-.089	1.0												
PL	.118	.093	**.828**	1.0											
G	.112	-.202	**.364**	**.349**	1.0										
e	**-.481**	**.928**	.072	.247	.170	1.0									
n	**-.370**	**.850**	.126	.250	-.009	**.879**	1.0								
wbd	.341	**-.804**	-.034	-.145	.398	**-.693**	**-.908**	1.0							
sand	-.104	.140	-.333	-.345	**-.602**	-.083	.057	-.266	1.0						
silt	.167	-.132	.062	.065	-.191	-.202	-.183	.076	-.068	1.0					
clay	-.155	.085	.096	.099	**.427**	.243	.171	.016	-.281	**-.927**	1.0				
M	.362	**-.348**	-.020	-.214	-.007	-.367	-.418	.379	-.126	.327	-.300	1.0			
I	-.320	.259	.079	.230	.007	.279	.340	-.317	.135	-.169	.156	**-.839**	1.0		
K+C	-.212	.272	-.076	.068	.003	.280	.287	-.247	.039	-.362	.329	**-.635**	-.416	1.0	
SS	**.428**	**-.425**	.120	.029	.259	-.320	-.282	.324	-.124	.368	-.298	.334	-.178	-.362	1.0

Level of significance = 99.9 %, n = 157

Table 5.3: Correlation coefficients on properties of calcareous sediments from the CIB.

	Dep	WC	LL	PL	G	e	n	wbd	sand	silt	clay	M	I	K+C	SS
Dep	1.00														
WC	-.228	1.00													
LL	.404	-.644	1.00												
PL	.645	-.443	.677	1.00											
G	.512	.195	-.199	.362	1.00										
e	-.143	**.989**	-.647	-.370	.338	1.00									
n	.130	**.988**	-.625	-.349	.334	.998	1.00								
wbd	.224	-.872	.527	.388	.020	-.832	-.833	1.00							
sand	-.378	.558	**-.755**	-.613	.027	.539	.520	-.514	1.00						
silt	.480	-.440	.677	.675	.025	-.419	-.401	.313	**-.932**	1.00					
clay	-.347	-.266	.218	-.334	-.531	-.333	-.329	.434	-.255	-.008	1.00				
M	.130	.389	-.472	-.383	.249	.412	.411	-.088	.270	-.288	.292	1.00			
I	.276	-.528	.309	.285	.045	-.507	-.517	.383	-.267	.237	-.086	-.547	1.00		
K+C	-.447	.137	.187	.147	-.252	.099	.112	-.276	-.038	.058	-.194	.520	-.416	1.00	
SS	.049	-.583	.404	.245	.000	-.560	-.575	.422	-.307	.262	-.153	-.636	.609	.033	1.00

Level of significance = 99.9 %, n = 14

Table 5.4: Geotechnical properties of sediments from the Pacific Ocean.

	Siliceous			*Calcareous*				*Pelagic*	
	min.	*max.*	*ave.*	*min.*	*max.*	*ave.*	*min.*	*max.*	*ave.*
Water content (%)	315	400	-	70	80	-	180	300	-
Liquid limit (%)	206	275	239	-	-	70	138	192	160
Plastic limit (%)	-	-	-	-	-	-	35*	70*	-
Plasticity Index (%)	48	78	61	-	-	18	36	78	36
Liquidity Index	-	-	-	-	-	-	1.1[a]	4.6[a]	-
Specific gravity	2.3	2.6	-	~~9~~	~~10~~	-	2.66[a]	2.84[a]	-
Wet density (g/cm^3)*	1.2	1.7	-	1.2	1.6	-	1.22[a]	1.50[a]	-
Void ratio	8	10	-	1.9	2	-	5.5	7	-
Shear strength (kPa)	10	20	-	1	30	-	1	7	-
Shear strength (kPa)*	10	19	-	5	10	-	5	13	-

Tisot and Gerarad (1981) North Central Pacific Ocean
* Richrds etal. (1976) from NE Central Pacific Ocean
[a] Noorany (1985) for 60 cm depth.

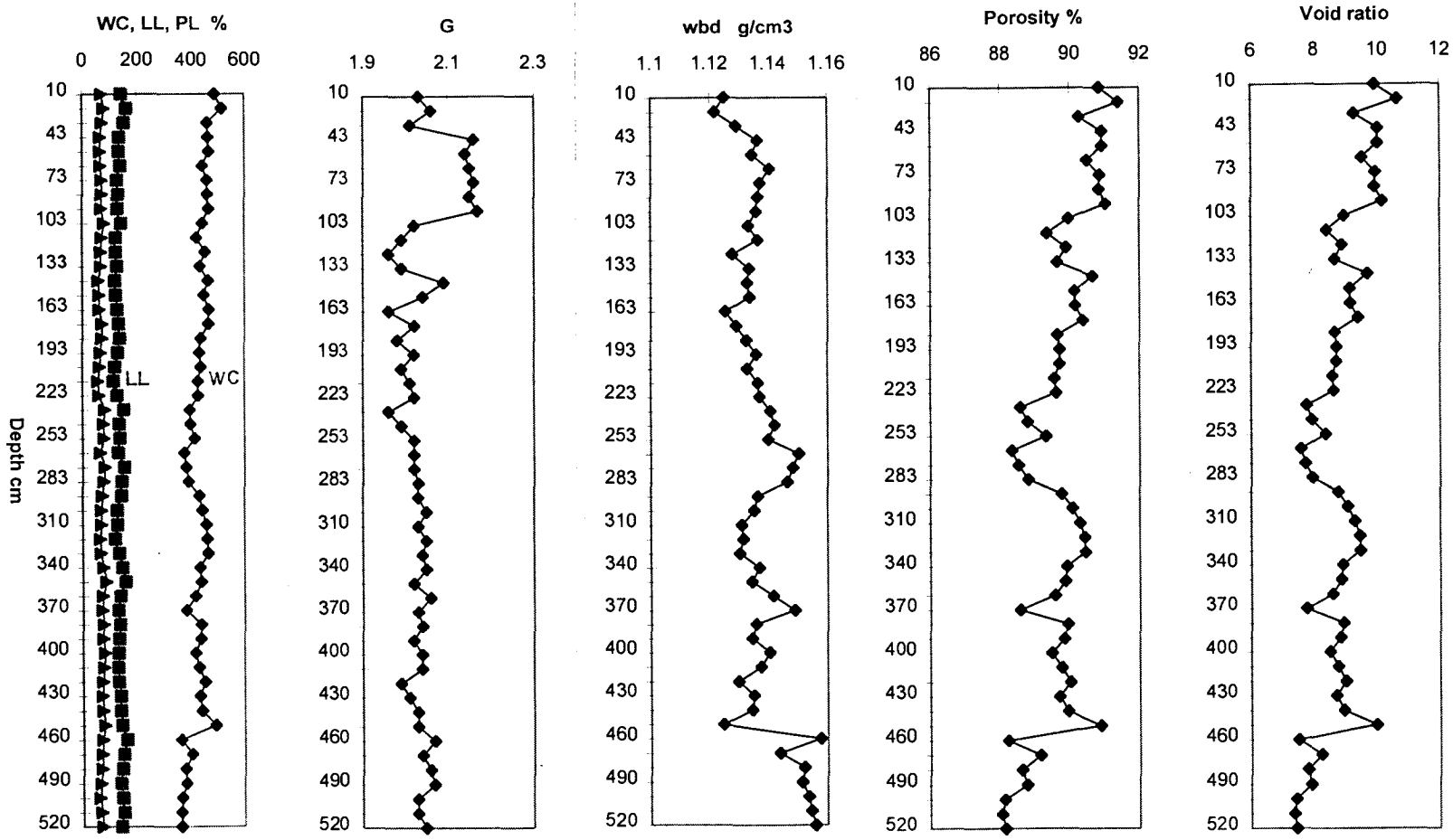

Figure 5.1: Down core variation in physical properties of the core A4/1.

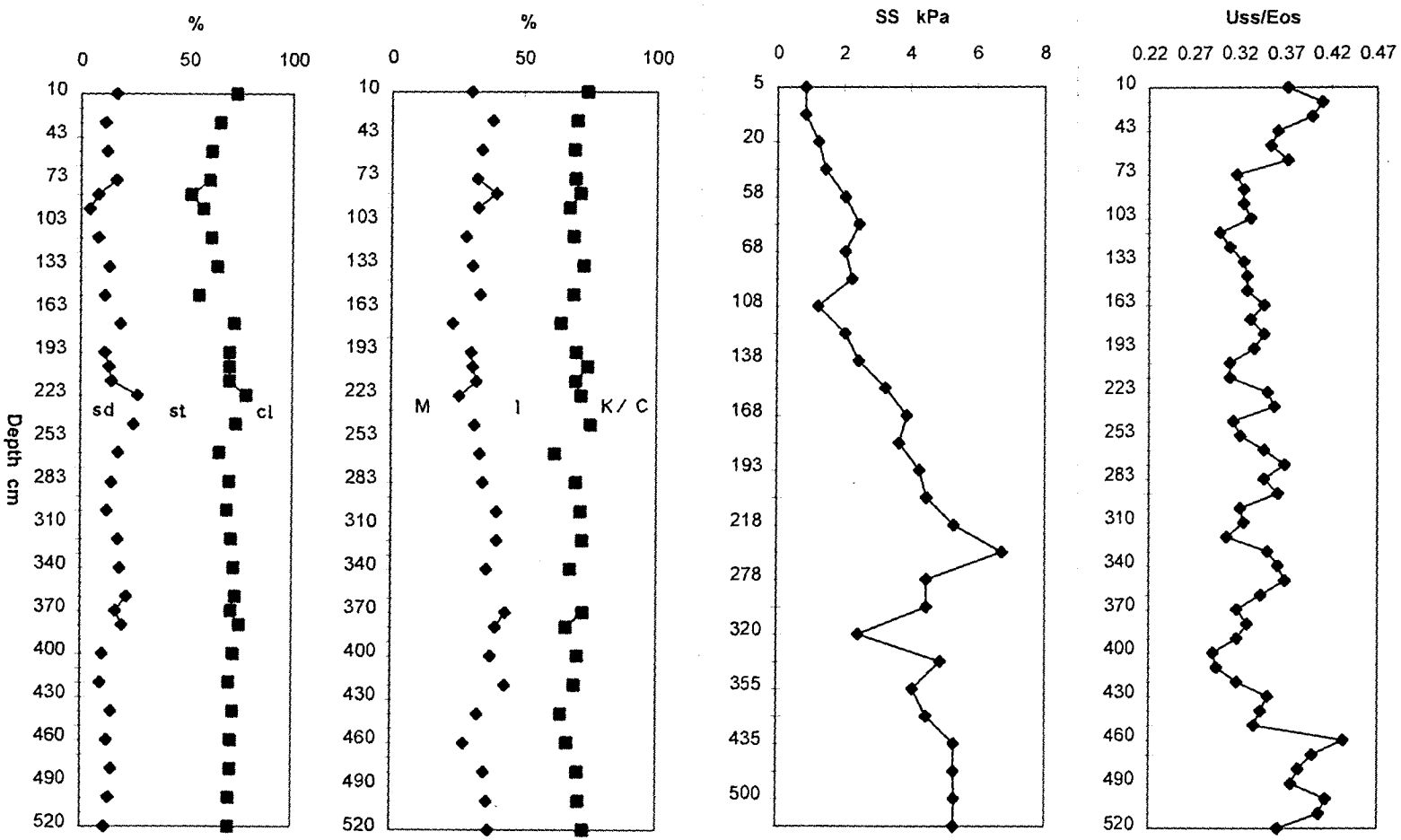

Figure 5.2: Depthwise variation in grain size, clay mineralogy and shear strength of the core A4/1.
(sd = >63μm fraction, st = silt, cl = clay, M = montmorillonite, I = illite, K/C = kaolinite/chlorite)

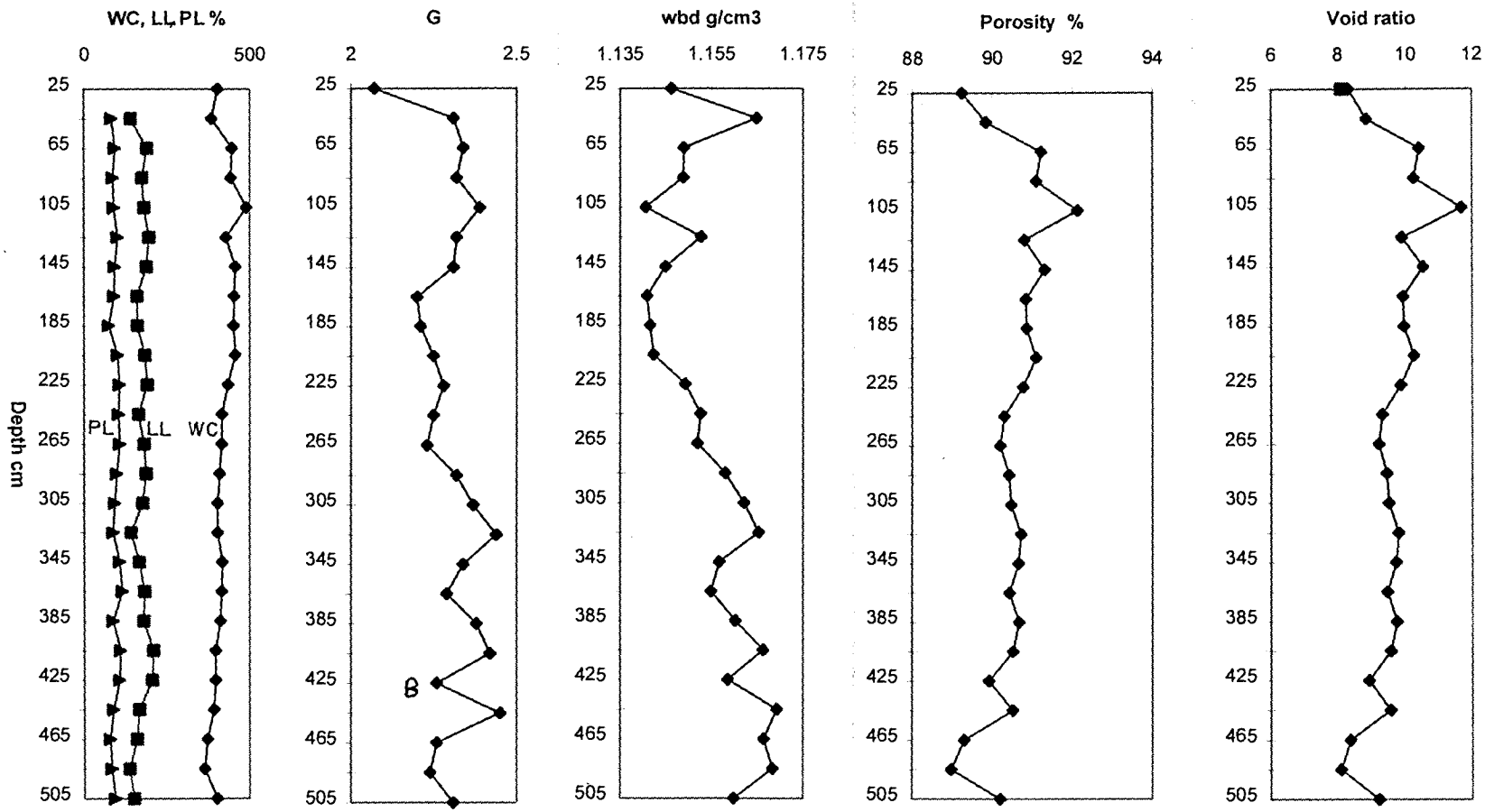

Figure 5.3: Down core variation in physical properties of the core GC-1.

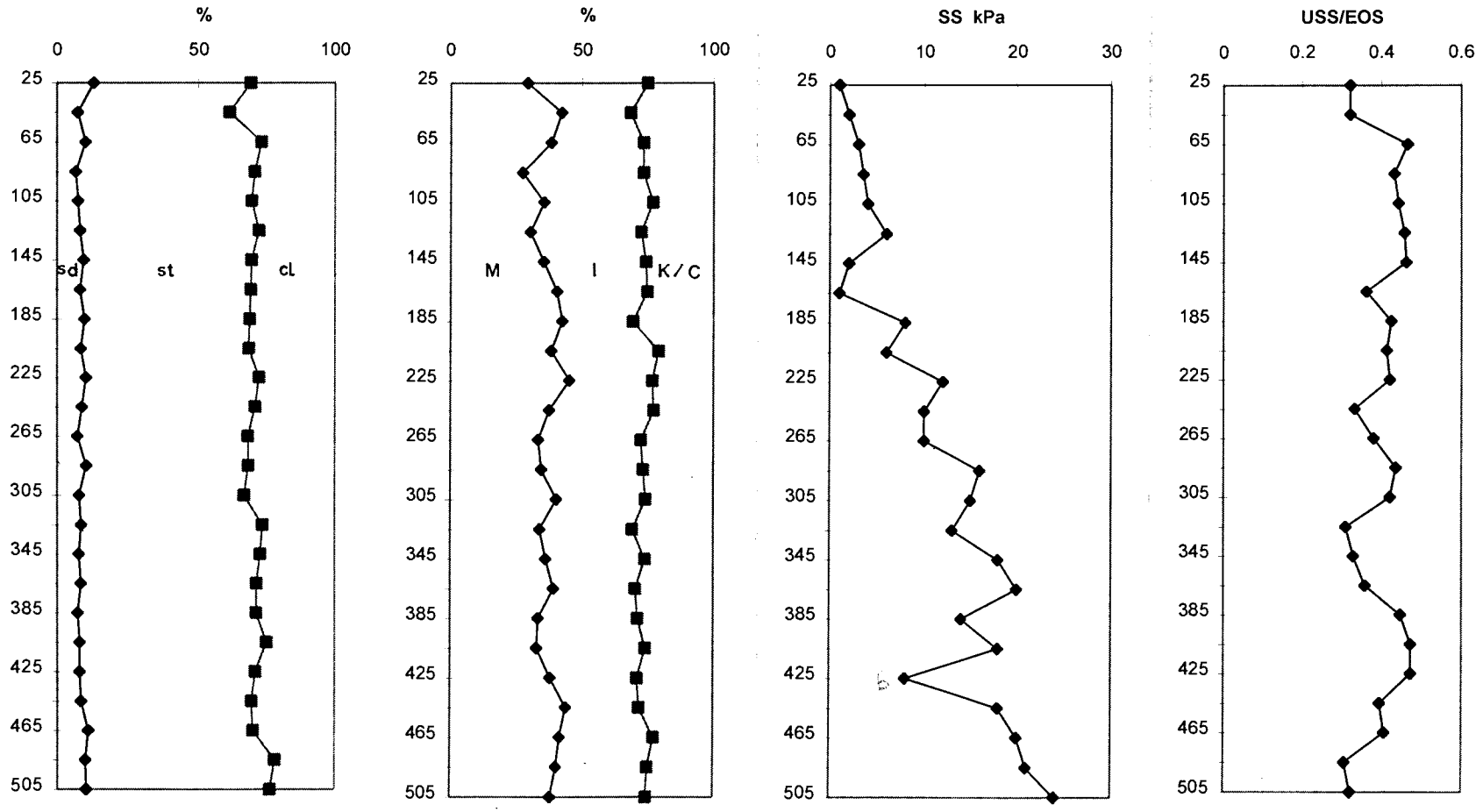

Figure 5.4: Depthwise variation in grain size, clay mineralogy and shear strength of the core GC-1.
(sd = >63μm fraction, st = silt, cl = clay, M = montmorillonite, I = illite, K/C = kaolinite/chlorite)

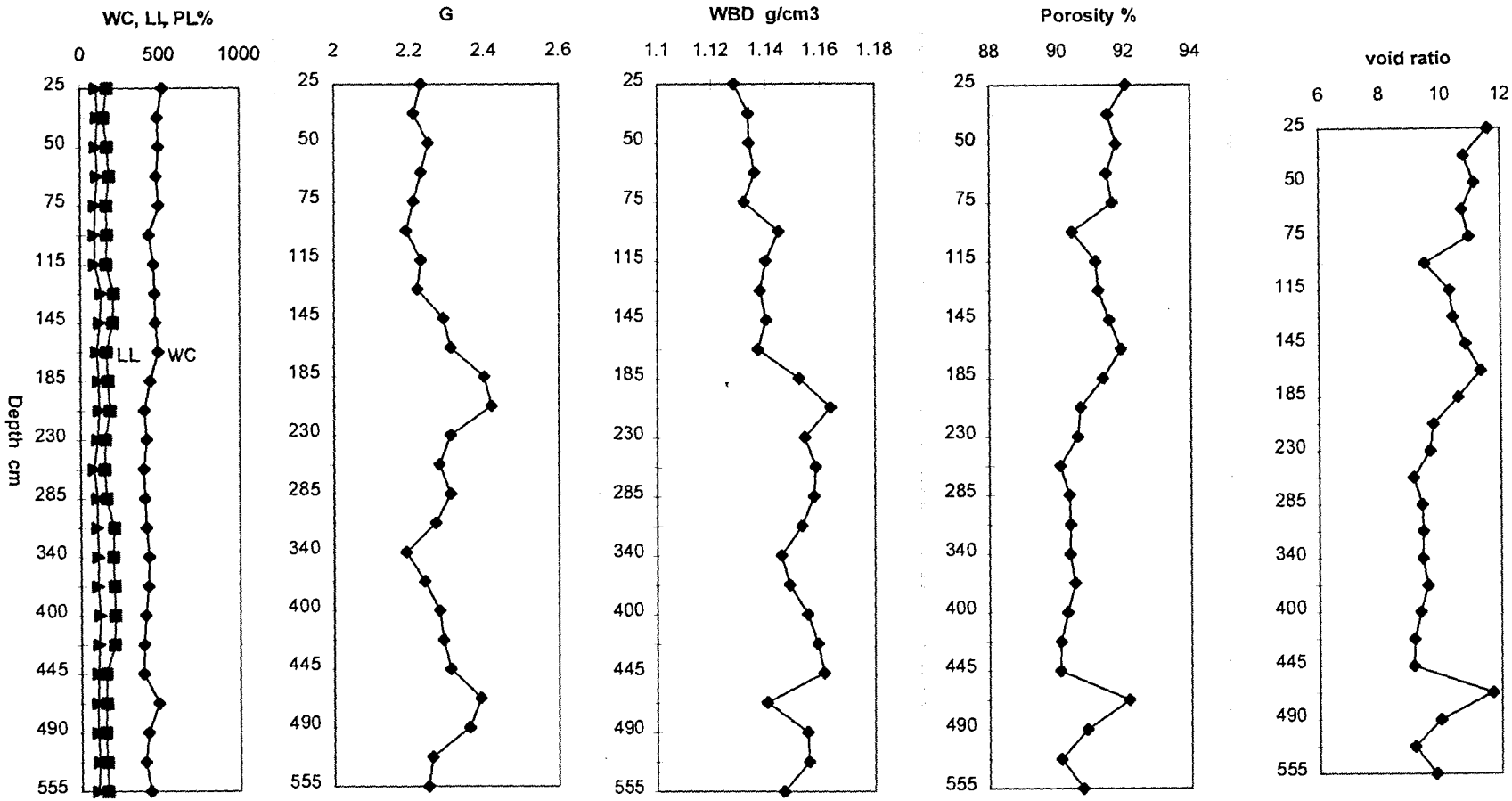

Figure 5.5: Down core variation in physical properties of the core A 4/2.

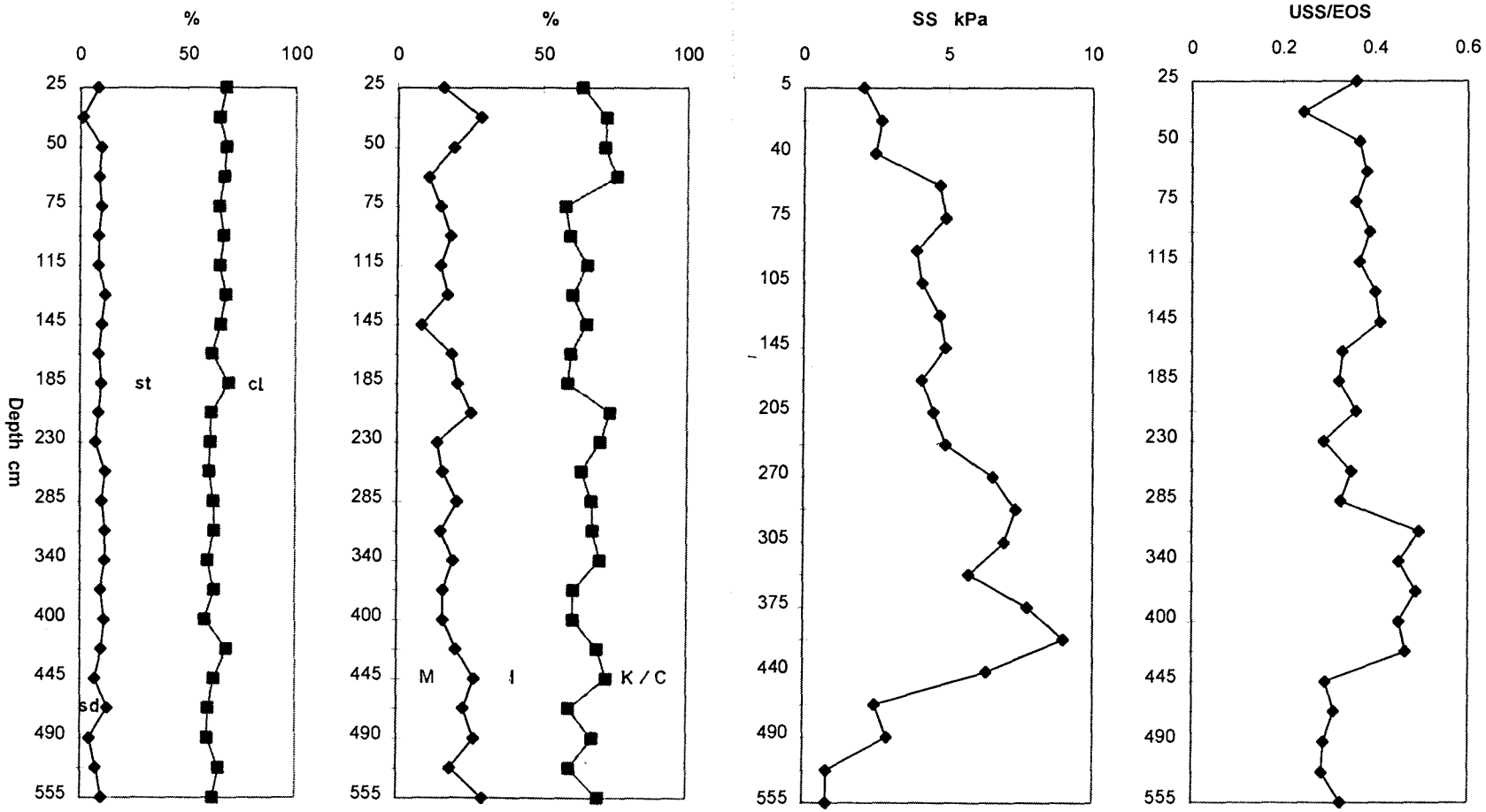

Figure 5.6: Depthwise variation in grain size, clay mineralogy and shear strength of the core A4/2.
(sd = >63μm fraction, st = silt, cl = clay, M = montmorillonite, I = illite, K/C = kaolinite/chlorite)

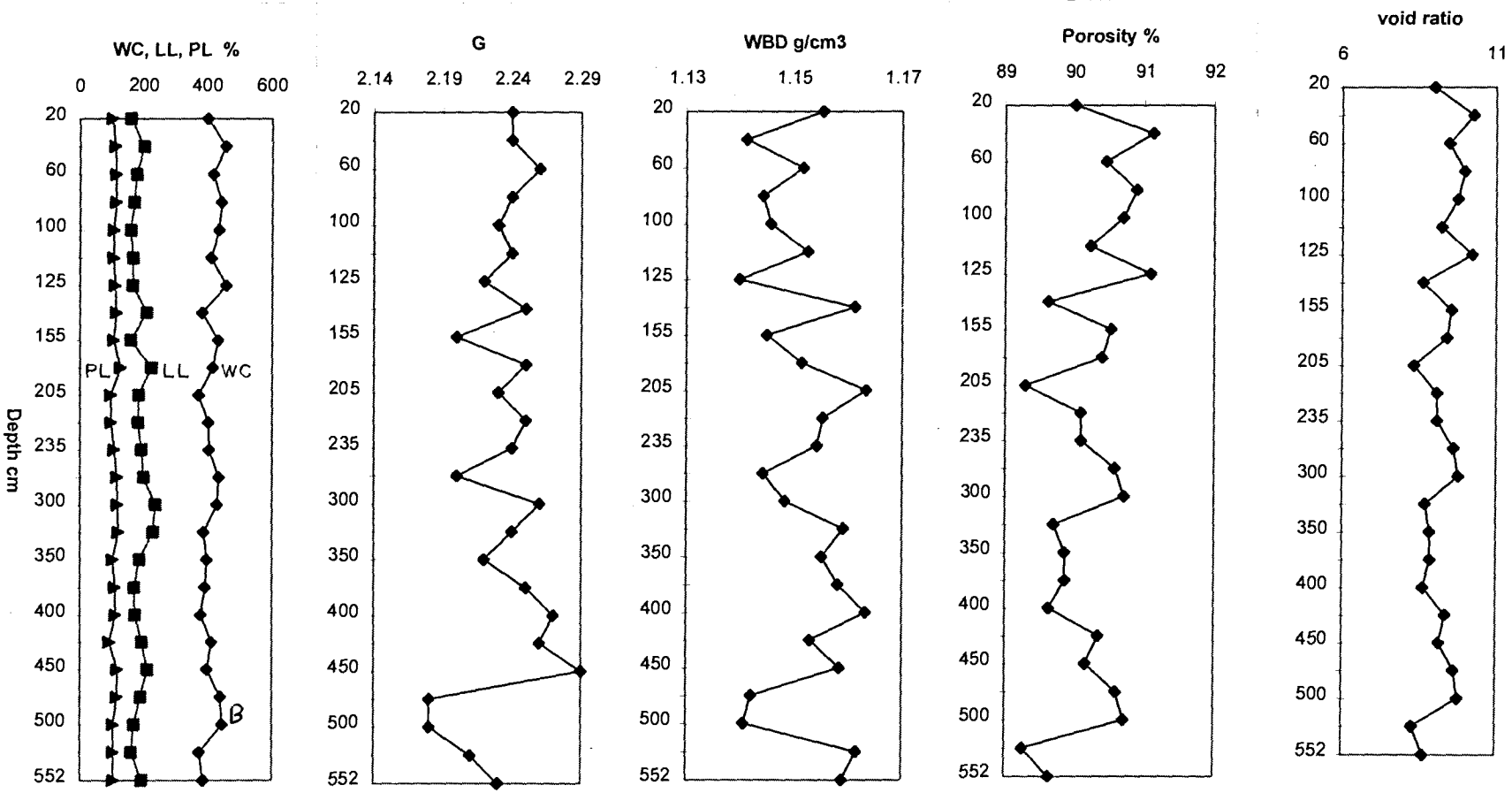

Figure 5.7: Down core variation in physical properties of the core A4/5α.

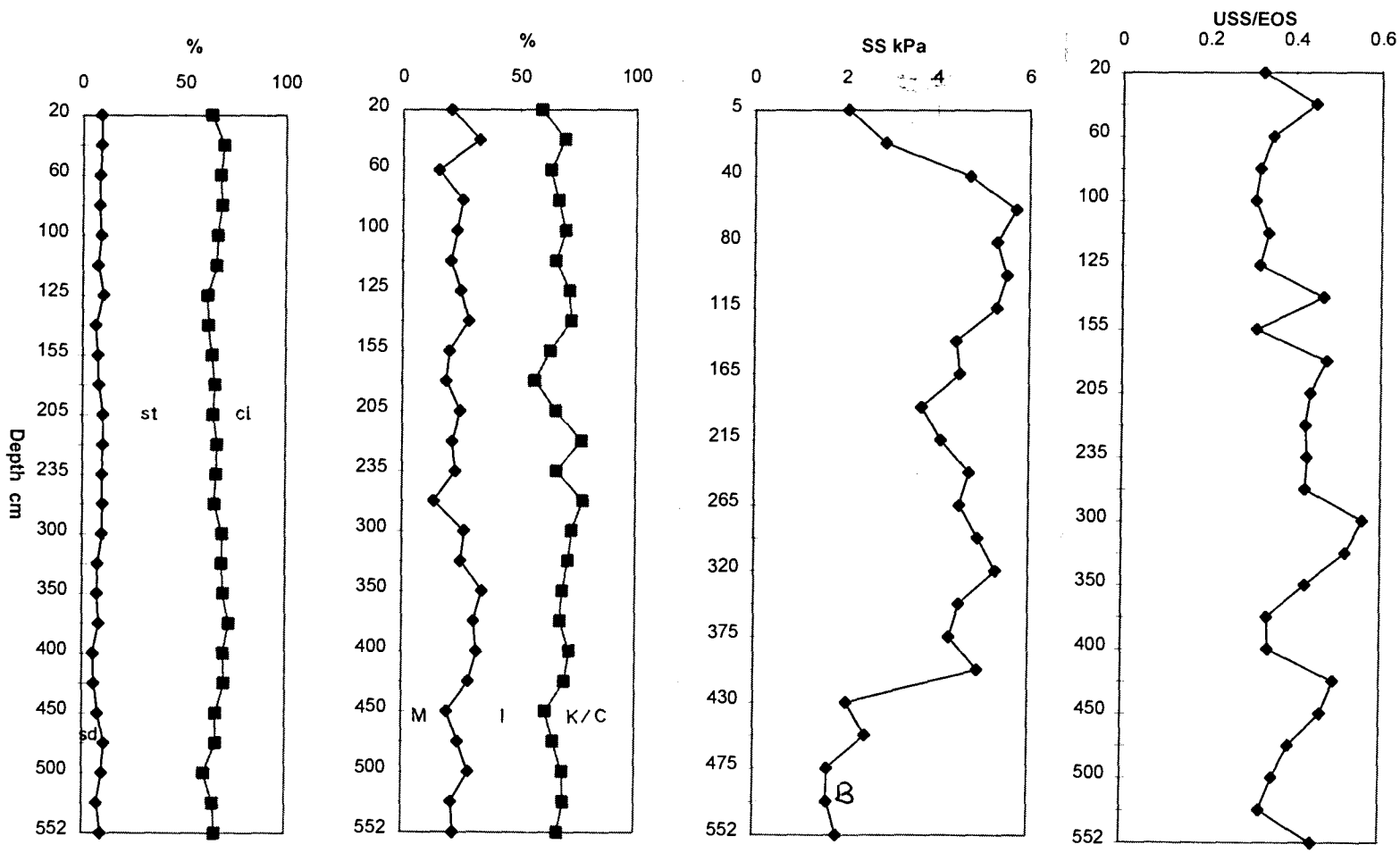

Figure 5.8: Depthwise variation in grain size, clay mineralogy and shear strength of the core A4/5a
(sd = >63μm fraction, st = silt, cl = clay, M = montmorillonite, I = illite, K/C = kaolinite/chlorite)

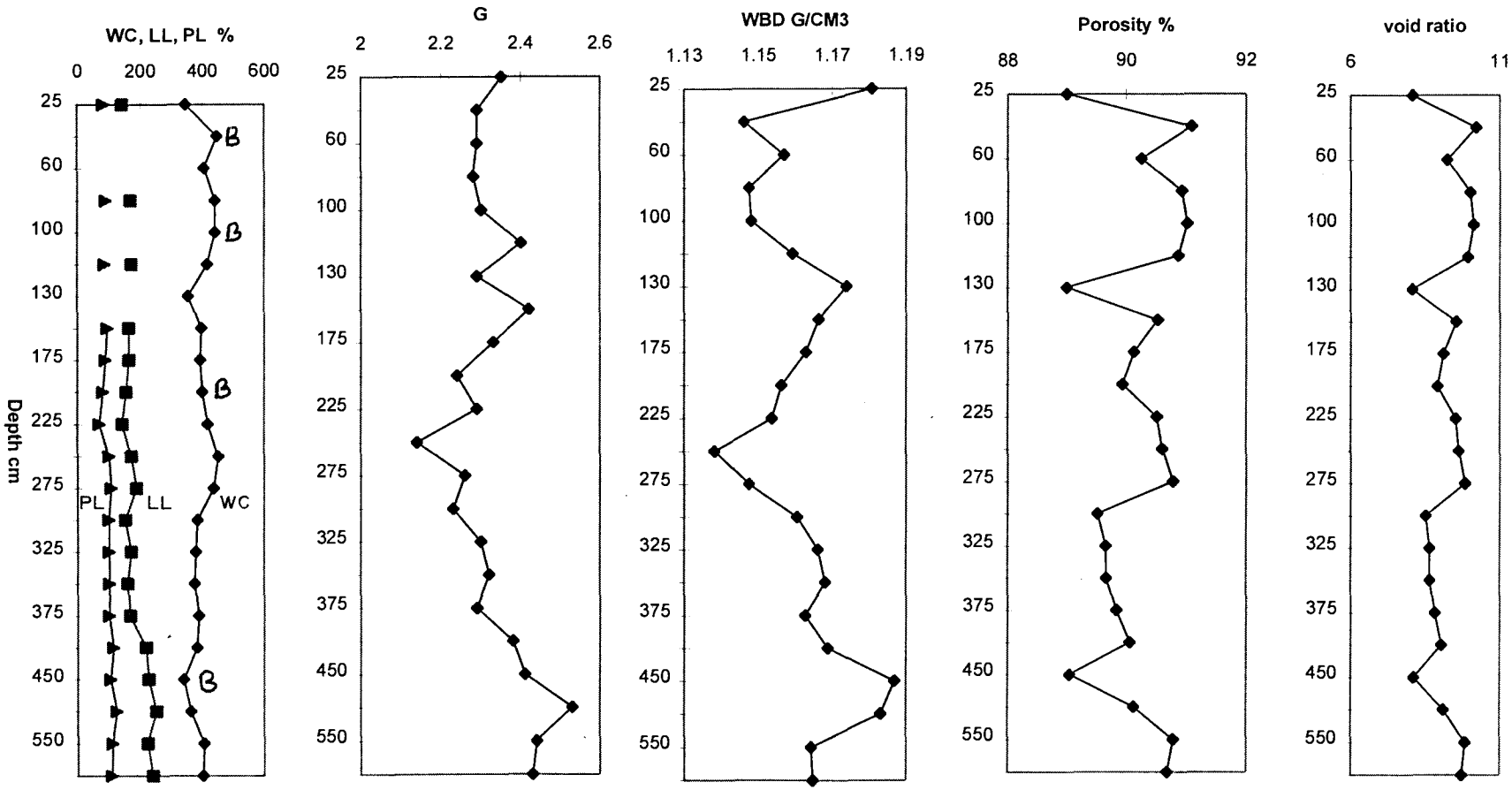

Figure 5.9: Down core variation in physical properties of the core A4/6.

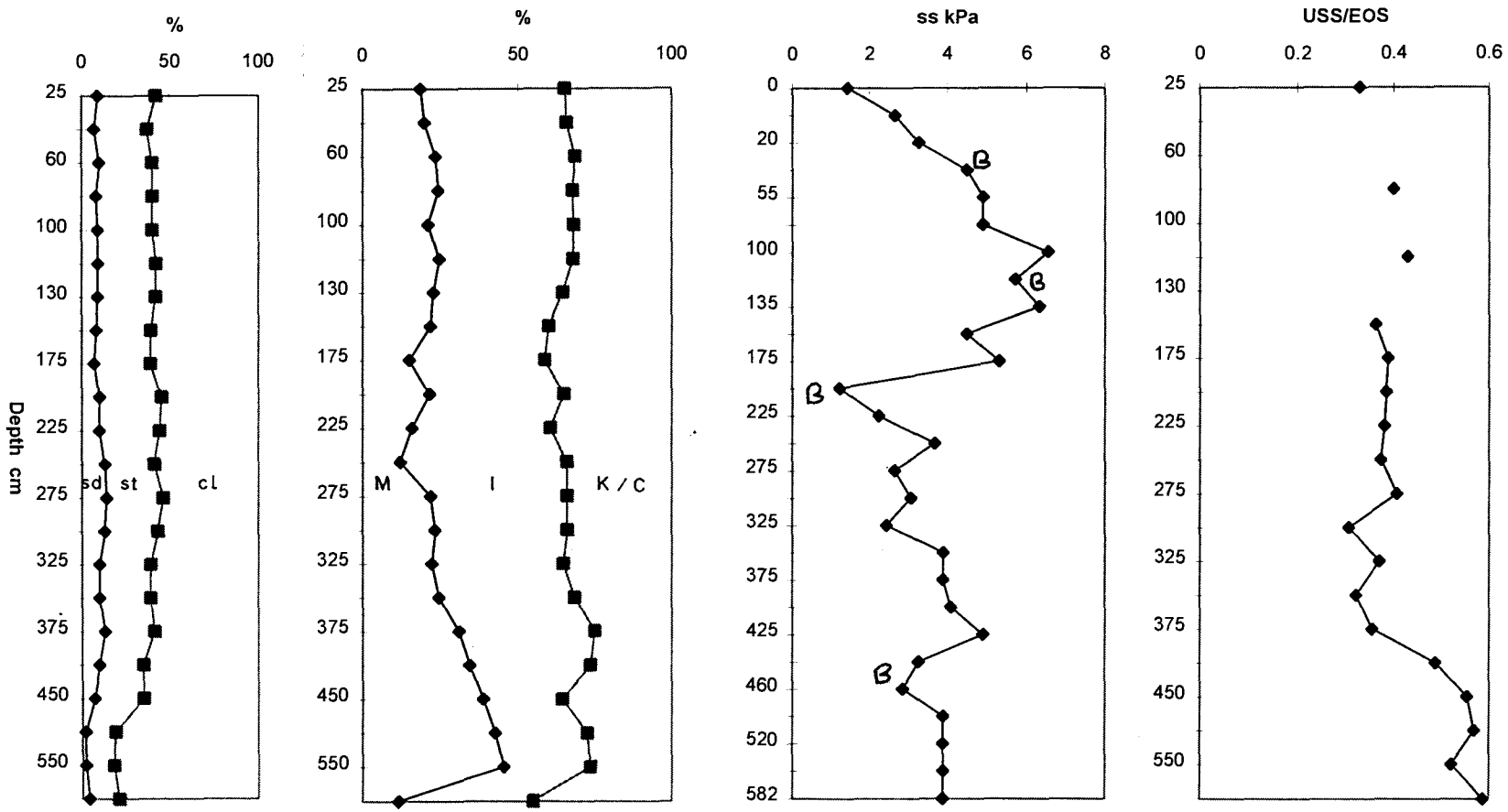

Figure 5.10: Depthwise variation in grain size, clay mineralogy and shear strength of the core A4/6.
(sd = >63μm fraction, st = silt, cl = clay, M = montmorillonite, I= illite, K/C = kaolinite/chlorite)

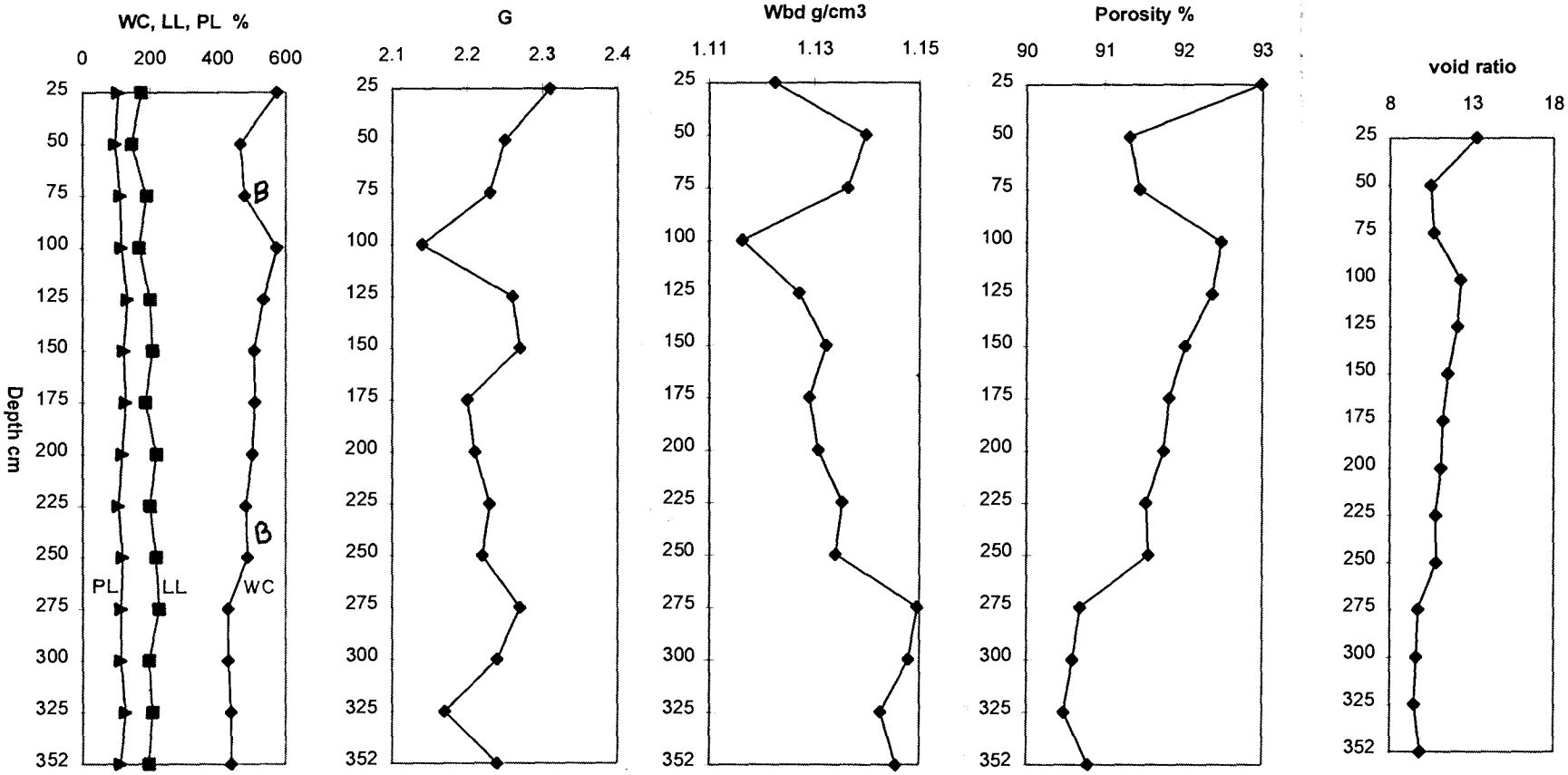

Figure 5.11: Down core variation in physical properties of the core A4/12.

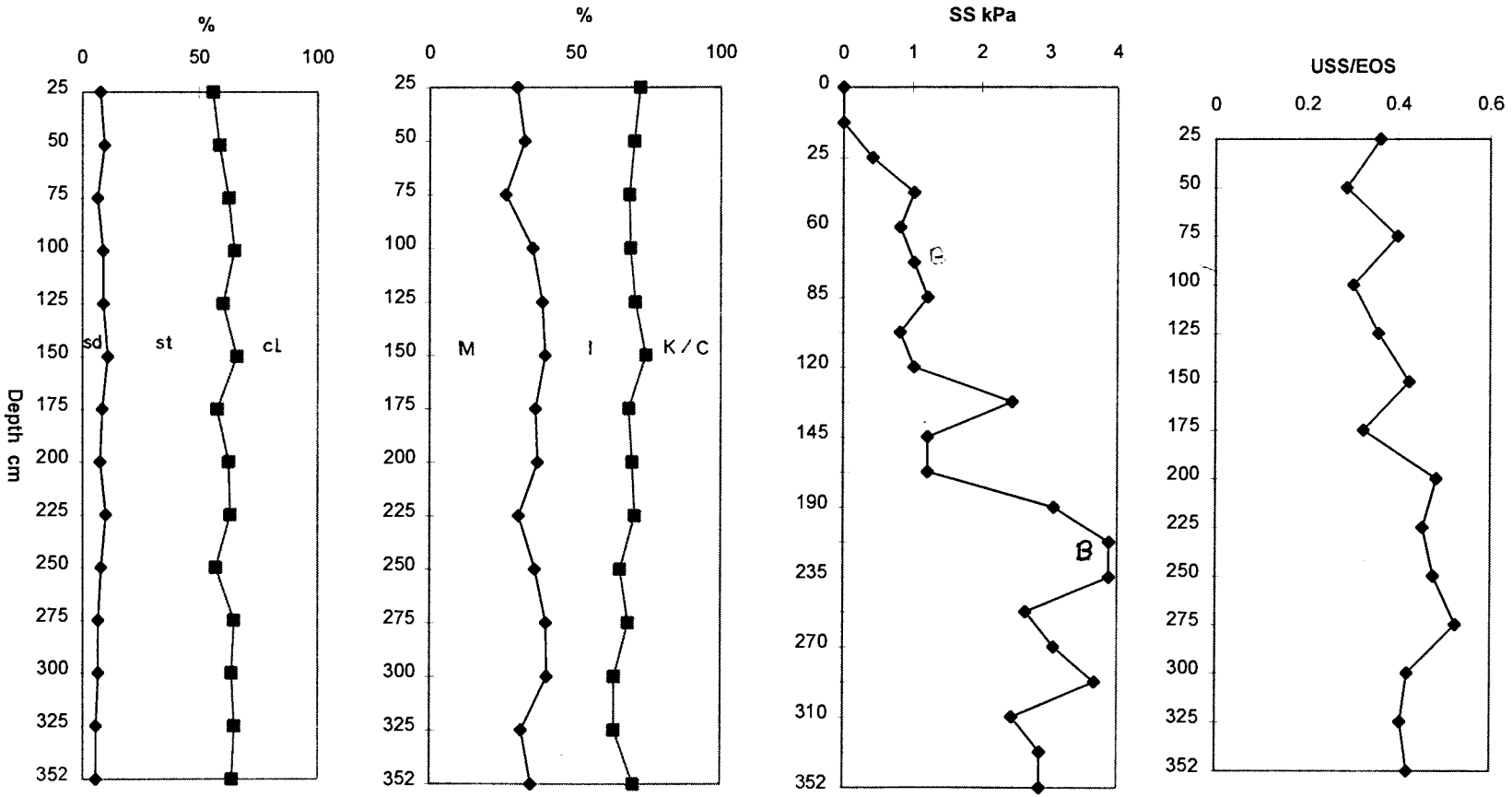

Figure 5.12: Depthwise variation in grain size, clay mineralogy and shear strength of the core A4/12.
(sd = >63μm fraction, st = silt, cl = clay, M = montmorillonite, I = illite, K/C = kaolinite/chlorite)

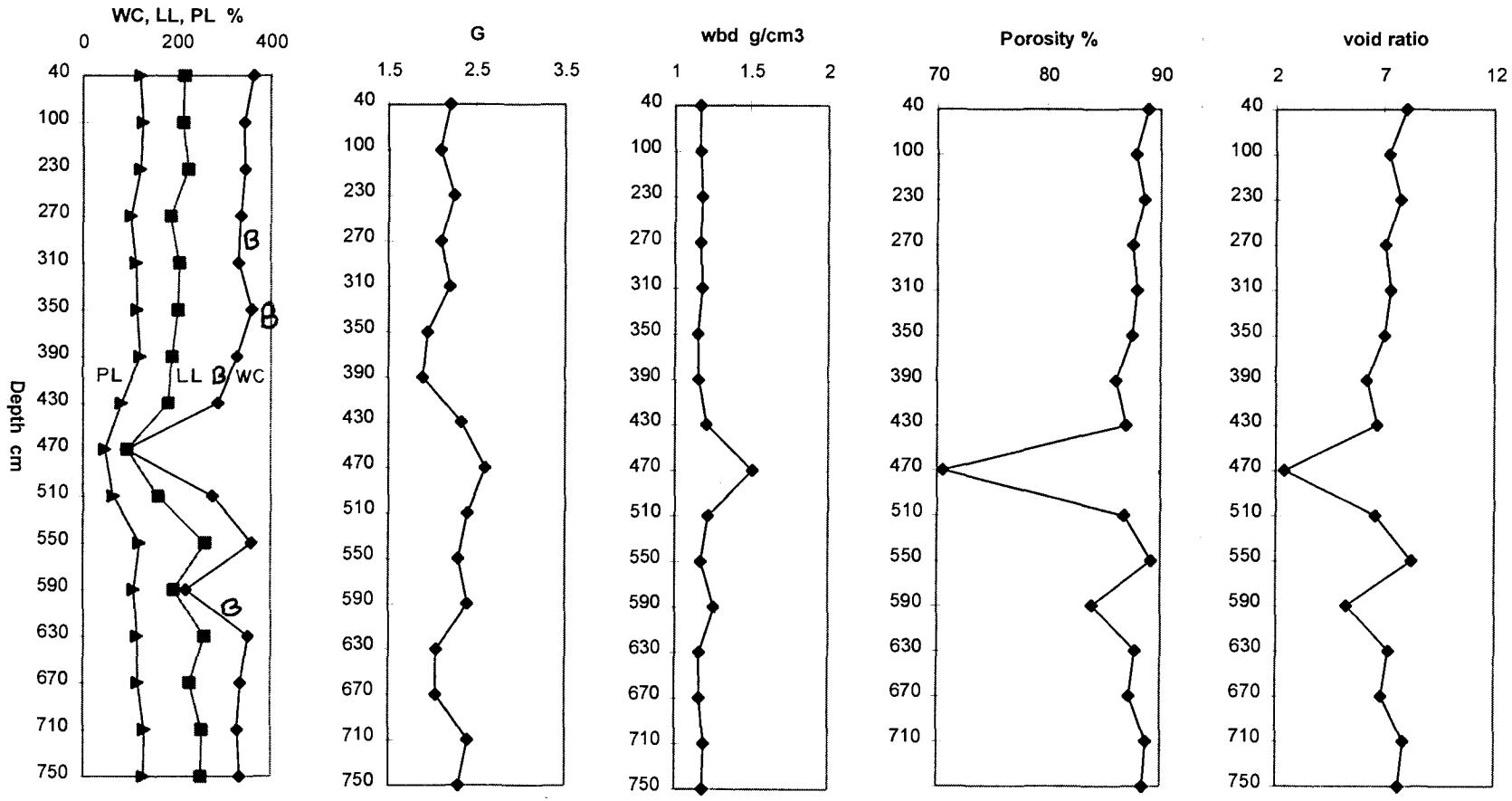

Figure 5.13: Down core variation in physical properties of the core SK69/2.

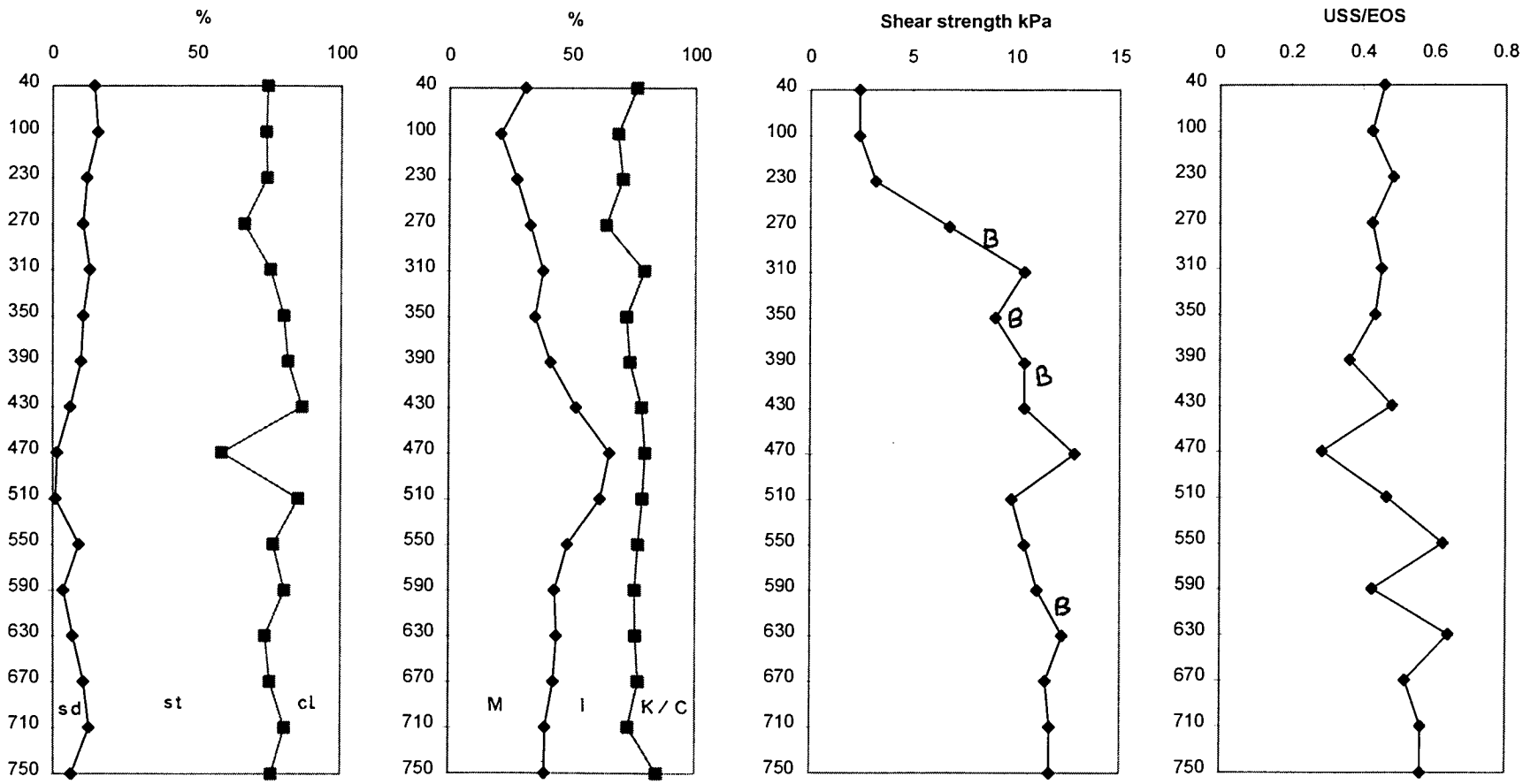

Figure 5.14: Depthwise variation in grain size, clay mineralogy and shear strength of the core SK69/2.
(sd = >63μm fraction, st = silt, cl = clay, M = montmorillonite, I = illite, K/C = kaolinite/chlorite)

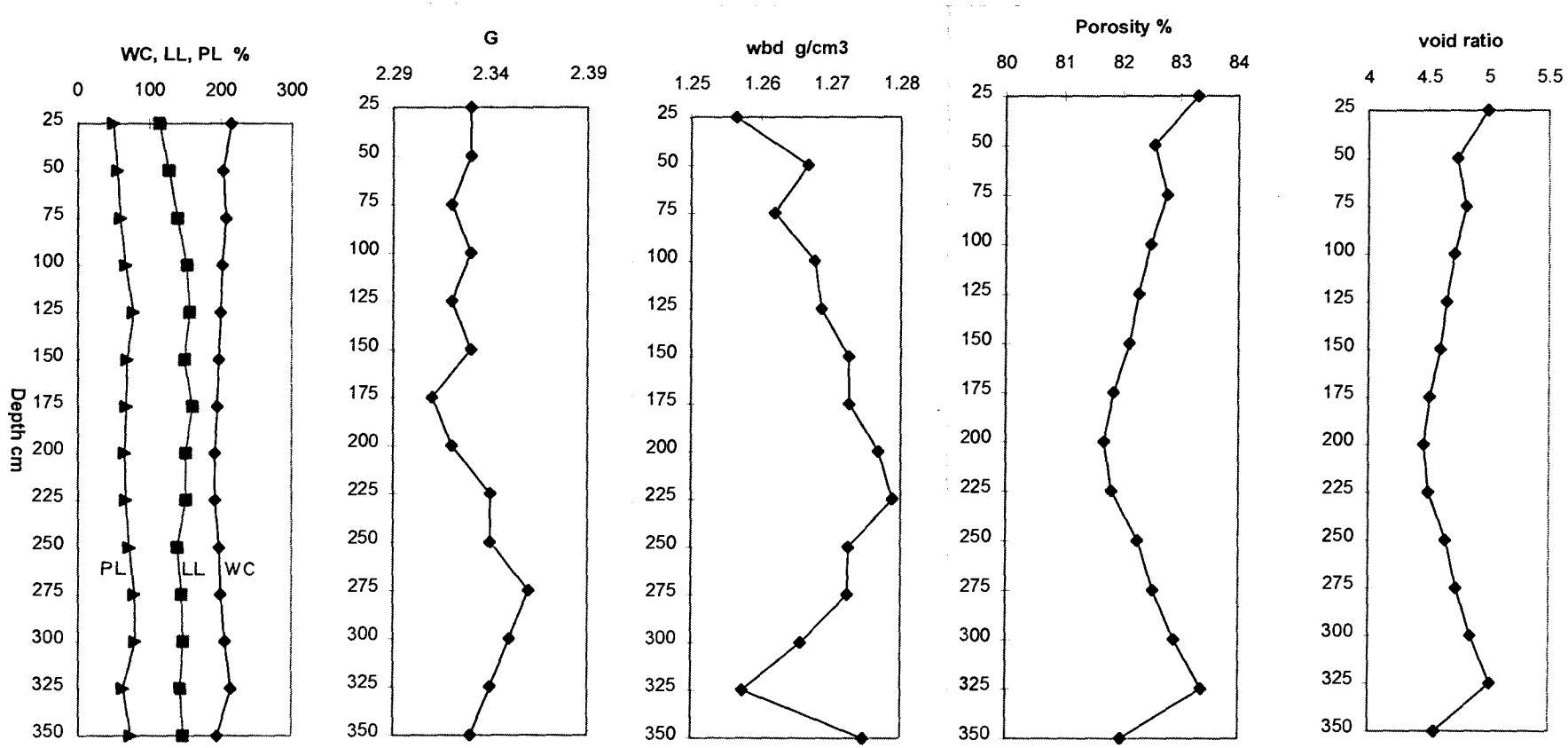

Figure 5.15: Down core variation in physical properties of the core A4/13.

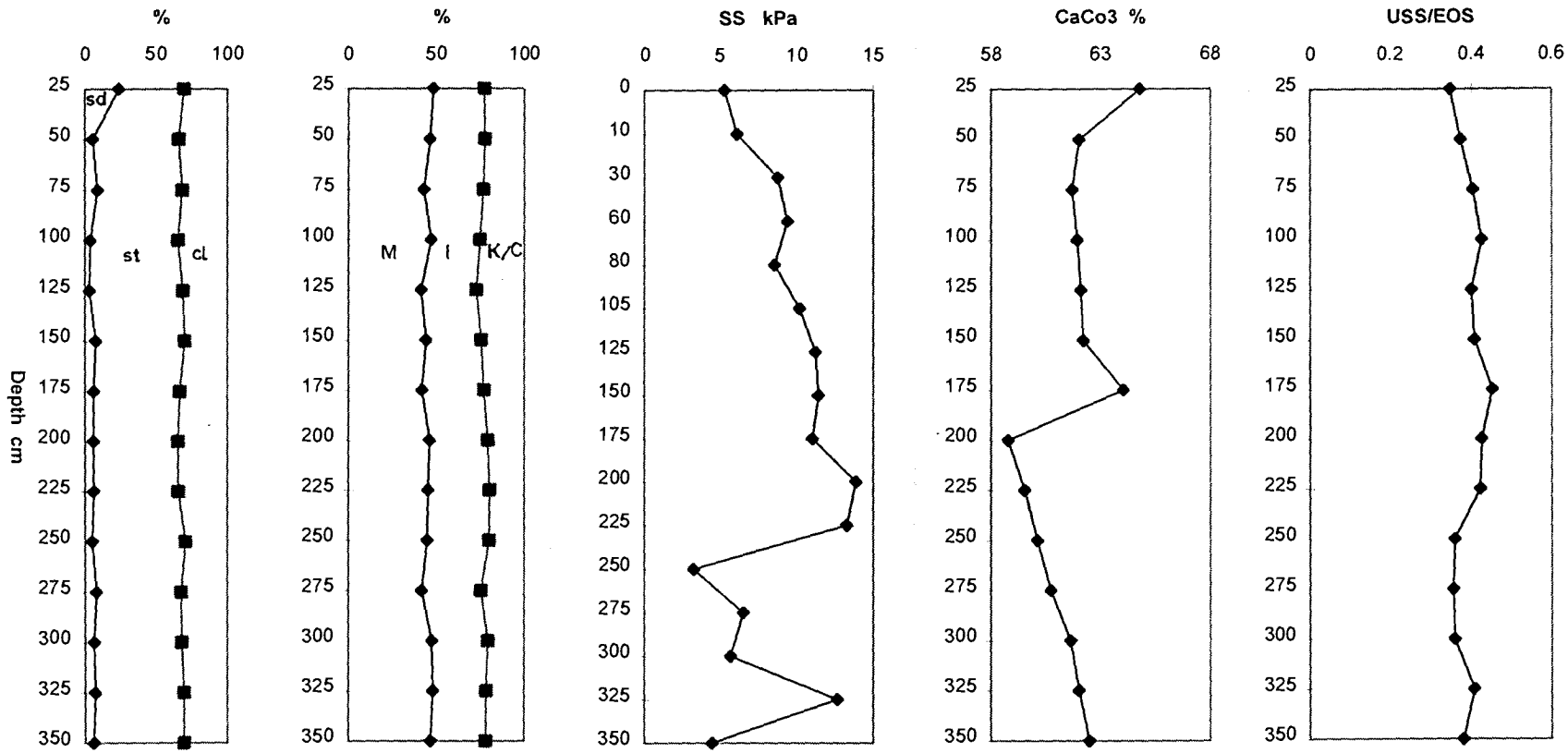

Figure 5.16: Depthwise variation in grain size, clay mineralogy and shear strength of the core A4/13.
(sd = >63μm fraction, st = silt, cl = clay, M = montmorillonite, I = illite, K/C = kaolinite/chlorite)

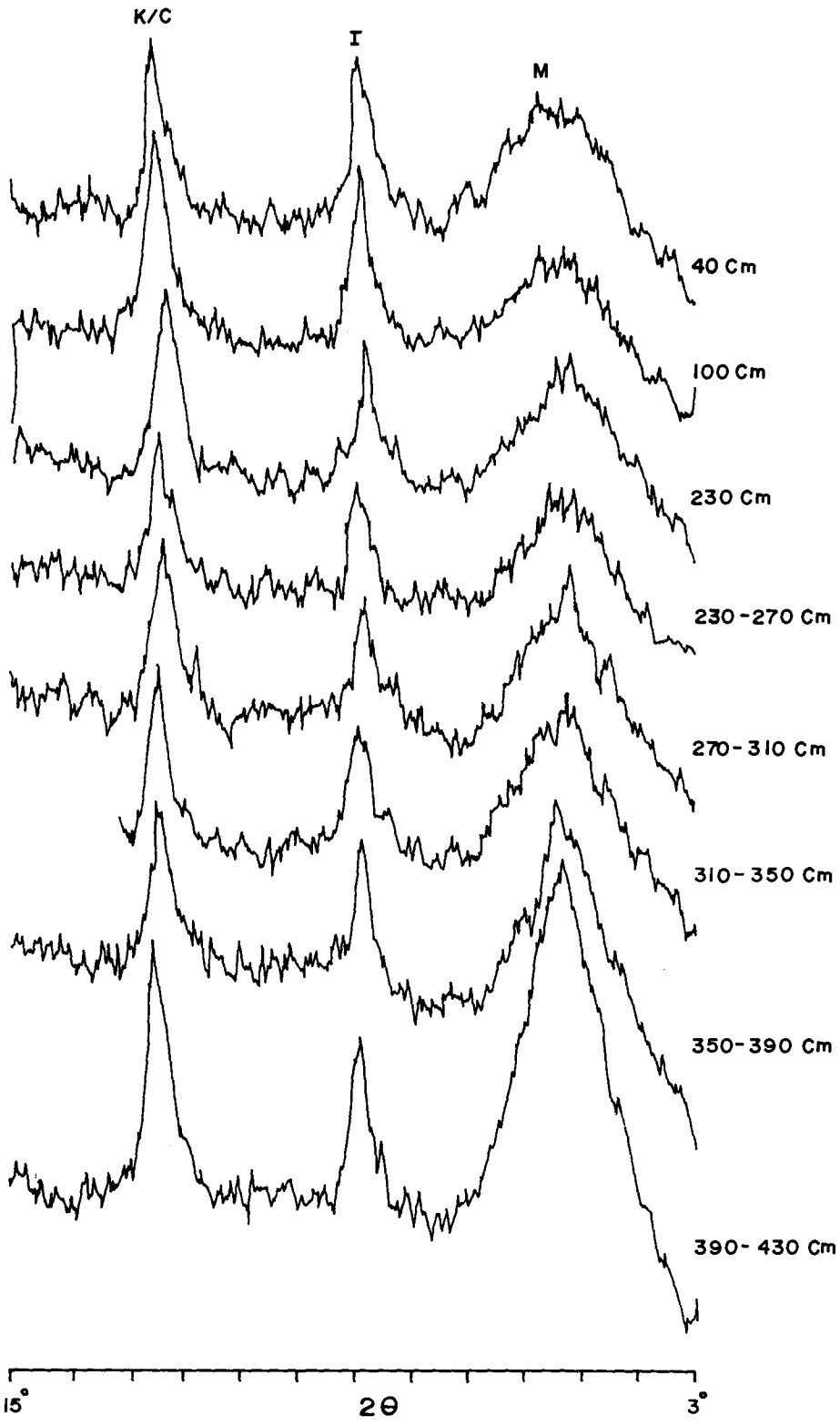

Fig. 5.17 X-RAY DIFFRACTOGRAMS OF CLAY MINIRALS (SK 69/2) AFTER GLYCOLATION ; M Montmorillonite, I = Illite K/C = Kaolinite / Chlorite

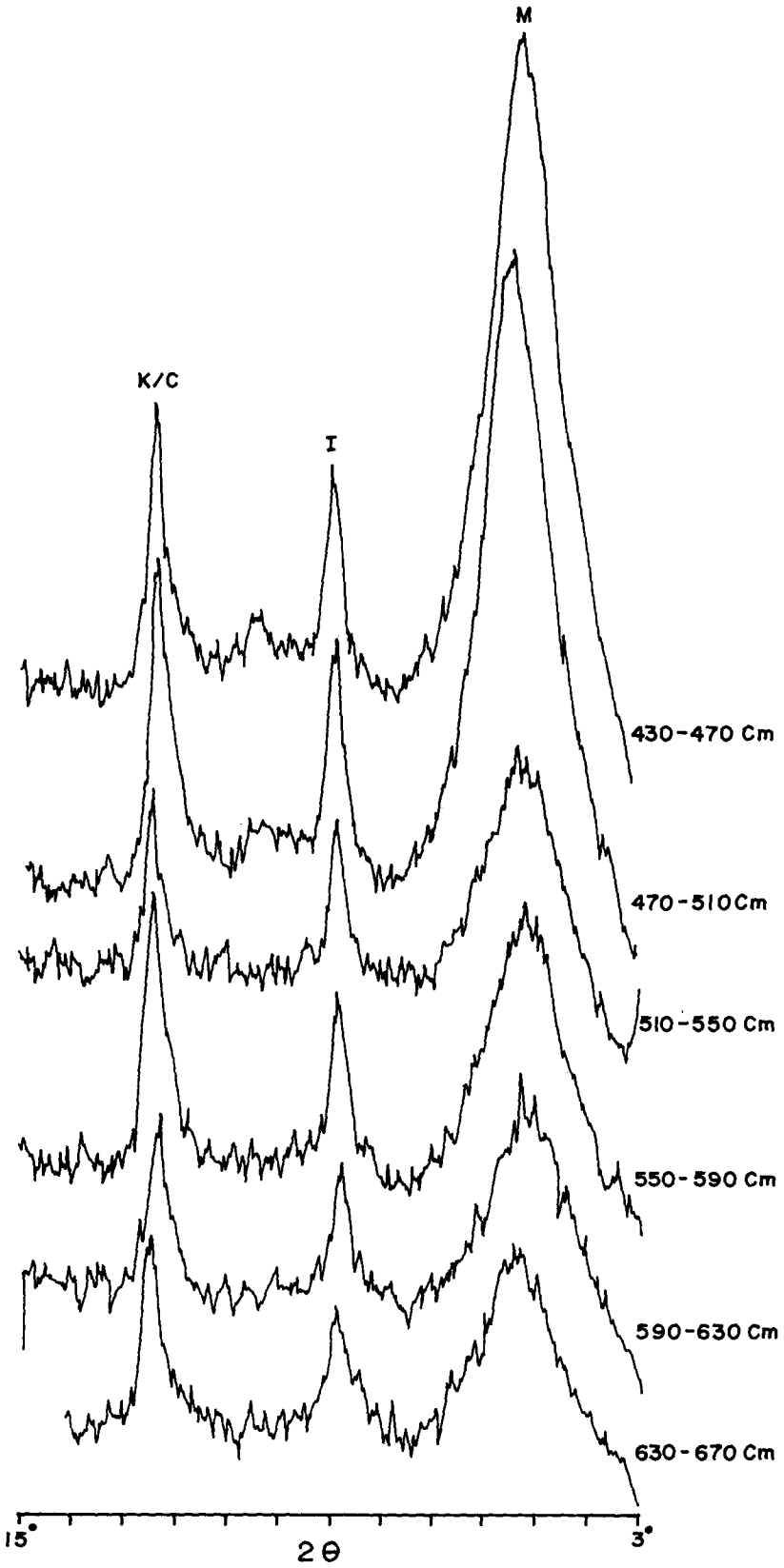

Fig.5.18 X-RAY DIFFRACTOGRAMS OF CLAY MINIRALS (SK69/2) AFTER GLYCOLATION ; M=Montmorillonite, I = Illite K/C = Kaolinite / Chlorite

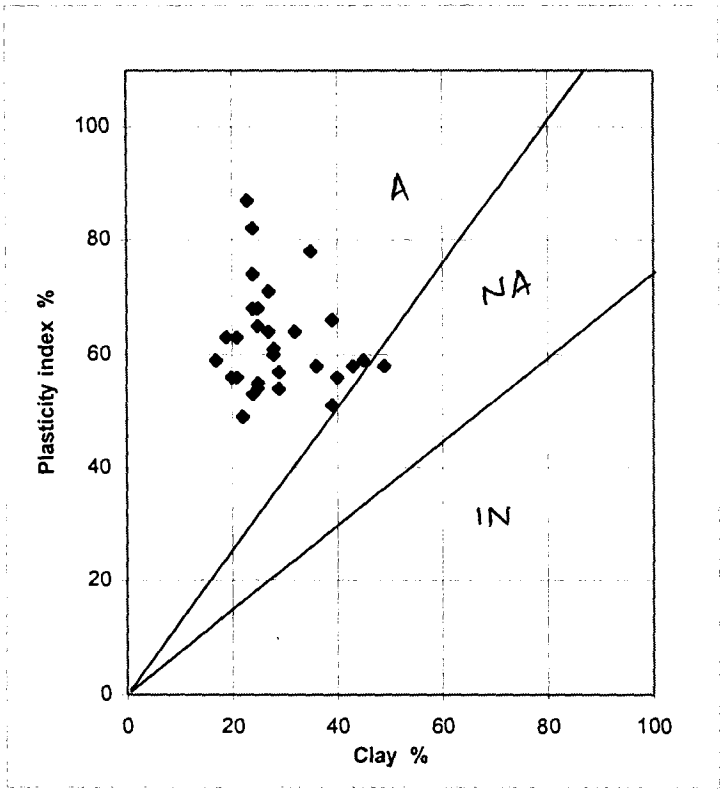

Activity chart

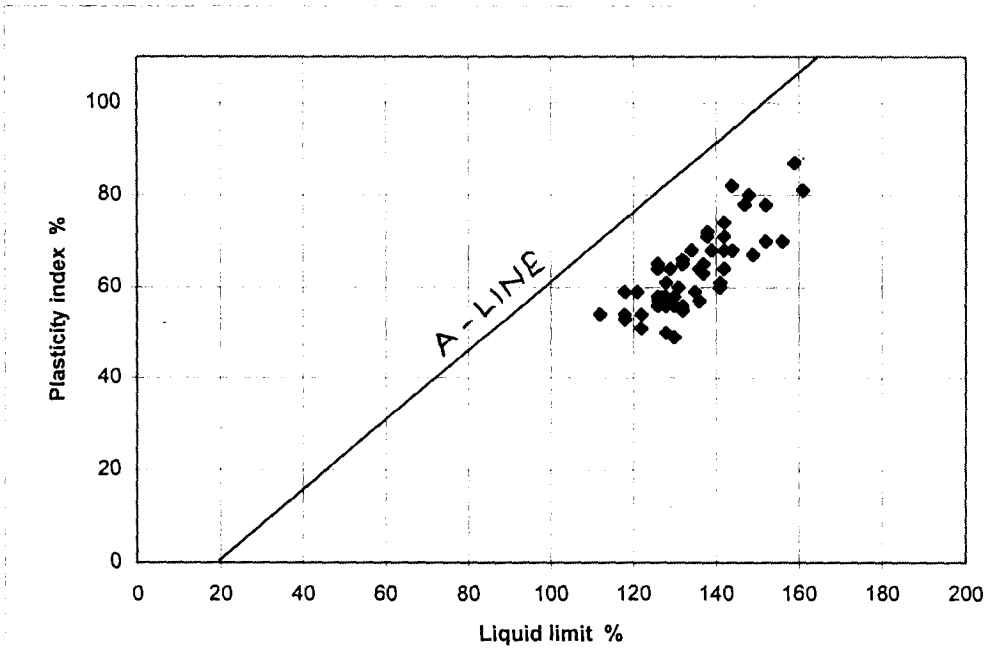

Plasticity chart

Figure 5.19: Activity and plasticity charts for the core A4/1

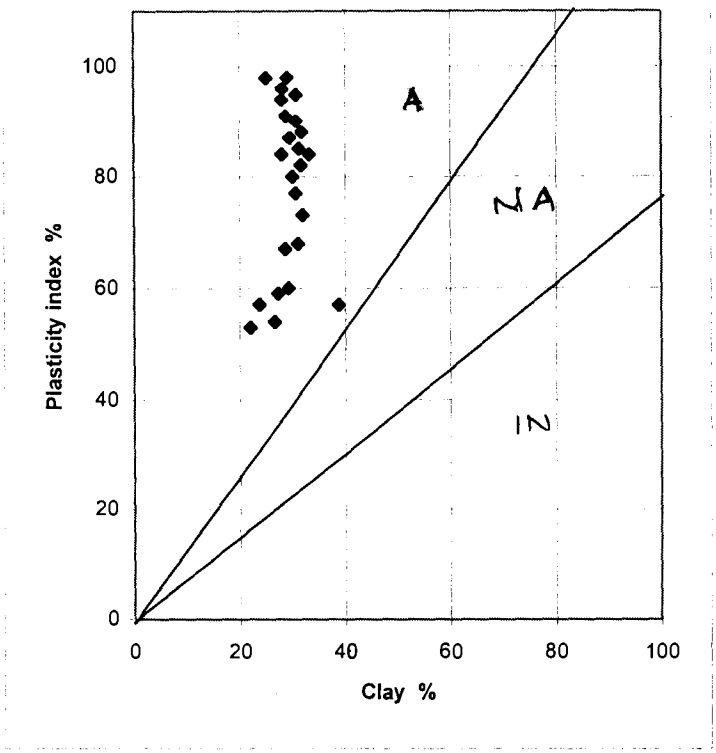

Activity chart

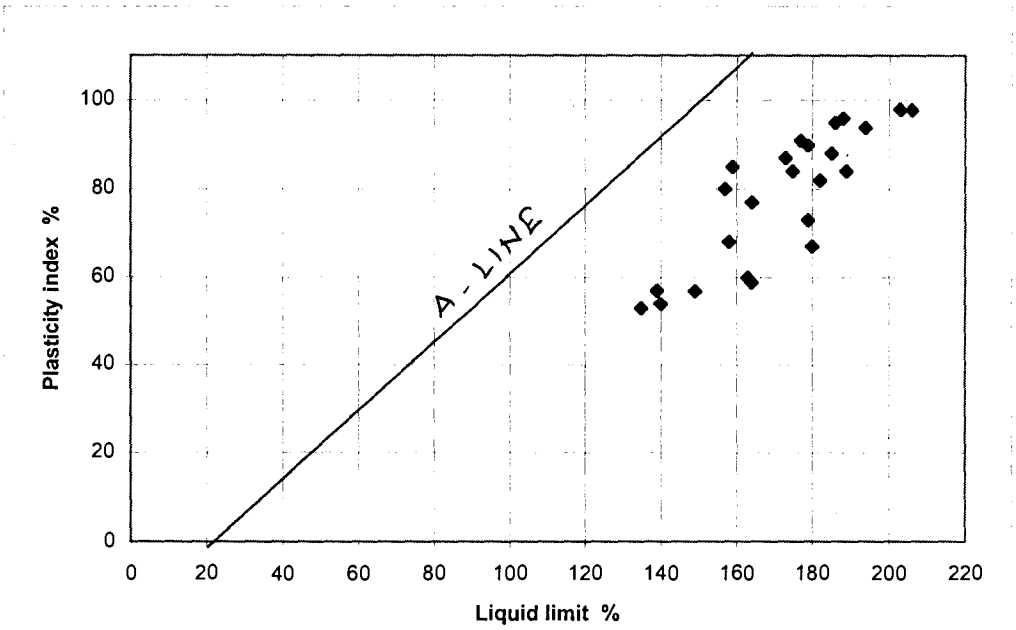

Plasticity chart

Figure 5.20: Activity and plasticity charts for the core GC-1

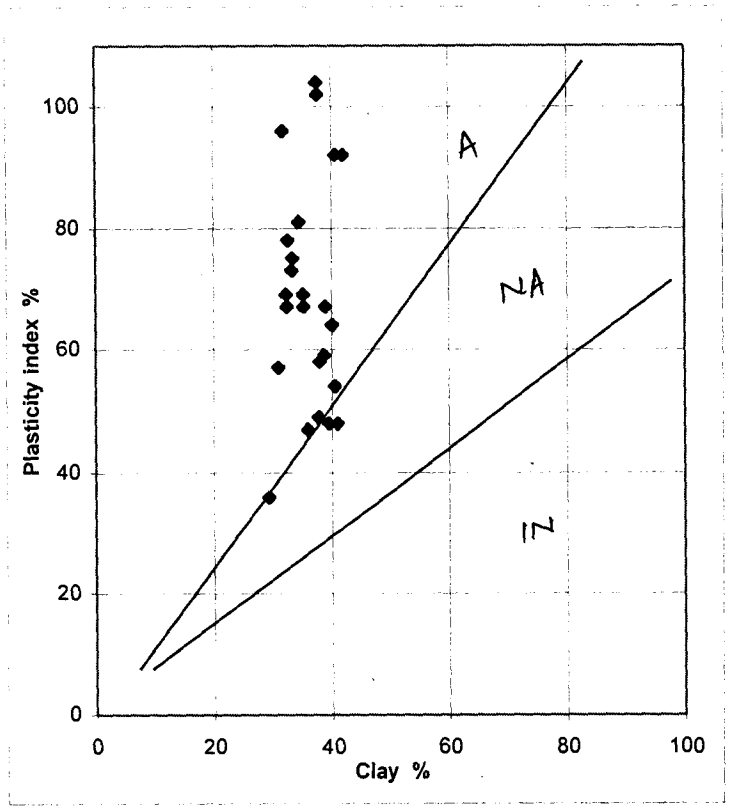

Activity chart

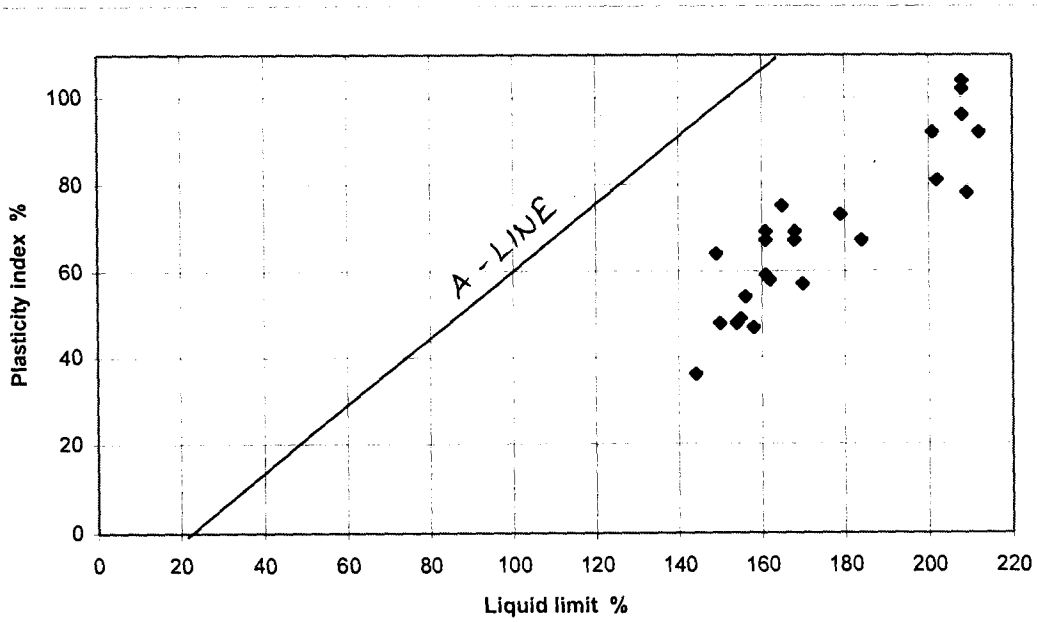

Plasticity chart

Figure 5.21: Activity and plasticity charts for the core A4/2

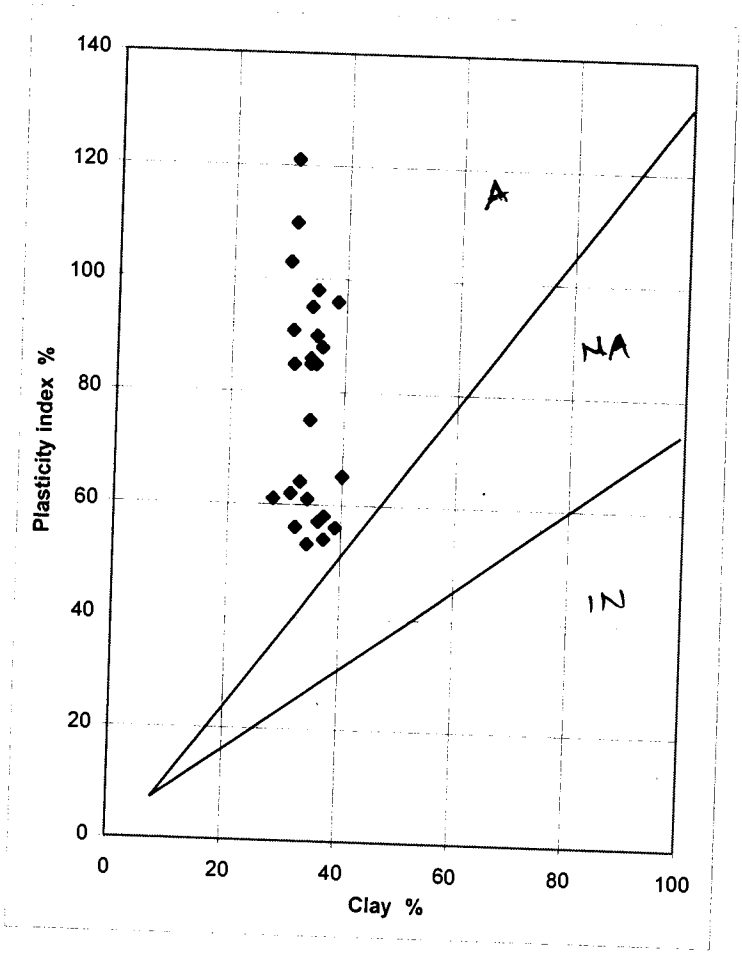

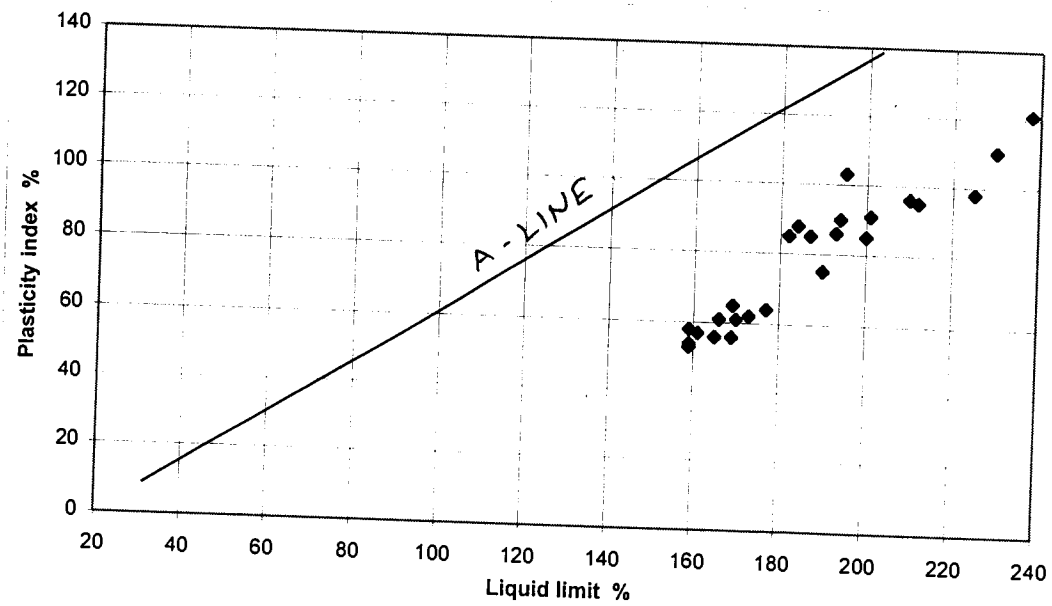

Figure 5.22: Activity and plasticity charts for core A4/5a

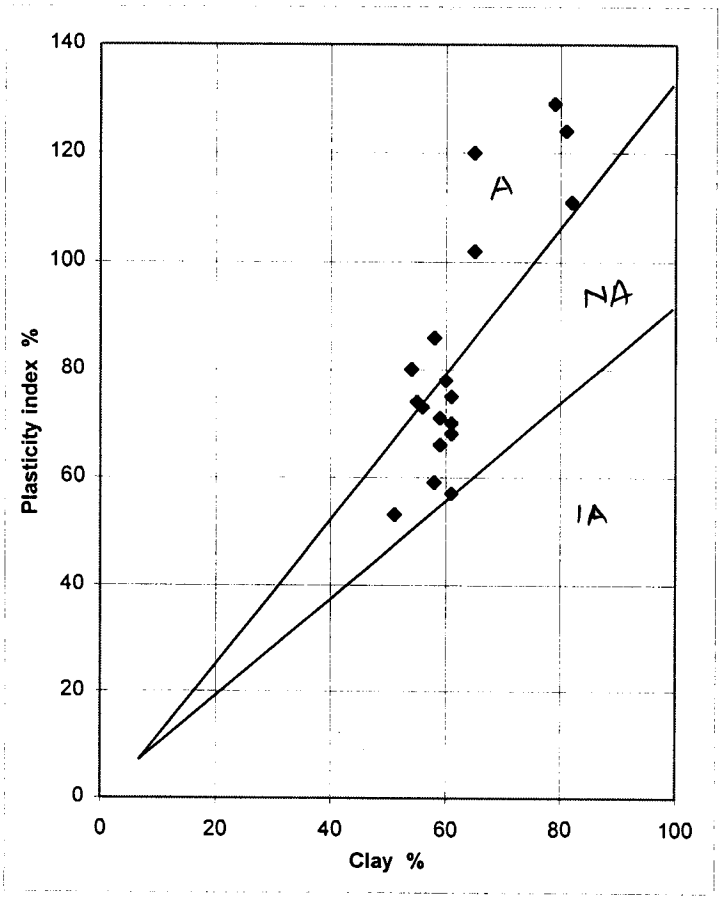

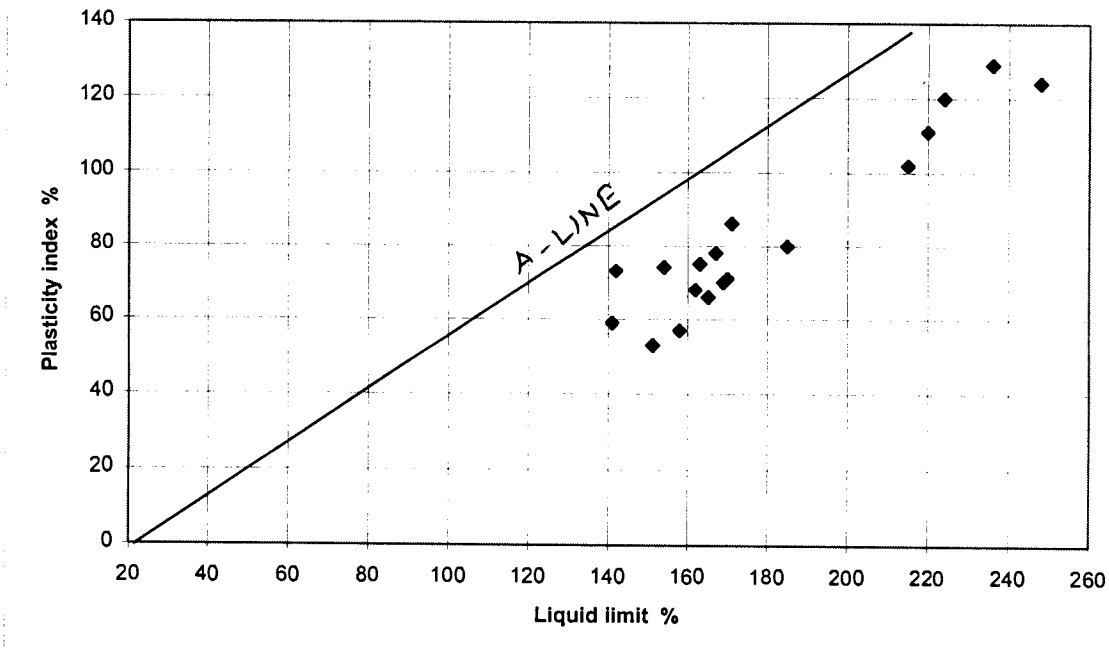

Figure 5.23: Activity and plasticity charts for core A4/6

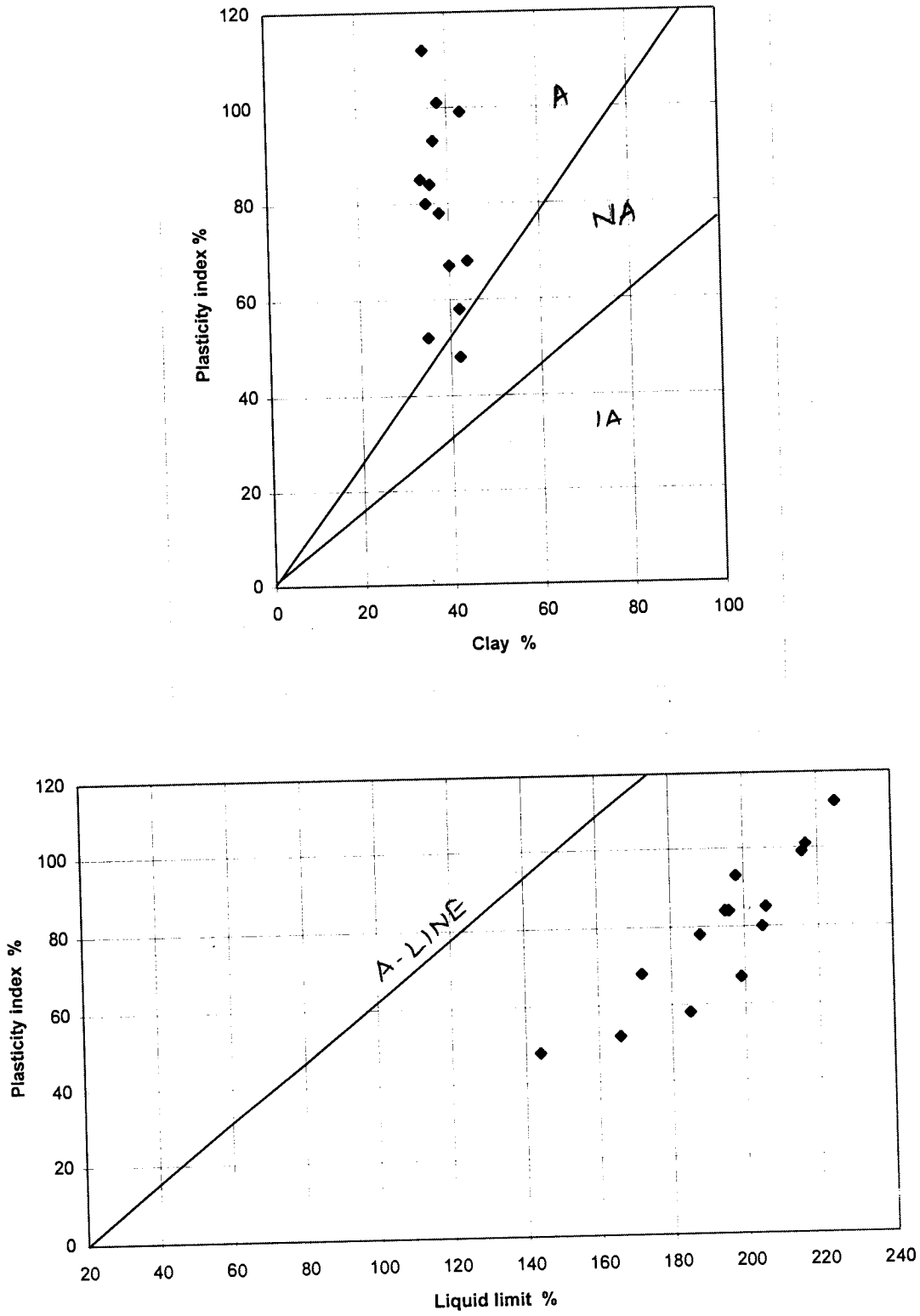

Figure 5.24: Activity and plasticity charts for the core A4/12

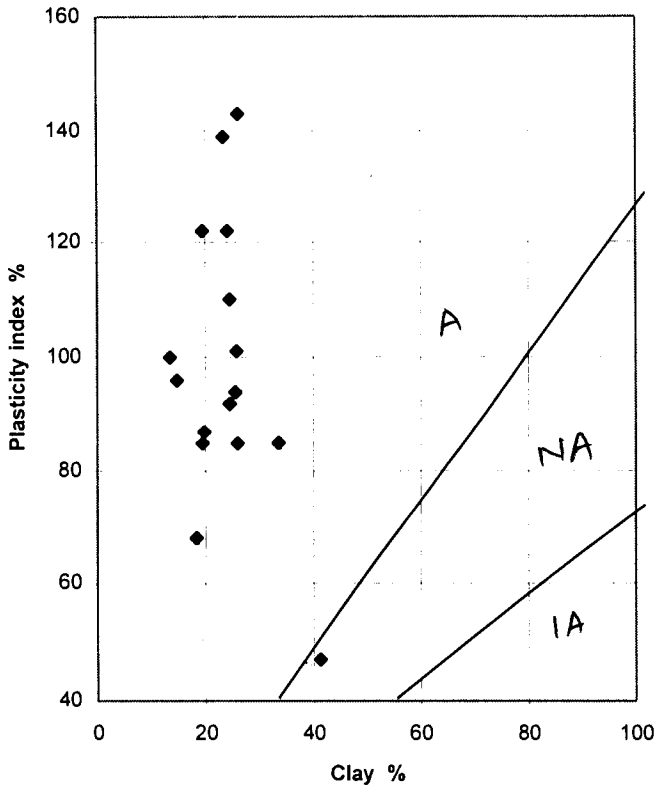

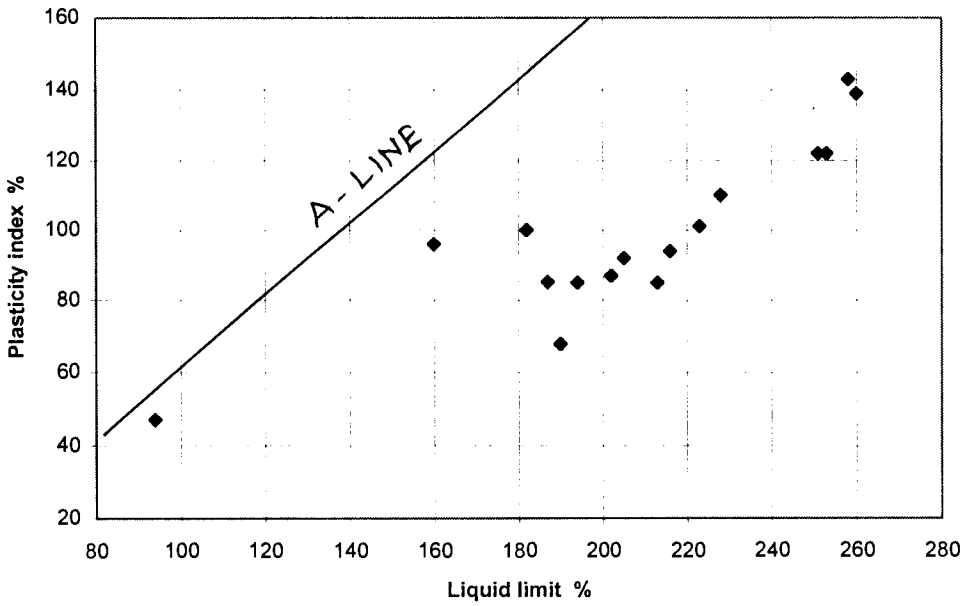

Figure 5.25: Activity and plasticity charts for core SK69/2

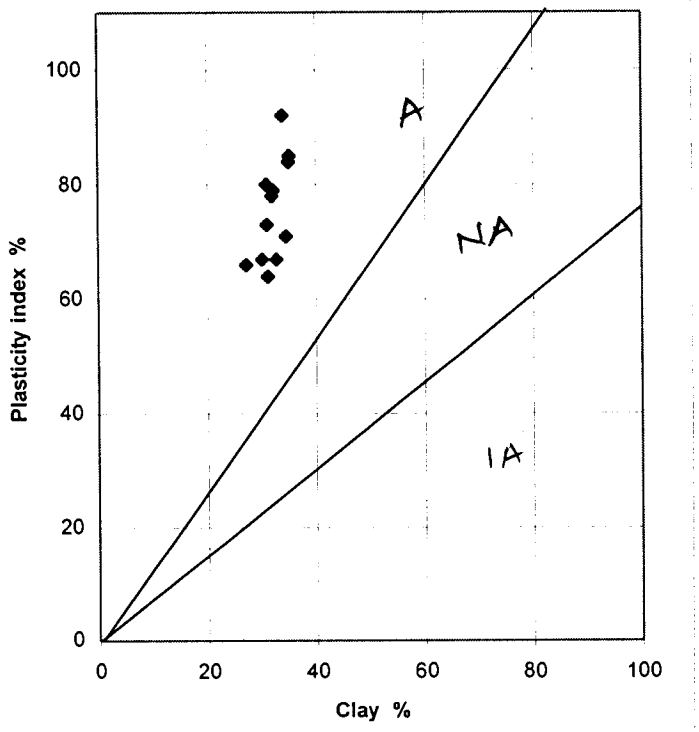

Activity chart

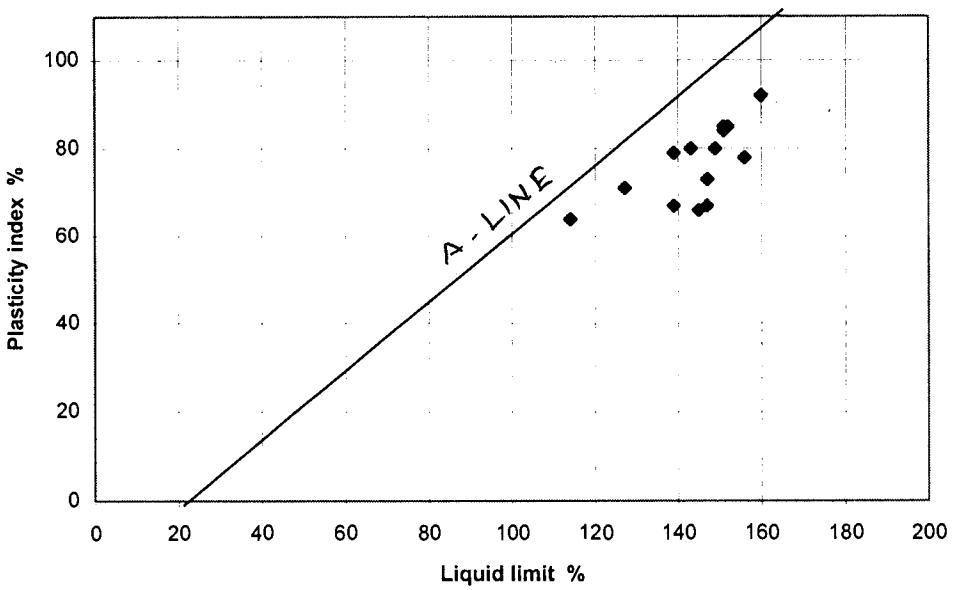

Plasticity chart

Figure 5.26: Activity and plasticity charts for core A4/13

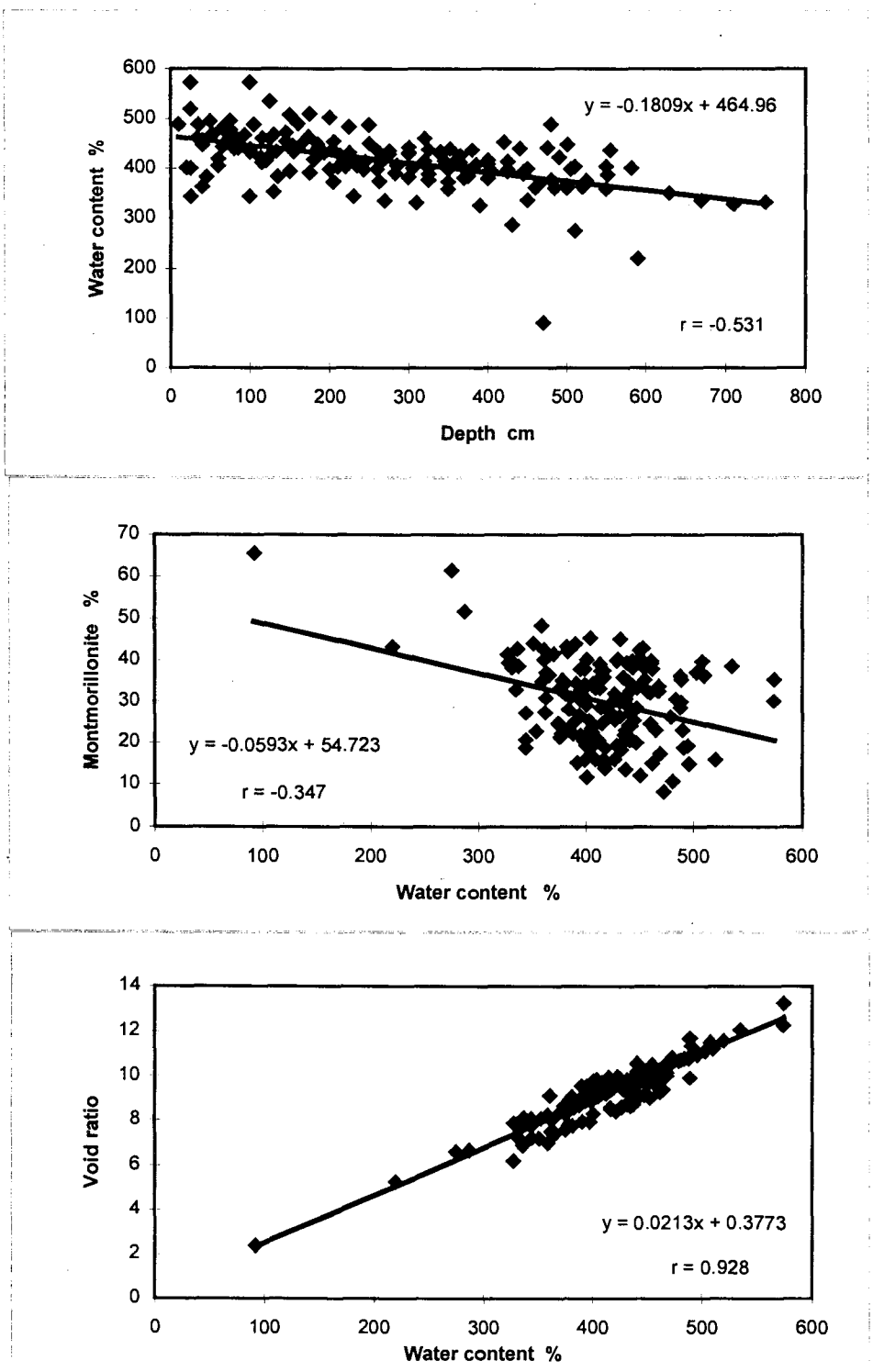

Figure 5.27: Variation of water content with depth, montmorillonite and void ratio in siliceous sediments from the CIB.

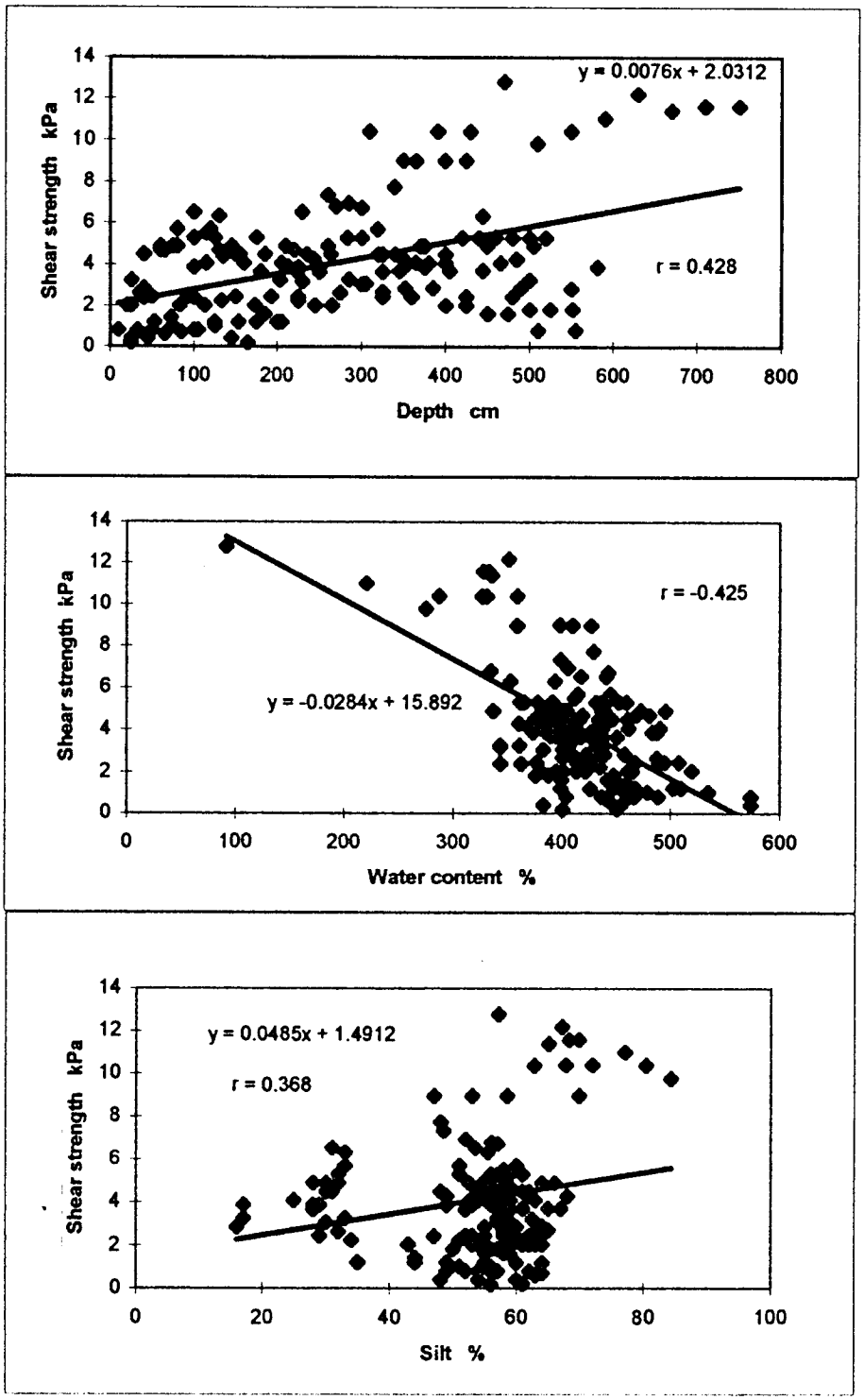

Figure 5.28: Relationship of shear strength with depth, water content and silt in siliceous sediments from the CIB.

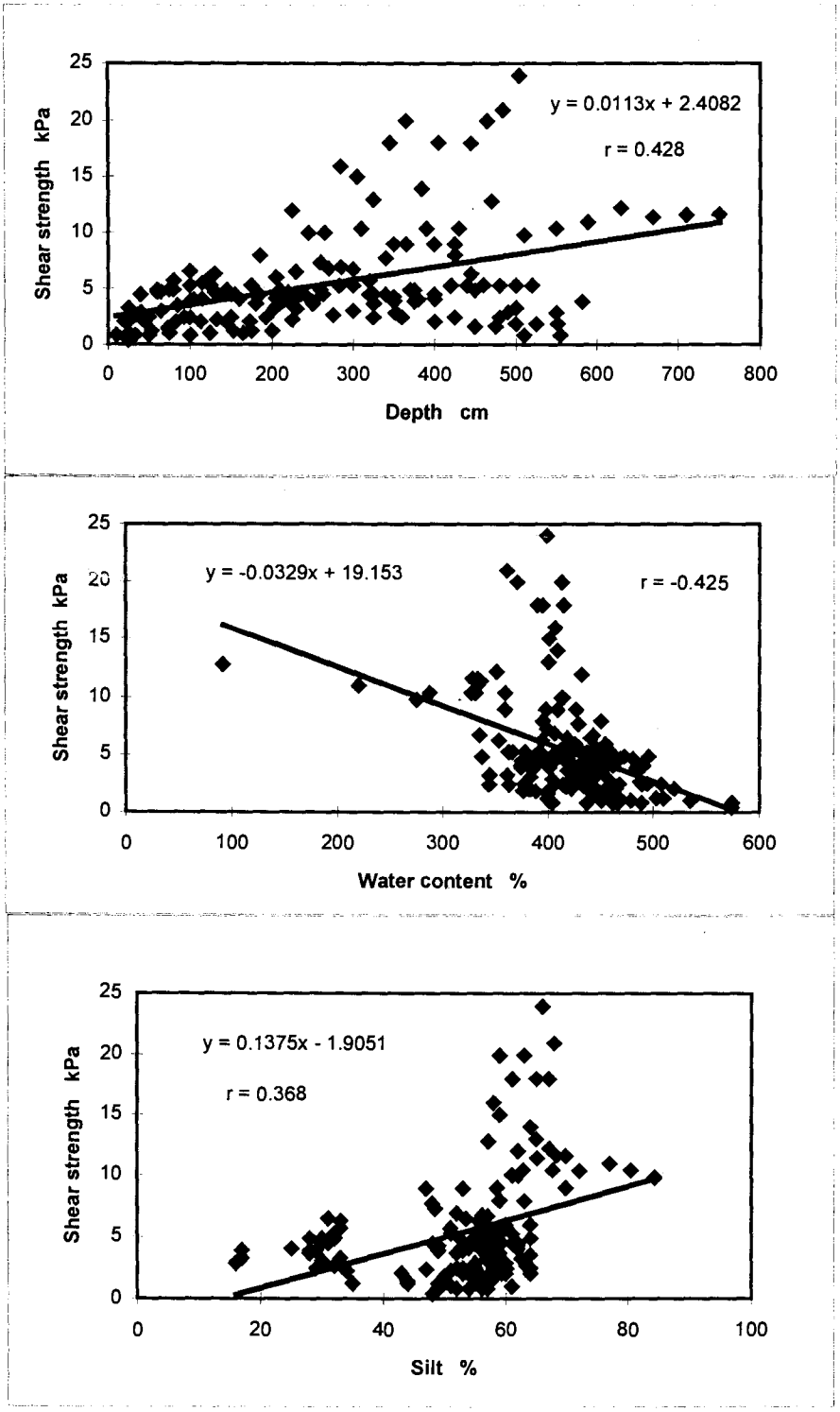

Figure 5.28: Relationship of shear strength with depth, water content and silt in siliceous sediments from the CIB.

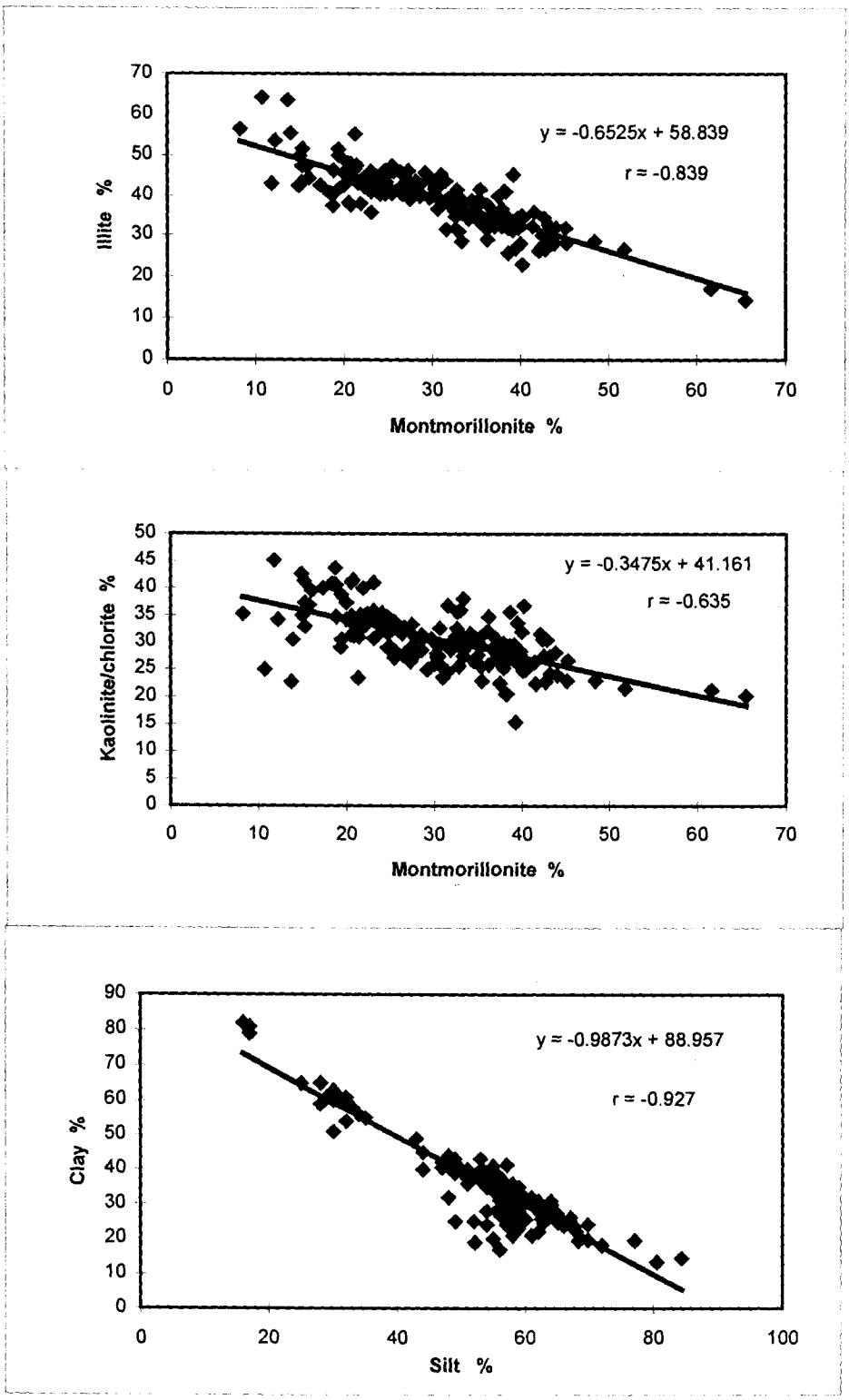

Figure 5.29: Relationships among grain size and clay minerals from siliceous sediments from the CIB.

CHAPTER 6

BENTHIC DISTURBANCE STUDIES

As nodule mining activity involves large instruments and infrastructure, it is likely to create a set of entirely new conditions on the seafloor and benthic environment. The sediment plume caused by mining head while collecting nodules would lead to increase in density and turbidity of the bottom waters. A study (Amos and Roels, 1977) reported that with every tonne of nodule collection, about 2.5 - 5.5 tonnes of sediments ~~will~~ would be resuspended. This may create ~~non~~un suitable conditions at bottom waters for the benthic community.

As an UNCLOS requirement, the environmental impact assessment studies in the Central Indian Basin are essential before mining. For this geological, biological and chemical parameters were studied in sediment cores collected before and after the simulated disturbance on the seafloor. A square shaped area of 10 x 10 nautical mile with plain topography was chosen at 10°0'S and 10° 10'S latitudes and 75° 55'E and 76° 05'E longitudes. A NW - SE trending strip of 3000 m length and 200 m width was disturbed (Figure 6.1). The area has siliceous ooze sediments with very few nodules (abundance, 2 kg/m^2) and flat topography with relief of 20 m. Disturbance was created by hydraulic device which fluidises, resuspends and discharges sediment slurry 5 m above the seafloor. The overall disturbance was carried out for 88 km distance (26 tows) which resulted in resedimetation of 6000 cubic meter of sediments. Similar disturbance techniques were used in the Pacific Ocean by Japan and Russia.

The benthic disturber is developed by Sound Ocean System Inc., USA and operated by National Oceanographic and Atmospheric Administration

(NOAA, USA). It comprises of a tow frame, a discharge stack, two pumps, a TV camera, a depressor, a rossete, cable and deck unit. Tow frame is 4.8 x 2.4 x 5 m (Figure 6.2). This is connected with coaxial cable which tows and transmits signals and power to the disturber unit. The sleds at the bottom of frame can collect nodules while moving on the sediments. Discharge stack is 5 m high and 30 cm in diameter with funnel shaped bottom, where sediments are sucked in and discharged from the top at 5 m height. Out of two pumps, one is used for fluidising sediments through 16 nozzles and the another for sucking in and discharging it. The TV camera is attached to view functioning of disturber, which is monitored on deck unit. This can be attached on top to view discharge or at front of the frame to view seafloor. Depressor weighs about one tonne and is attached 200 m ahead of disturber to dampen ship's motions affecting disturber. A 21 mm coaxial cable is used for deploying, operating and transmitting power and signal to and from the system. Deck unit is a PC based system to monitor and control the operation of disturber. The choking of pumps can be sensed through the current levels and corrective measures can be taken. The camera, lights, rossette can be operated from this unit. Also the video images transmitted by slow scan camera can be seen on TV screen.

6.1 Operation of disturber

The disturber is lowered in the water with stabilizing fins which keep it oriented forward and right side up. The depressor along with transponder for acoustic positioning of the body is 200 m before the disturber, reduces effect of rolling and pitching, and cable movement on the disturber.

Once the disturber touches Seafloor, its functioning can be monitored from the altitude, roll, pitch and heading which are displayed on the deck unit, and where the functioning of pumps is also controlled. The plume generation

can be seen on the video monitor and the average sediment pumped can be estimated by taking intermittent water samples in the rossette on the disturber. The positioning of the disturber is observed real time on acoustic navigation system and recorded for post processing.

6.2 Effect of disturbance

The effect of disturbance was observed from deep tow photography and sediment core analyses. The photographic observations show the disturbance is confined to the seabed and the resedimentation due to plume migration is restricted to adjacent area of the tow zone. Due to disturbance, the seafloor microrelief undergoes a change, sediments from lower depths are exposed and benthic population decreases in the areas as compared to undisturbed areas. It is revealed that physical properties of sediments show minor changes after disturbance whereas biological and chemical variations are beyond 10 cm depth of cores. The three subbottom profiles taken along the disturbance area showed variable sediment thickness of 40-90 m with four distinct layers. The top two layers are very thin (3 - 5.5 m) whereas lower two layers are thicker (average 22 and 35.5 m, Figure 6.3). There are no rock outcrops and entire area is covered with sediments which was an advantage for smooth functioning of the disturber as well as to evaluate effect of disturbance.

Preliminary results showed that no significant sediment plume remains in the area within few days of disturbance, the effect can be seen on seafloor in the form of deep trenches of disturbance tracks, piles of sediments at the edge of tracks, resedimentation in the disturbed zone with no traces of megabenthic activity and undisturbed areas with numerous trails, fecal casts, burrows and mounds of benthic organisms (Anonymous, 1997).

6.3 Geotechnical properties

As far the physical properties are concerned, the effect of disturbance was not much significant. Nevertheless, the change in the water content and shear strength was observed at various depths. All the cores are siliceous ooze/clay in composition with abundant radiolarian tests (Gupta SM, pers. comm.). Figures 6.4 and 6.5 show water content variation with depth and Figures 6.6 and 6.7 depict shear strength change in each core with depth, before and after the disturbance. Figures show that water content increases and shear strength decreases after the disturbance in the surface layer only. In all 11 cores for water content and 10 cores for strength were analyzed for the comparison purpose. Each core was subsampled at 2 cm upto 10 cm and at 5 cm below 10 cm depth. Therefore, the number of measurements of water content ~~were~~ was more than shear strength measurements. In all about 55 samples were analyzed for water content. The shear strength was measured at 3-4 depth intervals as the cores have short length. Table 6.2 shows average water content and strength of all the studied cores. It is clear from the figures and table that no significant change in the two parameters is seen. The Table 6.2 also shows changes in other physical properties observed after disturbance. The parameters like specific gravity, wet density, porosity void ratio did not show any notable change. For example average specific gravity values before and after disturbance are 2.31 and 2.40 respectively. Similarly, porosities before and after the disturbance are 91.6 % and 92.2 % respectively whereas wet bulk density remains 1.14 g/cm^3 in both the conditions. Average water content in predisturbed sediments is 495 % which increases to 498 % in post disturbed condition thus showing little (3 %) increase. Average shear strength showed a change from 3.51 to 3.64 kPa. The increase in strength may be due to the fact that stations outside the disturbed area are more (7 i.e. stations 4, 6, 8, 11, 13, 14, 15) and have more influence on the data than those in the area (3 i.e. stations 2,3,5).

However, small variations are encountered in case of strength of the surface sediments up to 10 cm (Table 6.3). If only the stations in the disturbed track are considered (Stations 2,3,5), then increase in water content is higher (from 514 % to 563 %) and decrease in shear strength is higher (from 3.12 kPa to 1.13 kPa). Therefore, the effect of disturbance is severe in the disturbance track than the areas around.

Figure 6.8 depicts relationship of values of water content and shear strength before and after the disturbance. Natural water content before and after disturbance show significant positive relationship (r = 0.657) which clearly implies that water content of surface siliceous sediments gets affected to considerable extent after the disturbance, especially in the track of disturber than around it. Similar observation could not be seen in case of undrained shear strength which exhibits non-significant correlation (r = 0.203), implying that change in shear strength of surface sediments may not be like the change in water content after disturbance. This point has to be given importance while designing the nodule mining system.

Table 6.1: Locations of box cores in the disturbance area.

Stn. No.	Latitude (deg.)	Longitude (deg.)
1	1003.189	7600.155
2	1002.397	7601.216
3	1002.071	7600.712
4	1001.548	7559.706
5	1002.108	7600.165
6	1002.724	7601.709
7	1002.514	7600.766
8	1001.815	7601.088
9	1001.172	7601.505
10	1001.663	7601.348
11	1002.140	7601.332
12	1001.335	7600.689
13	1001.675	7600.508
14	1002.133	7600.298
15	1002.669	7600.322
16	1002.758	7601.116

Table 6.2: Summary of properties observed before and after the disturbing the area.

	Pre-disturbance			***Post-disturbance***		
	max.	min.	ave.	max.	min.	ave.
Water content (%)*	741	328	485	768	302	498
Specific gravity	2.94	1.79	2.31	3.18	2.10	2.40
porosity (%)	94.4	89	91.6	95.4	86	92.2
wet bulk density (g/cm^3)	1.21	1.10	1.14	1.20	1.10	1.14
Shear strength (kPa)**	7.36	0.0	3.51	6.82	0.0	3.64

* based on 11 cores

** based on 10 cores

Table 6.3: Water content and shear strength changes observed in the disturbance strip (station 2,3,5)

		Pre-disturbance			***Post-disturbance***		
Depth (cm)		0-10	10-15	> 15	0-10	10-15	>15
Water content(%)	max.	637	465	455	716	476	468
	min.	436	390	356	454	372	436
	ave.	**514**	429	395	**563**	434	452
Depth (cm)		0-10	10-15	> 15	0-10	10-15	>15
Shear strength (kPa)	max.	3.84	5.12	6.52	5.39	6.82	5.39
	min.	0.0	2.06	3.09	1.18	2.51	3.23
	ave.	**3.12**	3.12	3.32	**1.13**	3.95	5.03

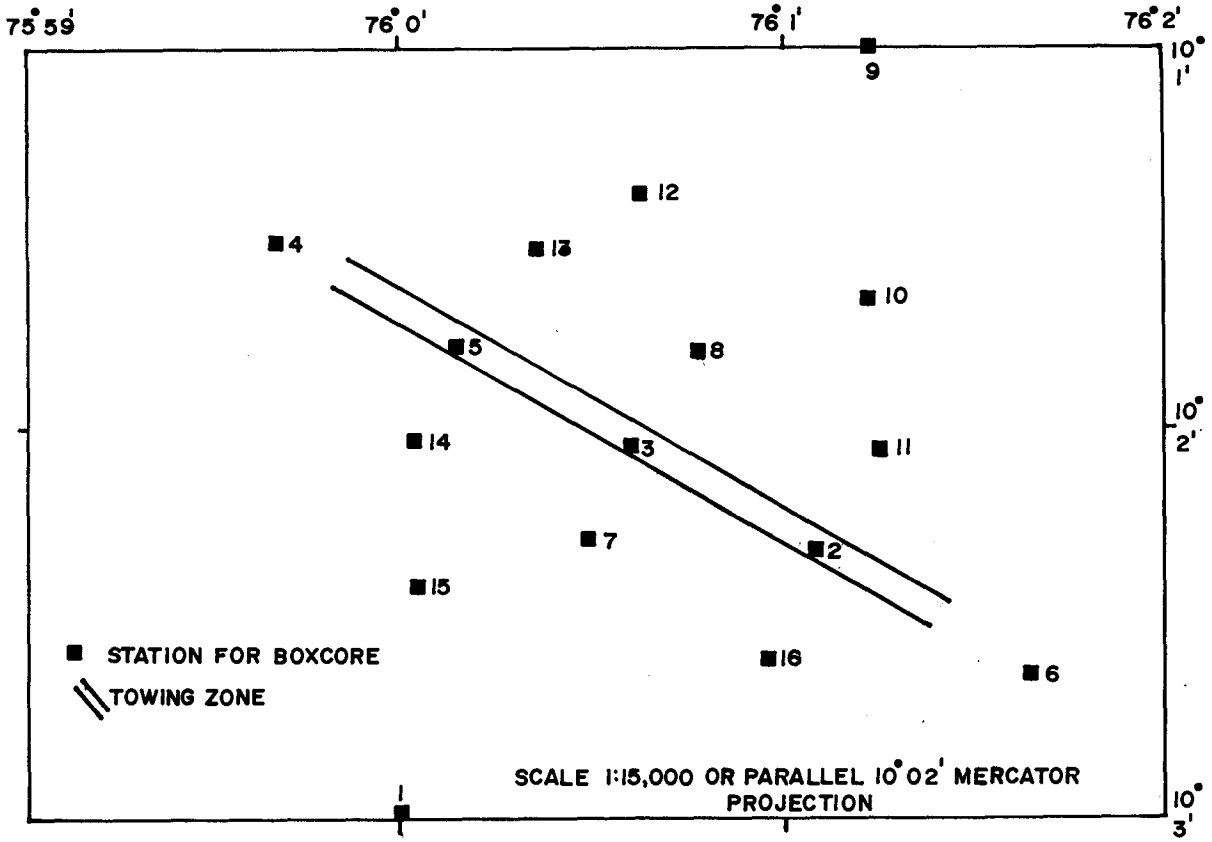

Fig.6.1 LOCATIONS OF CORING STATIONS IN AND AROUND THE SITE OF DISTURBANCE.

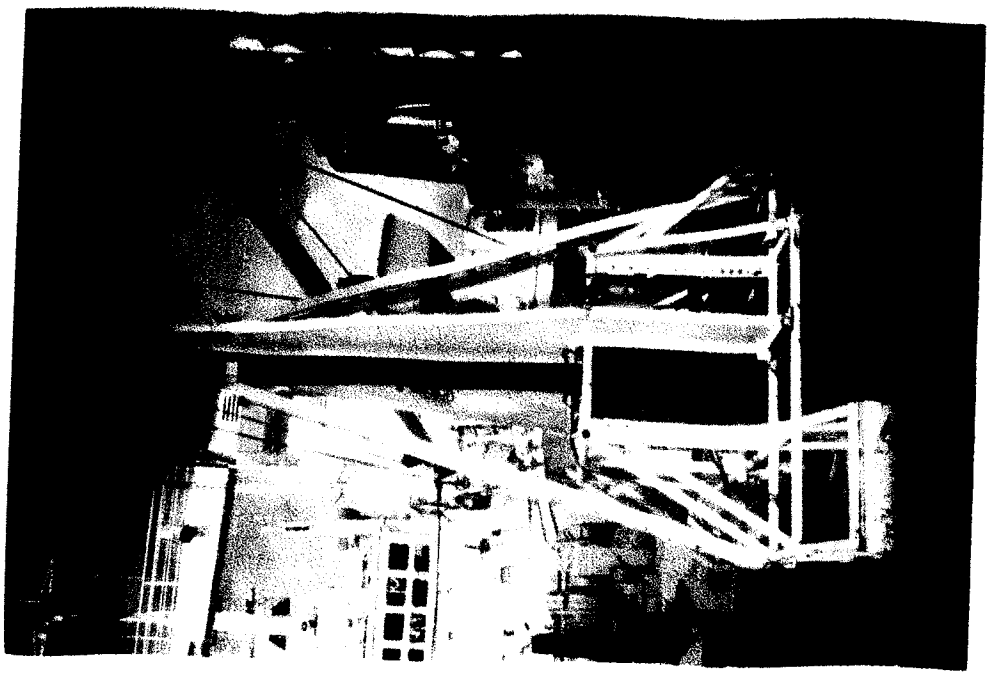

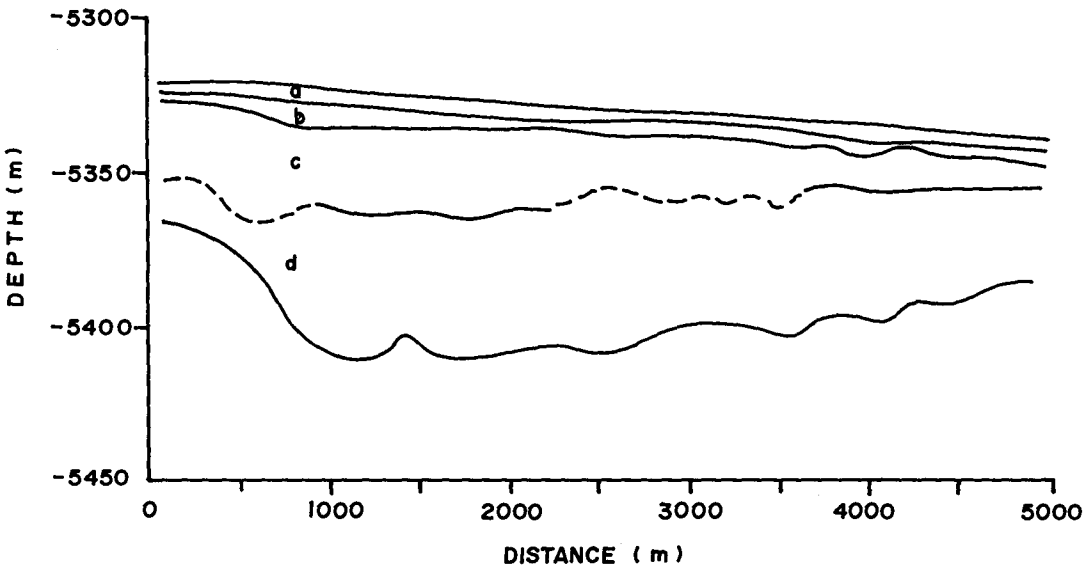

Fig.6.3 SURFACE SEDIMENTS OBSERVED FROM SUB BOTTOM PROFILE SHOWING FOUR LAYERS

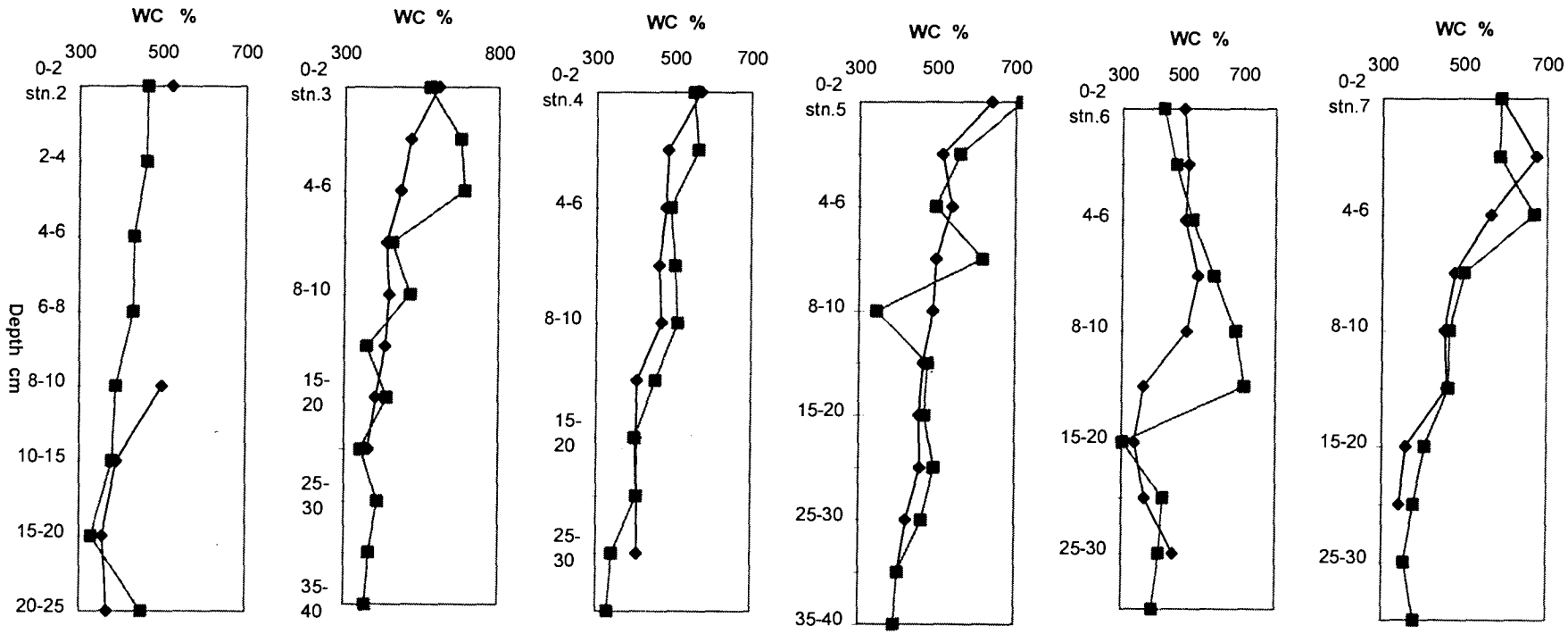

Figure 6.4: Water content variations in sediments before and after the disturbance.
(◆ = pre-disturbance, ⧈ = post-disturbance)

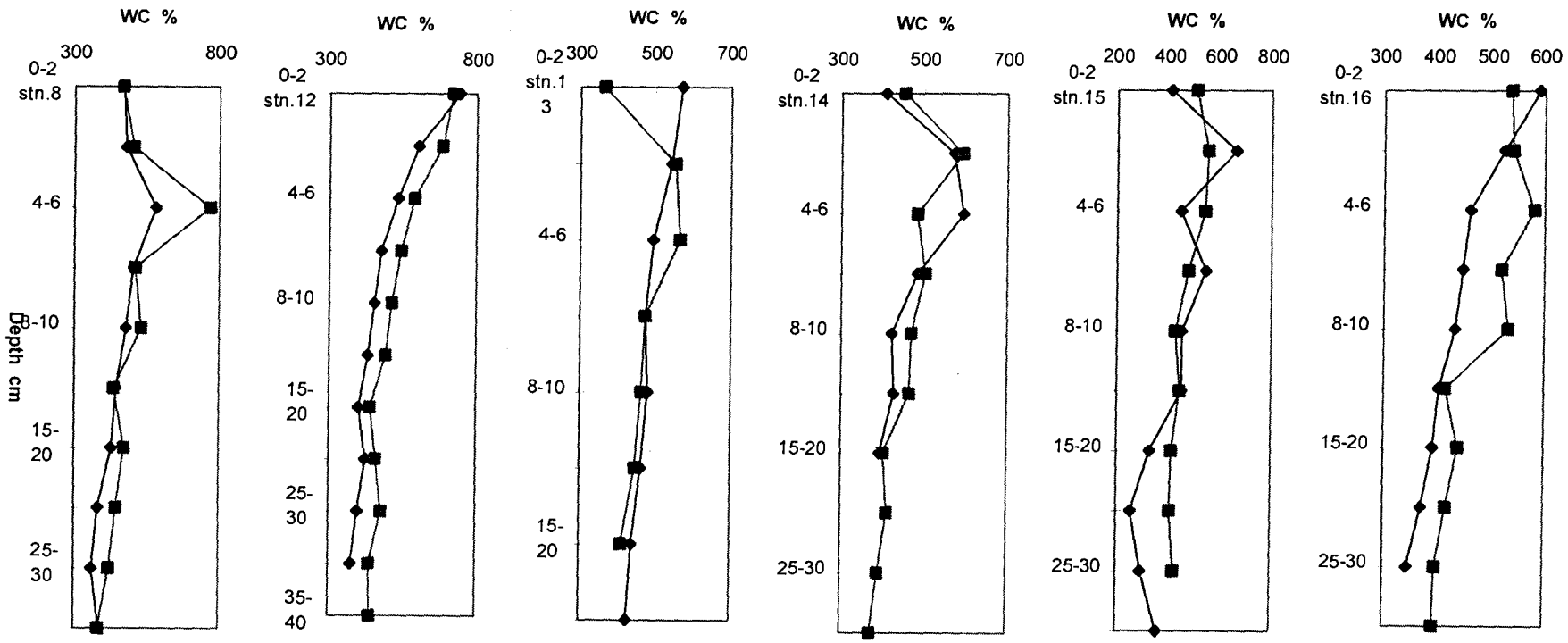

Figure 6.5: Water content variations in sediments before and after the disturbance.
(◆ = pre-disturbance, ■ = post-disturbance)

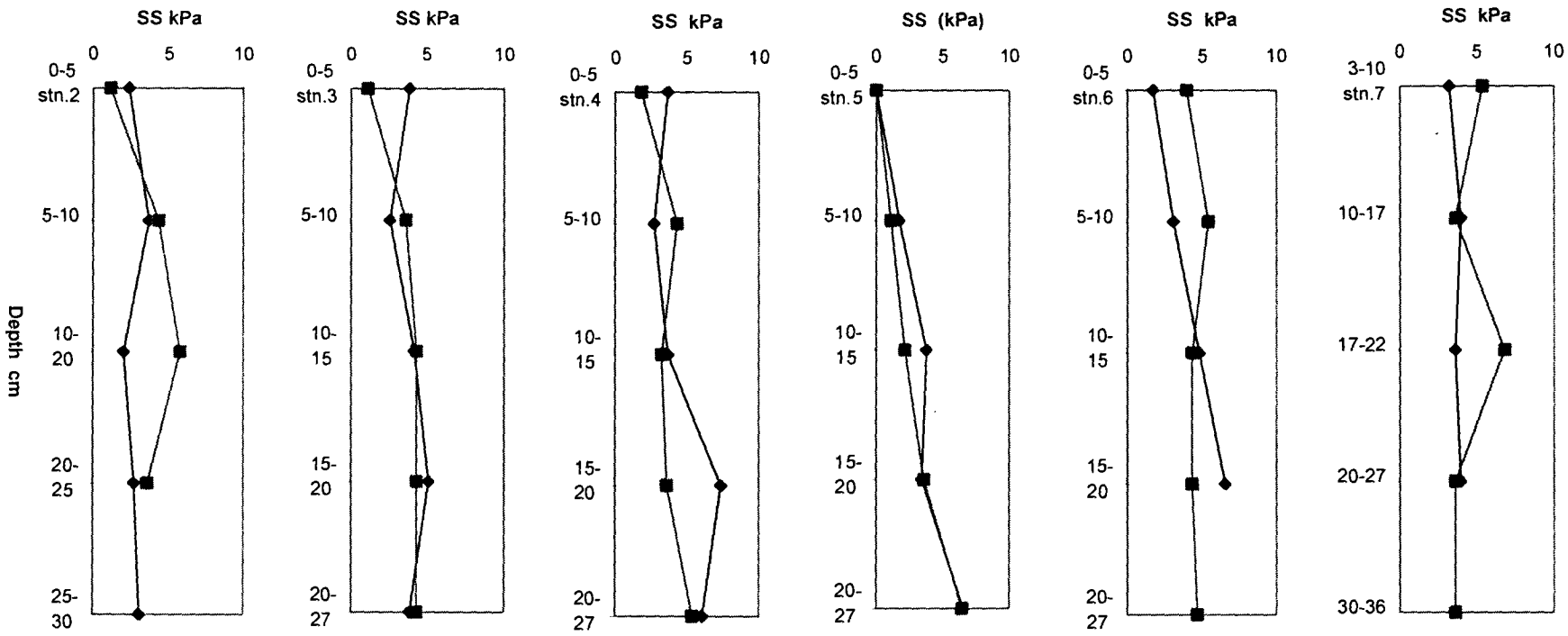

Figure 6.6: Shear strength variations in sediments before and after the disturbance.
(◆ = pre-disturbance, ▣ = post-disturbance)

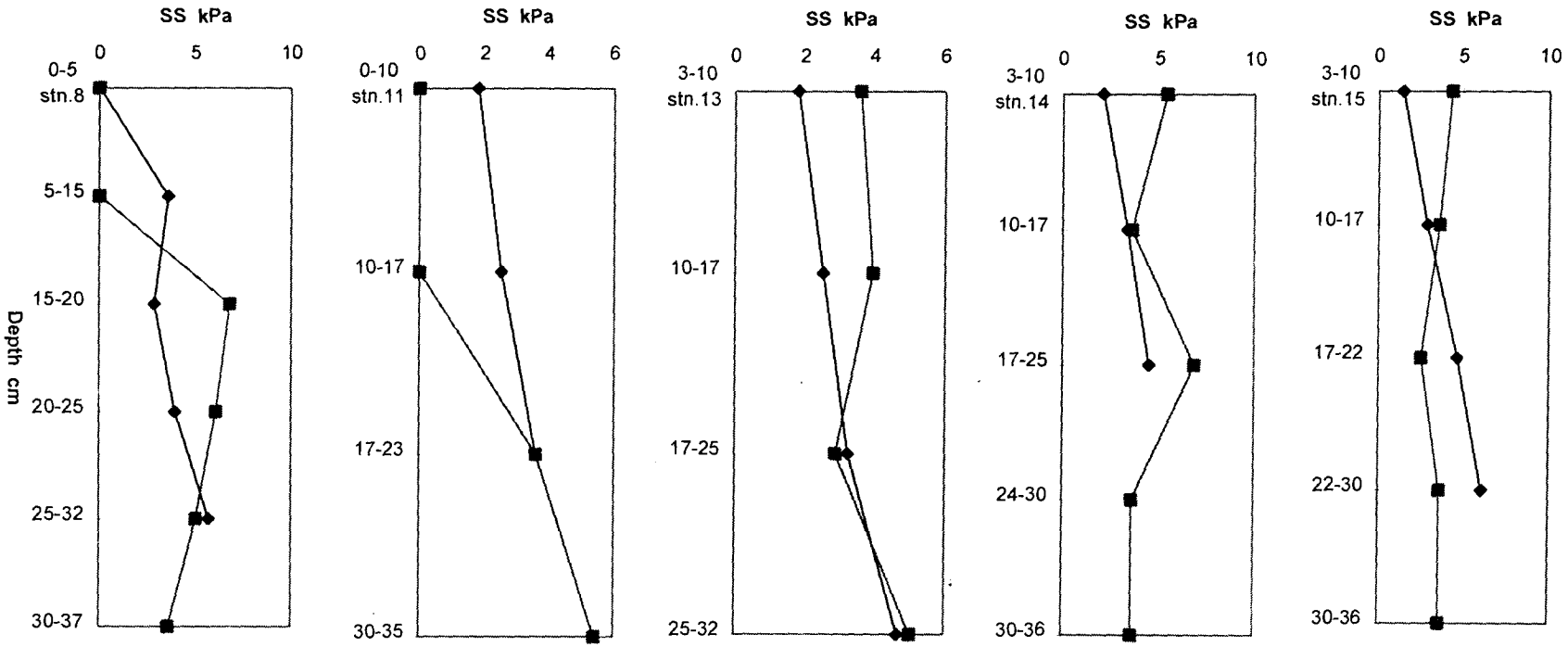

Figure 6.7: Shear strength variations in sediments before and after the disturbance.
(◆ = pre-disturbance, ◘ = post-disturbance)

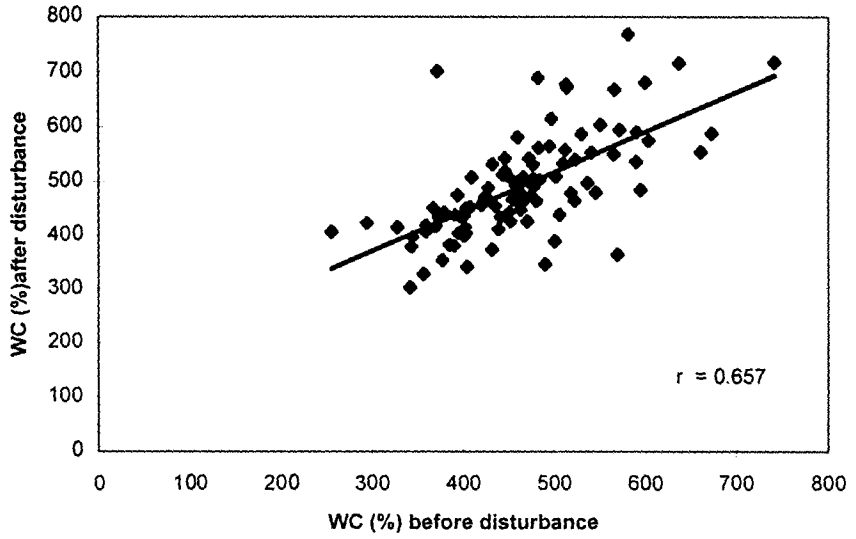

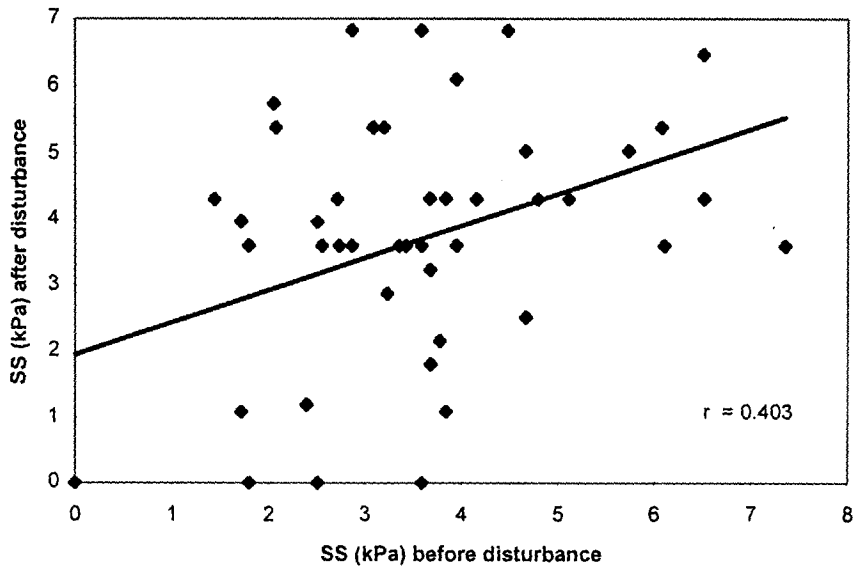

Figure 6.8: Scatter diagrams of water content and shear strength of surface sediments before and after disturbance

CHAPTER 7

SUMMARY AND CONCLUSIONS

The study is the first attempt to determine geotechnical properties of the deep sea sediments from the Indian Ocean and is based on mostly siliceous cores collected from the relatively flat topographic terrain in the Central Indian Basin. The sediments are siliceous, fine grained in texture and silty clay to clayey silt in composition with very little amount of sand size fraction. The sediments are cohesive and exhibit medium to high plastic characteristics. The siliceous sediments are highly porous, less dense and hence show high water content at all the depths. The clay mineralogy shows that illitic component is dominated over montmorillonite, and both are inversely related. Kaolinite and/or chlorite do not play any role in controlling the properties though they are present in considerable amount in all the cores. The plasticity charts show that sediments have little scatter indicating their deposition from the same source except core A4/6 and sk69/2 which do show more than one source of supply. The activity of clay indicates that the sediments are normal to highly active due to high content of montmorillonite fraction. The effect of bioturbation on siliceous sediments is mixed and does not show firm variation in parameters such as porosity, water content and shear strength.

Shear strength and physical properties of siliceous sediments show variations with the depth of burial below the seafloor. Shear strength variation is more dependent on water content and depth below the seafloor than any other parameter.

Physical properties of siliceous sediments show interdependencies among themselves barring few exceptions. Overall, the water content, void ratio, porosity decrease with depth whereas wet bulk density, montmorillonite,

and shear strength increase with depth. The significant inverse relationship of montmorillonite with water content is unexpected and could be explained through overconsolidated nature of sediments. These properties could be used for geological interpretation as they can be measured immediately. The depositional break during Plio-Pleistocene in core SK69/2 is well reflected in the geotechnical properties and could be used as an additional tool for geological interpretation. The CIB sediments indicate less cohesiveness than the Pacific Ocean sediments from the nodule bearing areas.

Calcareous sediments are more cohesive than siliceous sediments and exhibit medium to high plasticity. Despite uniform nature of these sediments, the shear strength shows increase with depth which could be attributed to the cementation of voids as indicated by low values of water content and porosity, high values of wet bulk density and shear strength. The study on calcareous samples is too meager to draw any firm conclusions. Therefore, in future more calcareous and pelagic sediment core should be collected and studied for geotechnical properties.

The impact of simulated disturbance on the geotechnical properties of surface sediments is not as much as it was expected. Very little increase in water content and decrease in shear strength is observed after disturbing the sediments. Nevertheless, effect of disturbance is highest in the disturbance track than its surroundings. Therefore, the change in shear strength can not be ignored for nodule mining activity which would actually cover larger area of the seafloor.

Recommendations

The results presented here form a part of the on going geotechnical program for the Central Indian Basin. This type of studies are not very common for the deep sea sediments though lot of work is published from the coastal areas on these aspects. The number of cores studied is rather low as

compared to the area covered by polymetallic nodules in the Pioneer Area. More data need to be generated from additional cores. Based on the present work, the following studies are recommended in the future.

Cores of calcareous and pelagic sediment should be collected to know the geotechnical properties and their variation. In situ measurements using submersible dives in selected sediment facies and areas of the Central Indian Basin should be carried out in future to correlate the on board determination of shear strength and other characteristics. The clay fabric studies are needed on sediment samples using transmission electron microscope to know the control over various parameters. Depositional processes in the CIB are varied and therefore, the continuous property measurements e.g. porosity, could be useful for application of data to geological interpretation such as those done (Wetzel, 1990) on DSDP cores in the Bay of Bengal. The exclusive undisturbed cores for triaxial test and compression test should be collected. The consolidation and triaxial tests on sediment samples will give data on the compression index, overconsolidation ratios and angle of friction which should be used to know settlement behaviour and compressibility characteristics of sediments. These data would be required by mining engineers to know bearing capacity of sediments and trafficability of nodule miner on the seabed.

The area of simulated disturbance is small as compare to size of the Pioneer Area. Though the impact of disturbance is not much seen on all properties, the change in shear strength and water content should be monitored in future from the Pioneer area. Also larger area could be disturbed in the siliceous sediments and its effect on properties could be studied by in situ measurements.

REFERENCES

REFERENCES

Anonymous (1989) Post depositional processes in deep-sea sediments. In: *Ocean chemistry and deep-sea sediments* prepared by Open University Course Team, U.K. Pergamon, Oxford. 134p.

Anonymous (1995) Status Report of the PMN project. NIO Goa submitted to DOD, New Delhi (unpublished).

Anonymous (1997) Report on benthic disturbance and impact studies. NIO, Goa, submitted to DOD, New Delhi (Unpublished).

Amos AF and Roels AO (1977) Environmental aspects of manganese nodule mining. Marine Pollution International Bull., 1, 160-162.

Ahmed SM and Hussain A (1987) Geochemistry of ferromanganese nodules from the Central Indian Basin. Mar. Geol., 77, 165-170.

ASTM (1978) Annual book of ASTM standards, Vol, 19, Philadelphia, 580p.

ASTM (1987) Annual book of ASTM standards, Vol 04.08, Soil and rock, building stones, geotextiles. Philadelphia, Pa, 1189p.

Atterberg AM (1911) Die Plastizitat der Tone. Int. Mitt. Bodenkunde 1, 4-37.

Banakar VK and Kodagali VN (1988) Nodules of the Central Indian Ocean basin. In: *From the first nodule to the first mine site* : An account of the polymetallic project. Quasim SZ and Nair RR (Editors), DOD & NIO, Goa, 7-13.

Banakar VK, Gupta SM and Padmavati VK (1991) Abyssal sediment erosion in the CIB : evidence from radiochemical and radiolarian studies. Mar. Geol., 96, 167-173.

Belyaeva NV and Burmistrova II (1985) Critical carbonate levels in the Indian Ocean. J . Foraminiferal Res., 15, 337-341.

Bennett RH and Lambert DN (1971) Rapid and reliable technique for determining unit weight and porosity of deep sea sediments. Mar. Geol., 11, 201-207.

Biscaye PE (1965) Mineralogy and sedimentation of recent deep sea clays in the Atlantic Oceans and adjacent seas and oceans. Bull. Geol. Soc. Am., 76, 803-832.

Bonatti E, Kraemar T and Rydell YR (1972) Classification of genesis of submarine iron and manganese deposits. In: Horn DR (Ed) Ferromanganese deposits on the ocean floor. NSF, Washington DC, 149-166.

Bouquillon A, Chamley H and Fröhlich F (1989) Sedimentation argileuse recente dans l'Ocean Indaien Nord-Oriental. Oceanol. Acta, 12, 133-147.

Bryant WR, Bennett RH and Katherman CE (1981) Shear strength, consolidation, porosity and permeability of oceanic sediments. In: Emiliani C (Editor) *The Ocean Lithosphere, The Sea*, Vol 7, John Wiley, New York, 1555-1615.

Burns RG and Burns VM (1977) Mineralogy. In: Glasby GP (Editor) *Marine manganese deposits.* Elsevier, Amsterdam, 185-248.

Carroll D (1970) Clay minerals: a guide to their x-ray identification. Geol. Soc. Am., Special Paper, 126, 80p.

Casagrande A (1932) Research on the Atterberg limits of soils. Public roads, 13, 121-136.

Chernow RM, Frey RW and Ellwood BB (1986) Biogenic effects on development of magnetic fabrics in coastal Georgia sediments. J. Sed. Petrol., 56,160-172.

Cochonat P, Le Suave R, Charles C, Greger B, Hoffert M, Lenoble JP, Meunier J and Pautot G (1992) First in situ studies of nodule distribution and geotechnical measurements of associated deep-sea clay (Northeastern Pacific Ocean). Mar. Geol., 103, 373-380.

Cronan DS and Tooms JS (1967) Geochemistry of manganese nodules from the north-west Indian Ocean. Deep-Sea Res., 14, 239-249.

Cronan DS (1980) *Underwater minerals*. Academic Press, London, 362p.

Cronan DS and Moorby SA (1981) Manganese nodules and other ferromanganese oxide deposits from the Indian Ocean. J. Geol. Soc., London, 138, 527-539.

Debrabant P, Fagel N, Chamley H, Bout V and Caulet JP (1993) Neogene to quaternary clay mineral fluxes in the Central Indian Basin. Palaeogeogr. Palaeoclim. Palaeoecol., 103, 117-131.

Folk RL (1968) *Petrology of sedimentary rocks.* University of Texas, Hemphills, 170p.

Fraser HJ (1935) Experimental study of the porosity and permeability of clastic sediments. J. Geology, 43, 910-1010.

Frazer JZ and Wilson LL (1980) Manganese nodule resources in the Indian Ocean. Mar. Min., 2,257-292.

Glasby GP (1972) The geochemistry of manganese nodules from the north west Indian Ocean. In : Horn DR (Editor) *Ferromanganese deposits on the ocean floor.* Washington, DC, National Science Foundation, 93-104.

Goldberg ED and Arrehnius G (1958) Chemistry of Pacific pelagic sediments. Geoch. Cosm. Acta, 13,152-212.

Goldberg ED and Griffin JJ (1970) The sedimentation of the northern Indian Ocean. Deep-Sea Res., 17, 513-537.

Gupta SM (1996) Tropical sea surface temperatures and the Earth's orbital eccentricity cycles. Geophy. Res. Lett., 23, 3159-3162.

Hamilton, EL (1970) Sound velocities and related properties of sediments, North Pacific. J. Geophy. Res., 75, 4423-4446.

Hamilton EL (1972) Compressional wave attenuation in marine sediments. Geophysics, 37, 620-646.

Jauhari P (1987) Classification and inter element relationships of ferromanganese nodules from the Central Indian Ocean Basin. Marine Mining, 6, 419-429.

Jauhari P and Pattan JN (1998) Ferromanganese nodules of the Central Indian Ocean Basin. *In: Cronan DS (Editor) Handbook of marine mineral deposits. (in press).*

Keller GH (1974) Geotechnical properties ; interrelationships and relationships to depth of burial. In: Inderbitzen AL (Editor) *Deep Sea Sediments physical and mechanical properties.* Plenum Press, New York, 45-76.

Keller GH and Lambert DN (1980) Variations of sedimentary geotechnical properties between the greater Antilles Outer Ridge and Nares Abyssal Plain. Mar. Geotech., 4, 125-143.

Khadge NH (1992) Geotechnical properties of deep sea sediments from the Central Indian Ocean Basin. Ind.J. Mar. Sci., 21, 80-82.

Khadge NH (1995) Preliminary geotechnical properties of deep sea sediments from the Central Indian Basin. Proc. ISOPE-Ocean Mining Symposium, 21-23 November, 1995, Tsukuba, Japan, 55-60.

Khadge NH (1997) Physical properties of a long sediment core from the Central Indian Basin. In: Wijayananda, NP, Cooray, PG and Mosley, P (Editors), *Geology in South Asia - II,* Geological Survey & Mines Bureau, Sri Lanka, Professional Paper 7, 191-196.

Kodagali VN, Kameshraju KA, Ramprasad T (1995) Seafloor mapping of large areas using multibeam system - Indian experience. In: Maul G and Seeber G (Editors) Proceedings of Int. Symp. on Marine Positioning, MTS, Washington, 365-373.

Kolla V and Biscaye PE (1973) Clay mineralogy and sedimentation in the eastern Indian Ocean. Deep-Sea Res., 20, 727-738.

Kolla V and Hayes J (1974) Sedimentation in the Indian ocean. In: Inderbitzen AL (Ed) *Deep Sea Sediments physical and mechanical properties*, Plenum Press, New York, 401-415.

Kolla V, Henderson L and Biscaye P (1976a) Clay mineralogy and sedimentation in the western Indian Ocean. Deep-Sea Research, 23, 949-961.

Kolla V, Be AWH and Biscaye PE (1976b) Calcium carbonate distribution in the surface sediments of the Indian Ocean. J. Geophy. Res.(Ocean and Atmosphere), 81, 2605-2616.

Kravitz JH (1970) Repeatability of three instruments used to determine the undrained shear strength of extremely weak, saturated, cohesive sediments. J. Sed. Petrol., 40 (3), 1026-1037.

Lambe TW and Whitman RV (1969) *Soil mechanics.* Wiley Eastern Ltd, New Delhi, 553p.

Lee HJ (1985) State of the art : laboratory determination of the strength of marine soils. In:Chaney RC and Demars KR (Editors) *Strength testing of marine sediments-Laboratory and in situ measurements*, ASTM STP 883, Philadelphia, 181-250.

Lyle M, Dymond J and Heath GR (1977) Copper-Nickel enriched ferromanganese nodules and associated crusts from the Bauer Basin, Northwest Nazca Plate. Earth Planet. Sci. Lett., 35, 55-64.

McManus J (1988) Grain size determination and interpretation In: Tucker M (Ed) *Techniques in sedimentology*, Blackwell Scientific Press, London, 63-85.

Mero JL (1965) *The mineral resources of the sea.* Elsevier, Amsterdam, 312p

Mitchell JK (1976) *Fundamentals of soil behavior.* Wiley, New York, 422p.

Mudholkar AV, Pattan JN and Sudhakar M (1988) Techniques and results. In: *From the first nodule to the first mine site.* An account of the polymetallic project. Quasim SZ and Nair RR (Editors), DOD & NIO, Goa, 29-36.

Mukhopadhyay R (1987) Morphological variations in the polymetallic nodules from the selected stations from the Central Indian Ocean Basin. Geo-Mar. Lett., 7, 45-51.

Mukhopadhyay R and Nath BN (1988) Influence of seamount topography on the local facies variation in ferromanganese deposits in the Indian Ocean. Deep-Sea Res., 35 (8), 1431-1436.

Mukhopadhyay R and Khadge NH (1990) Seamounts in the Central Indian Ocean Basin: indicators of the Indian plate movement. Proc. Ind. Acad. Sci. (Earth and Planet. Sci.), 99, 357-365.

Murray J and Irvine R (1894) On the manganese oxides and manganese nodules in the marine deposits. Transactions of Royal Society of London, 37,52-55.

Murray J and Renard AF (1891) Deep sea deposits. Report of Scientific Results of Challenger voyage. p525.

Nath BN, Rao VP and Becker KP (1989) Geochemical evidence of terrigenous influence in deep-sea sediments upto 8OS in the Central Indian Basin. Mar. Geol., 87, 301-313.

Nath BN, Roelands I, Sudhakar M and Pluger W (1992) Rare earth element patterns of the CIB sediments related to their lithology. Geophy. Res. Lett., 19, 1197-1200.

Noorany I (1985) Shear strength properties of some deep sea pelagic sediments. In: Chaney RC and Demars KR (Eds.) *Strength testing of marine sediments : laboratory and in situ measurements*. ASTM STP 883, Philadelphia, 251-257.

Pattan JN (1988) Internal microfeatures of manganese nodules from the CIOB. Mar. Geol, 8, 215-226.

Pattan JN, Gupta SM , Mudholkar, AV and Parthiban, G (1992) Biogenic silica in space and time in sediments from the Central Indian Ocean. Ind. J. Mar. Sci., 21, 116-120.

Pattan JN and Banakar VK (1993) Rare earth element distribution and bahavior in the buried manganese nodules from the Central Indian Basin. Mar. Geol., 112, 303-312.

Peck RB, Hanson, WE and Thornburn TH (1974) *Foundation engineering.* John Wiley, New York, p514.

Poulos HG (1988) *Marine geotechnics.* Unwin Hyman, London, 465p.

Purushothama Raj P (1995) *Geotechnical engineering.* Tata-McGraw Hill Publihing, New Delhi, 712p.

Rabitti S, Boldrin A and Vitturi LM (1983) Relationships between surface area and grain size in bottom sediments. J. Sedimentary Petrology, 53, 665-667.

Rao VP (1987) Mineralogy of polymetallic nodules and associated sediments from the Central Indian Ocean Basin. Mar. Geol., 74, 151-157.

Rao VP and Nath BN (1988) Nature, distribution and origin of clay minerals in grain size fractions of sediments from the Central Indian Ocean Basin. Marine. Ind. J. Mar. Sci, 17, 202-207.

Rhoads DC and Boyer LF (1982) The effect of marine benthos on physical properties of sediments: a successional perspective. In: McCall PL and

Tevesz MJS (Eds) *Animal-sediment relations* (Topics in Geobiology, Vol 2) Plenum, New York, 3-52p.

Richards AF (1961) Investigations of deep sea sediment cores, Part I: Shear strength, bearing capacity and consolidation, US Naval Hydrographic Office Tech. Report, 63.

Richards, AF (1962) Investigations of deep sea sediment cores, Part II : Mass physical properties. US Navy Hydrographic Office Technical Report, 106, pp146.

Richards, AF and Hamilton EL (1967) Investigations of deep sea sediment cores, Part III : Investigations of deep sea sediment cores: Consolidation. In: *Marine Geotechnique.* Richards AF (Editor), University of Illinois press, 93- 117.

Richards AF, Hirst TJ and Parks JM (1976) Preliminary geotechnical properties northeast central Pacific nodule mining area. Oceans'76, MTS and IEEE, 2B1-2B3.

Richards AF and Parks JM (1976) Marine geotechnology: Average sediment properties, selected literature and review of consolidation, stability, and bioturbation-geotechnical interactions in the benthic layer. In: McCave IN (Editor) *The benthic boundary layer.* Plenum Press, New York, 157-181.

Richards AF and Parks JM (1977) Geotechnical predictor equations for east central north Pacific nodule mining area sediments. Proc. Off. Tech. Conf., 2773, 377-386.

Richardson MD, Young DK and Briggs KB (1983) Effects of hydrodynamic and biological processes on sediment geoacoustic properties in Long Island Sound, U.S.A. Mar. Geol., 52, 201-226.

Rowe GT (1974) The effects of the benthic fauna on the physical properties of deep-sea sediments. In Inderbitzen AL (Editor) *Deep Sea Sediments: physical and mechanical properties.* Plenum Press, New York 381-400.

Sharma R (1993) Quntitative estimation of seafloor features from photographs and their application to nodule mining. Mar. Geores. Geotech., 11(4), 311-331.

Siddiquie HN, Das Gupta DR, Sengupta NR, Srivastava PC and Mallik TK (1978) Manganese iron nodules from the Indian Ocean. Ind. J. Mar. Sci., 7, 239-253.

Silva AJ (1974) Marine geomechanics: overview and projections. In:Inderbitzen AL(Editor) *Deep Sea Sediments: physical and mechanical properties.* Plenum Press, New York, 45-76.

Simpson F (1976) Analysis of strength characteristics of deep-sea sediments from potential manganese nodule mining areas in the Northern Central Pacific. Oceans'76, 2, A1-2, A9.

Skempton AW (1953) The colloidal activity of clays. Proceedings of the Third International conference of soil mechanics and foundation engineering, Zurich, Vol. 1, 57- 61.

Skempton AW (1970) The consolidation of clays by gravitational compaction. Q. J. Geol. Soc., London, 125, 373-411.

Sudhakar M (1989) Ore grade manganese nodules from the Central Indian Basin: an evaluation. Mar. Min., 8, 201-214.

Terzaghi K (1926) Simplified soil tests for subgrades and their physical significance. Public Roads, 7, 153-162.

Terzaghi K (1955) Influence of geological factors on the engineering properties of sediments. Eco. Geol., (50^{th} Anniversary volume), 557-618.

Tisot JP and Gerard B (1981) Analysis of physical and mechanical properties of deep sea sediments from potential manganese nodule mining areas in the north central Pacific. Proc. Offshore Tech. Conf., OTC 4132, 139-146.

Tsurusaki K, Yamazaki T and Handa K (1994) Geotechnical properties of deep sea sediments and manganese nodules in the Penrhyn Basin, South Pacific. In: *Marine Geology, geophysics and Manganese nodule deposits in the Penrhyn Basin, South Pacific (GH83-3 Area).* Usui A (Editor) Cruise Report 23, Geological Survey of Japan, 225-240.

Udintsev GB (1975) *Geological-geophysical atlas of the Indian Ocean.* Pergamon, Oxford, 151p.

Valsangkar AB and Khadge NH (1989) Size analyses and geochemistry of ferromanganese nodules from the Central Indian Ocean Basin. Mar. Min., 8, 325-347.

Valsangkar AB (1995) Nodule size : an important factor in nodule mining? Proc. ISOPE-Ocean Mining Symposium, 21-23 November, 1995, Tsukuba, Japan, 113-118.

Wetzel A (1990) Interrelationships between porosity and other geotechnical properties of slowly deposited fine grained marine surface sediments. Mar. Geol., 92, 105-113.

Winters WJ (1988) Geotechnical testing of marine sediments. USGS Open file report, 88-36, 52p

List of Author's Publications

Valsangkar AB and **Khadge NH** (1989) Size analyses and geochemistry of geochemistry of ferromanganese nodules from the Central Indian Ocean Basin. *Marine Mining*, 8, 325-347.

R Mukhopadhyay and **Khadge NH** (1990) Seamounts in the Central Indian Basin: indicators of the Indian Plate movements. *Proc. Indian Academy of Sciences (Earth and Planetary Sciences)*, 99, 3, 357-365.

Valsangkar AB, **Khadge NH** and JAE Desa (1992) Geochemistry of polymetallic nodules from the Central Indian Ocean Basin. *Marine Geology*, 103, 361-371.

Khadge NH (1992) Geotechnical properties of deep-sea sediments from the Central Indian Ocean Basin. *Indian J. Marine Sciences*, 21, 80-82.

R Mukhopadhyay and **Khadge NH** (1992) Tectonic reactivation in the Indian Ocean: evidence from seamount morphology and manganese nodules characteristics. *Journal of Geological Society of India*, 40, 443-452.

R Mukhopadhyay and **Khadge NH** (1994) Growth constraints of the Indian Ocean seamounts. *Proc. of "Space applications in earth system science"*, 30th convention of IGU, 21-23 Dec., Hyderabad,1993.

Khadge NH (1994) Geotechnical properties of two siliceous cores from the Central Indian Basin. *Proc. of INCHOE-94,* June 94, Pune, E21-30.

Khadge NH (1995) Preliminary geotechnical properties of deep sea sediments from the Central Indian Basin. *Proceedings of the ISOPE - Ocean Mining Symposium*, Tsukuba, Japan, Nov., 1995 55-60.

Khadge NH (1997) Physical properties of a long sediment core from the Central Indian Basin. In:*Geology in South Asia - II*, Geological Survey & Mines Bureau, Sri Lanka, Wijayananda, N. P., Cooray, P. G. and Mosley, P. (Editors), Professional Paper 7, 191-196.

Sharma R, BN Nath, AB Valsangkar, **NH KHADGE**, SM Gupta and G Parthiban (1997) Seafloor and sediment characteristics in the INDEX area of the Central Indian Basin. *Proc. International symposium on environmental studies for deep sea mining*. Nov., 1997, Tokyo, Japan, 83-90.

Desa E and **INDEX project group** (1997) Initial reports of India's environmental impact assessment of nodule mining. *Proc. International symposium on environmental studies for deep sea mining*. Nov., 1997, Tokyo, Japan, 49-63.